

GH 4145.

AN EVALUATION OF THE FEASIBILITY OF USING THE GRAVITY  
METHOD TO RESOLVE THE STRUCTURE OF THE LITTLE KAROO  
CRETACEOUS BASIN WITH A VIEW TO DRILLING PRODUCTION  
BOREHOLES INTO THE UNDERLYING TABLE MOUNTAIN  
SANDSTONE AQUIFER  
With  
STRUCTURAL-GEOLOGICAL CONSIDERATIONS FOR FUTURE  
EXPLORATION

P. SMIT  
F.C. ANKE  
D. BRINK  
L.A. SMITH  
J. GROENEWALD

REPORT NO. GHP 3949

Geohydrological Resource Assessment and Monitoring

Directorate Hydrological Services

Department Of Water Affairs

GHP3949

## CONTENTS

	<i>PAGE</i>
1. INTRODUCTION	3
2. EXISTING INFORMATION	3
3. GEOPHYSICAL FIELDWORK	9
4. DATA REDUCTION	11
5. GRAVITY DATA INTERPRETATION AND MODEL	13
6. DISCUSSION OF GEOPHYSICAL WORK	23
7. STRUCTURAL GEOLOGY	25
8. DISCUSSION OF STRUCTURAL MEASUREMENTS	26
9. CONCLUSIONS AND RECOMMENDATIONS	37
10. REFERENCES	40
11. LIST OF FIGURES AND TABLES	42
12. ACKNOWLEDGEMENTS	44

APPENDIX A – GEOPHYSICAL DATA LISTING

APPENDIX B – GRAVITY MODEL DATA LISTING

APPENDIX C – SYNTHETIC GRAVITY MODELS

APPENDIX D – ADDITIONAL PHOTOGRAPHS: STRUCTURES

APPENDIX E – MAGNETIC DECLINATION INFORMATION

APPENDIX F – STRUCTURAL DATA LISTING

APPENDIX G – STRUCTURAL DATA PLOTS

## 1. INTRODUCTION

The Little Karoo valley is an arid region with little surface water flow and generally poor groundwater occurrences. The Little Karoo Rural Water Supply Scheme supplies piped water from groundwater sources outside the valley to rural communities throughout the valley. The present source areas are located in the Table Mountain Sandstone (TMS) outcrops east of Dysselsdorp and south-west of Calitzdorp. This intensely folded, fractured and jointed aquifer is well known for artesian wells in certain locations, and large yields are not uncommon. Excessive drawdown variations due to pumping schedules resulted in an exacerbated biofouling problem, with resultant impaired well efficiencies. Lowering of water levels and expected growth in demand initiated efforts to study the aquifer and to search for additional resource areas for future use.

Various options for future exploration exist: The valley is surrounded by TMS and various alternative sites for production wells probably exist, with accessibility and distance from the purification works the main constraints. Another option is the sinking of boreholes through the Cretaceous sediments that underlie the valley, to tap potable water from the underlying TMS. To initiate a study in this direction a preliminary gravity survey was carried out to

- Test the viability of the gravity method to delineate the bedrock topography
- Correlate the findings to results obtained by the CSIR and Council for Geoscience in earlier studies
- Find possible anticlinal structures or horst blocks in the bedrock at shallow depth as drilling targets.

The gravity survey was conducted along three profiles: One crossing the Cretaceous valley from south to north, starting and ending on TMS outcrops, and two west-east traverses at the western edge of the basin south of Calitzdorp. A total of 16 line km were surveyed during March 1997, and 7,2 line km during July 2002 by specialist personnel of the erstwhile Technology section of the Directorate: Geohydrology (Geohydrological Resource Assessment and Monitoring). This investigation was augmented by structural measurements to further delineate the basin structure.

## 2. EXISTING INFORMATION

### 2.1 GEOLOGY

The Little Karoo basin is surrounded by mountains formed by the folding of the Cape Supergroup, in the Cape Fold Belt (Figure 1). The basin itself is filled with sediments of Jurassic to Cretaceous age grouped under the Uitenhage Group, resting unconformably on a floor of Cape Supergroup rocks. The general strike direction of the mapped lithology and major faults are east-west.

#### 2.1.1 CANGO GROUP

The Cango Group rocks exposed in the study area consists of greywackes, shales, phyllites, schists, sub-arkose and conglomerates with limestone lenses, considered to represent both shelf-facies and deep-sea sediments. Overfolding and thrust faulting deformed the sediments, and many wide quartz veins occur in the shales. Metamorphic grade is low and does not exceed lower greenschist facies. Topography varies from rugged to gentle, with alluvium confined mainly to stream valleys. The groundwater potential of this intensely folded group is limited mainly to limestones occurring in the Matjies River and Groenewoerd Formations (Meyer 1996) in the lower part of the group. Various east-west faults occur, the most important one being the Cango fault (The local expression of the Swartberg Fault).

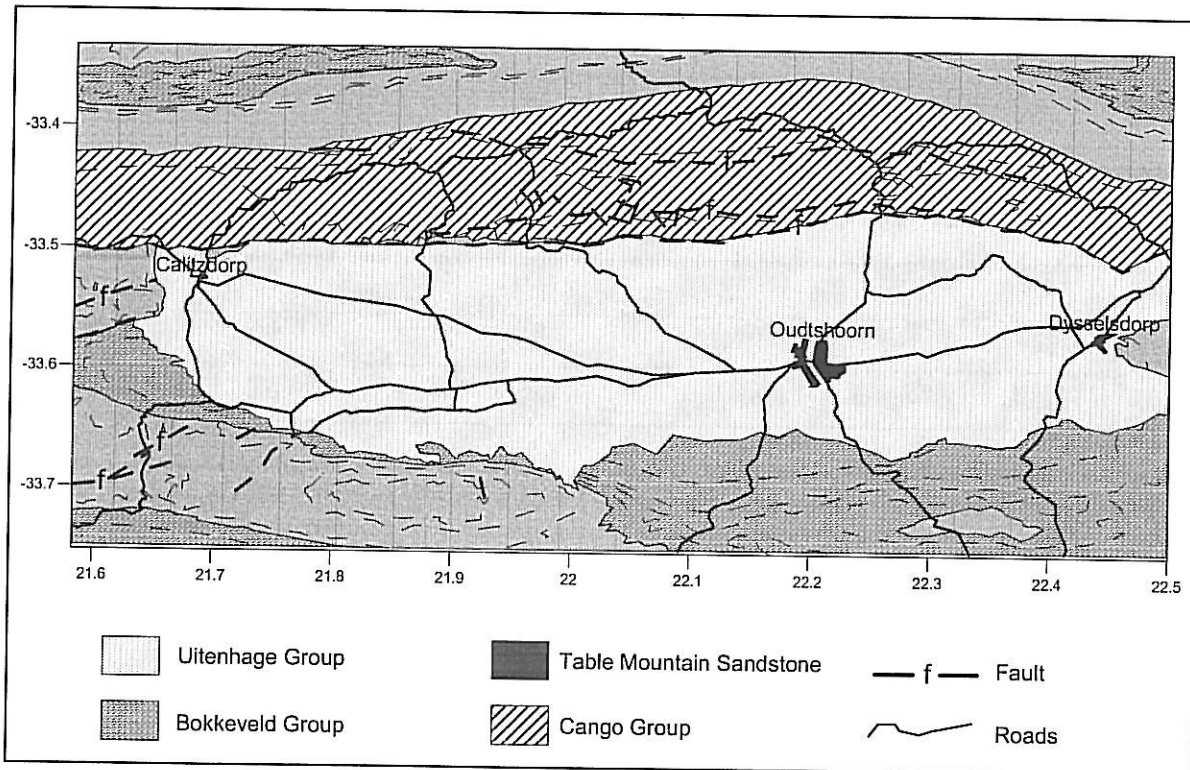


**Figure 1** Simplified Geology map of the study area.

### 2.1.2 CAPE SUPERGROUP

The Cape Supergroup comprises the Table Mountain, Bokkeveld and Witteberg Groups. The Table Mountain Group (TMG) consists mainly of super mature quartz sandstones, commonly known as the Table Mountain Sandstone (TMS). The TMS forms the mountain ranges in the Cape Fold Belt, and as such borders the Little Karoo valley to the north and south. The Bokkeveld Group is mainly argillaceous and is generally confined to the valleys of the Cape Fold Belt. The Witteberg Group consists of sandstones and shales.

The Cape Supergroup is of lower Palaeozoic age and the result of regional subsidence of a broad cratonic shelf with northward transgression of a marginal sea. Sedimentation progressed from shallow marine environments in the TMS to deltaic and shallow marine shelf conditions in the Bokkeveld and Witteberg. Sedimentation ended in a rather small basin due to sediment infilling and tectonic uplift in late Witteberg times. Although tectonism must have started in pre-Dwyka times, the main deformation of the Cape Supergroup did not start until after Dwyka sedimentation in the Karoo basin. Deformation started with the Swartberg folding, followed by Outeniqua folding, later folding of all pre-Beaufort age Karoo rocks with final uplift and horizontal tension. During this deformation, spanning almost 60 Ma, the Karoo basin to the north was supplied with material from both the Cape Supergroup and cratonic basement uncovered during tectonism. The subsequent rifting of Gondwanaland produced the graben structures in which the Cretaceous sediments collected.

The TMS is presently tapped for water supply to the Little Karoo, the tectonism having given rise to interbedding spaces, shear zones and joints, rendering the TMS an excellent aquifer. Recharge is fairly good in rainy years, due to the jointing and fracturing and large areas of mountainous outcrop, though storativity is deemed to be low. Due to the highly folded nature of the TMS, aquifer conditions can vary over relatively short distances. An example that can be cited is the results of pumping tests done during rehabilitation of the Dysselsdorp production field in 1996: Boreholes DP10 and DP27 are less than 10 m apart, yet DP27 had little response to pumping in DP10. On the other extreme, Borehole Television logging of borehole DP15 showed strong outflow at the bottom of the hole when the above mentioned boreholes were pumped. (Video 27, 1993)

#### 2.1.3 UITENHAGE GROUP

These late Jurassic to Cretaceous sediments were deposited in fault controlled basins after the completion of the Cape Orogeny (Söhnge and Hälbig). The Little Karoo basin developed by north-south extension and collapse faulting with sediment influx from the north, south and west. The mechanism is best explained by the major faults having a listric shape in depth: Extension of the region have thus resulted in thin-skin normal faulting, forming half-grabens and a relatively shallow east-west depression instead of a wide basin. The Uitenhage Group is divided into the Enon, Kirkwood and Buffelskloof Formations. The basal Enon Formation contains TMS fragments and is seen as a braided stream deposit, being an alluvial fan conglomerate transported from the south. This is followed by alluvial-plain sandstones and playa lake mudstones of the Kirkwood Formation. At the northern edge of the basin continued fault movement and unroofing of the pre-Cape Cango rocks led to southward spreading debris flows (Buffelskloof Formation). The whole succession is historically indicated to dip consistently northwards at up to 24° and was previously referred to as the Enon, differentiated into the Lower Enon conglomerate, Small-pebble conglomerate, Enon sandstone and Upper Enon red beds. The initial idea that the sedimentary wedge attains a thickness of around 3500 m at the Cango fault persisted in publications as late as 1999 (Tankard et al, Meyer), despite evidence to the contrary (Kleywelt (1972), Duvenhage (1992)) - this thickness is derived by the usual geological cross-section interpolation of a constant dip over a given distance to result in a certain thickness. The interpretation given by Kleywelt (1972) is of repeated step faulting and rotation of blocks to achieve a constant northward dip. (Measurements of bedding plane dips in this study refute this idea.) This interpretation implies a relatively thin succession of Uitenhage material, tilted after deposition to the attitude seen today, with renewed movement along the existing bedrock faults to explain the steps seen in the floor by geophysical investigations. Due to the extensive post-Cretaceous cover of alluvium and sediment, field mapping is difficult, and detailed, high resolution geophysical surveys with extensive drilling seem to be the only way to resolve the issue. No Uitenhage rocks are reported to the north of the Cango fault, seeming to indicate that the basin was probably about the size preserved today. Inspection of the topographic maps of the area indicates that there are places where the Uitenhage rocks lie at higher elevation than some of the rocks to the north of the Cango fault line, and outcrops at the southern and northern margins reach elevations of 400 m above the present valley: Cretaceous cover could have extended north of the fault line, subsequently being removed by extensive erosion. This is discussed further in the section on the structural investigations.

#### 2.1.4 TERTIARY SEDIMENTS

Large areas of the basin are covered with calcrete and mid- to late Tertiary gravel of unknown provenance. This gravel was probably derived from the exposed Cape rocks and reworking of the Uitenhage sediments. The amount of deposition and erosion after the Cretaceous period is unknown, but evidence of extensive erosion of the Cretaceous rocks exists near the Dysselsdorp water purification plant where remnants of Uitenhage material is present on TMS in a side valley above the present basin surface. In this area Uitenhage rocks outcrop high above the valley. The lack of Uitenhage material, whether consolidated or eroded, in the rugged topography to the north of the Cango fault was in the past taken to indicate that these sediments probably never occurred there, and that the fault remained active throughout the deposition of the Uitenhage Group. Block faulting and rotation of the Uitenhage group as postulated

by Kleywegt will also cause widespread erosion, giving rise to the extensive alluvium cover. Continued tectonics and uplift due to isostatic compensation for the Swartberg mountain range could have induced erosion of all Cretaceous material from the area north of the Cango fault. The presence of the Tertiary cover precludes detailed mapping of large parts of the basin itself, but many exposed outcrops are suitable for investigation.

## 2.2 GEOPHYSICAL INFORMATION

A relative wealth of information exists due to the early oil exploration programs. The surveys include reflection and refraction seismics, gravity observations and deep electrical resistivity soundings covering the valley. A set of 77 deep Schlumberger soundings were done by the CSIR in 1968 as part of a SOEKOR exploration study (Figure 2). Kleywegt published a paper on a gravity survey across the basin, also mentioning seismic studies, but no reference to the seismic work is given.

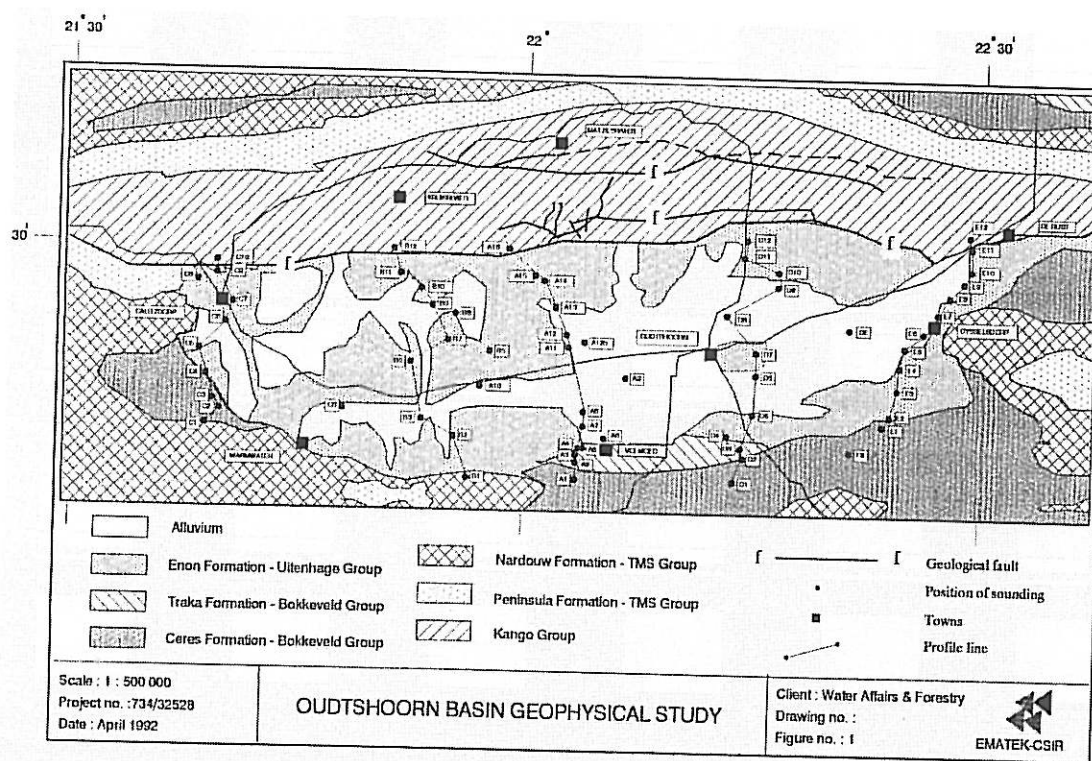


**Figure 2** Simplified geology map showing the positions of the deep resistivity soundings carried out by the CSIR. (From CSIR report EMA-C 92023)

The late sixties studies concentrated on the Cretaceous itself, and with newer ideas about the structure of the basin the deep electrical soundings were reinterpreted by the CSIR during 1992: Emphasis was placed on the later part of the sounding curve to evaluate the feasibility of locating faults in the floor rocks beneath the Cretaceous cover. The following areas were identified for further evaluation: Shallow sub-crops of TMS, fault zones within the TMS and the identification of the Cango fault in areas where the fault is not well documented. Further electric and time domain electromagnetic soundings and profiles

were done on three of these targets. Several faults in the floor rocks were identified and exploration borehole positions indicated.

The resistivity character of the various formations is shown in Table 1. From Table 1 it is clear that considerable overlap in the interpreted resistivities of the various formations exist, with a well-defined contrast between the TMS and Uitenhage/Bokkeveld rocks. Identifying fault contacts between the TMS and the Uitenhage/Bokkeveld is feasible, but at greater depths resolution is a problem and exact positioning of faults becomes risky. The pseudo-section of the CSIR profile B - B', approximating the position of the gravity Profile 1, is shown in Figure 3.

**Table 1:** Resistivities of lithologies in the study area (Duvenhage and Meyer)

Lithology	Resistivity range (ohm.m)
Alluvium	5 - 1 000
Uitenhage	10 - 110
Bokkeveld	10 - 150
TMS	200 - 12 000
Cango	1 000 - 5 000

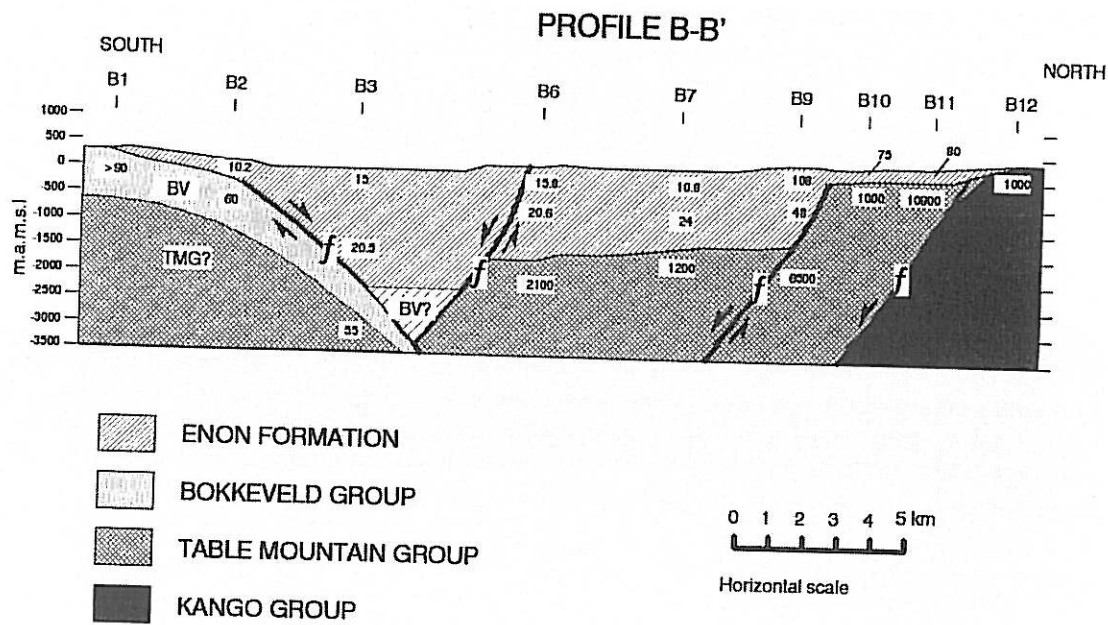


**Figure 3** The interpretation given by the CSIR for the deep sounding data along their Profile B - B'. (From CSIR report EMA-C 92023)

The earlier gravity survey (Kleywegt) was done along a profile with station spacing in the order of 132 m inside the basin and 1000m outside the basin. The resulting gravity profile is shown in Figure 4. Modelling of the residual gravity resulted in a cross section with pronounced steps in the thickness of the Uitenhage rocks (Figure 5). This was interpreted as normal faulting in the floor leading to half-graben type structures and block rotation. A result of this study was to put a limit on the maximum depth of the Cretaceous basin (2000 m), this maximum depth being attained in the middle of the basin and not against the Cango fault as previously presumed. The perception of the geologically interpolated depth of 3 000 - 4 500 m against the Cango fault still persists though ( Meyer, 1999, DWAF 1:500 000 geohydrological series). The structural model proposed by Kleywegt is shown in Figure 6.

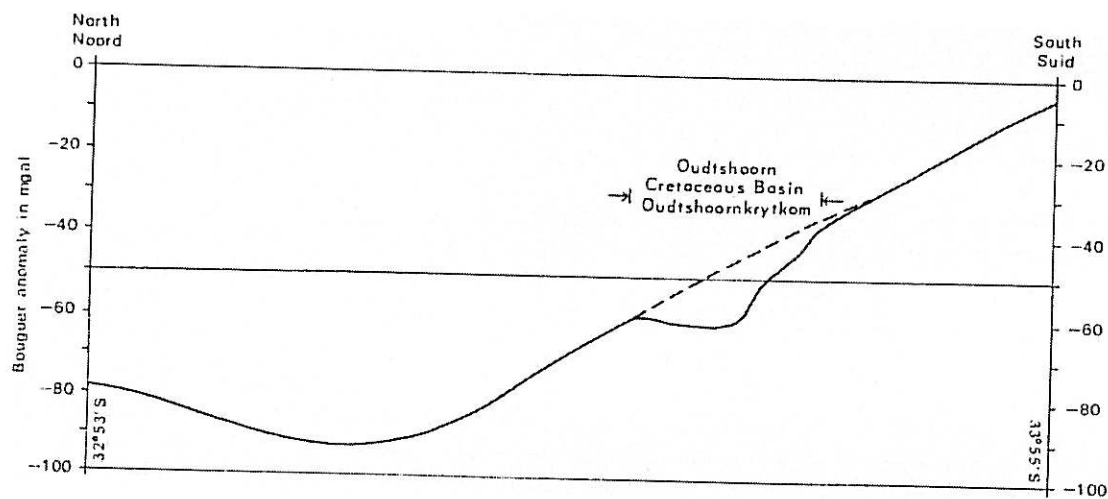


**Figure 4** Regional gravity profile of data as presented by Kleywegt. Note the size of the anomaly ascribed to the Cretaceous rocks in the Little Karoo basin. (From Kleywegt: 1972)

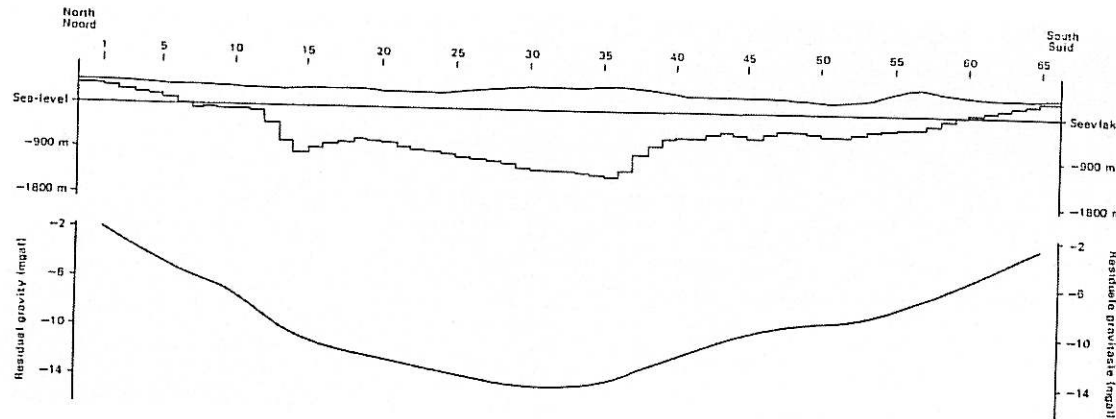


**Figure 5**

Model of the residual gravity anomaly caused by the Cretaceous rocks along the gravity profile of Kleywegt. Note the uneven basement floor, and the shape of the floor. (From Kleywegt: 1972)

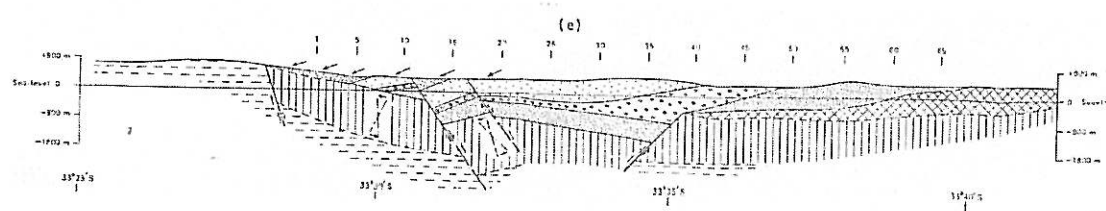


**Figure 6**

The structure of the Little Karoo Cretaceous basin as envisaged by Kleywegt. (From Kleywegt: 1972)

### 3. GEOPHYSICAL FIELDWORK

### 3.1 SITE SELECTION

It was decided to carry out a gravity survey along a traverse previously covered by electric soundings. The gravity survey carried out by Kleywegt was along a profile to the east of Oudtshoorn, and it was thus decided to do a South-North profile between Calitzdorp and Oudtshoorn. The position of this profile is shown in Figure 7 as Profile 1. The data was collected along a road from south to north, and the profile extended to the north to cross the Cango fault. The profile could initially not be extended to the south to reach the TMS outcrops, due to flooding damage to the roads in 1997, but during the 2002 fieldwork the profile was extended southwards to Bokkeveld outcrops close to the TMS. The gravity profile approximates the position of profile B - B' in the CSIR report on the reinterpretation of the electrical soundings (Figure 2), and is reproduced in Figure 8. To investigate the possibility of a south-north striking fault forming the western boundary of the basin, two short west-east profiles (Profile 2, Profile 3) were surveyed south of Calitzdorp during the 2002 fieldwork (Figure 7).

### 3.2 DATA COLLECTION

Stations in the 1997 survey were pegged at 200 m intervals, and relative elevations were obtained by levelling, using the first station as a base with an assigned elevation of 258 m. Gravity data were collected with a SCINTREX CG-3 automated gravity meter, with a resolution of 0.005 mgal. Prior to commencing data collection a stabilising period of two days was allowed, during which instrument sensor drift was checked and corrected. The first station was used as a base, and work was started and ended each day by taking a reading at this station. A close control on residual instrument drift was thus obtained.

The follow-up work in 2002 also utilised the Scintrex CG-3, with station spacing of around 100 m for the Profile 1 extension, and 15 m for Profiles 2 and 3. Profile 1 was extended to the south to cross Bokkeveld outcrops close to the Rooiberg TMS outcrops. This extension resulted in a gravity profile crossing the entire Cretaceous basin from south to north. The Profiles 2 and 3 were chosen to start on TMS outcrops at the western edge of the basin, continuing east to end on Cretaceous material. Time constraints precluded longer profiles in this area: data acquisition would have to be extended on foot with no existing roads or paths. This was determined to be a limiting factor to the usefulness of the profiles during the modelling phase.

During the 2002 survey a SOKKIA differential GPS system was used to obtain true coordinate as well as elevation data. Gravity and GPS work included an overlap between the 1997 and 2002 sections of Profile 1, to enable the coordinate and elevation data of the 1997 survey to be tied with the 2002 survey.

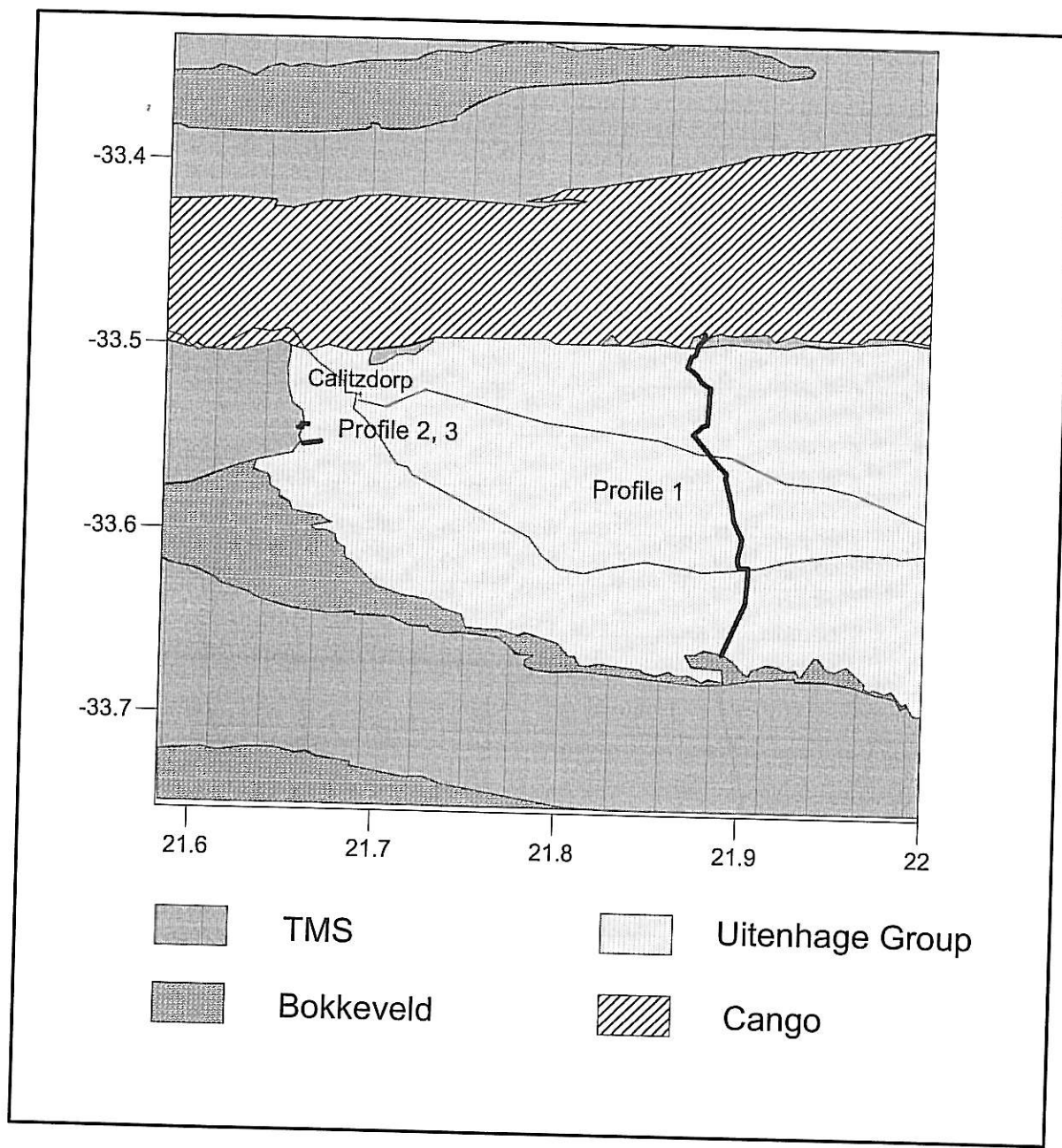


**Figure 7** Position of the gravity profiles done in 1997 and 2002. Profile 1 follows the general trend of the Profile B – B' of the CSIR resistivity soundings. (Refer Figures 1 and 2)

#### 4. DATA REDUCTION

The gravity data were dumped from the instrument to a laptop computer and imported into a spreadsheet program to do residual instrument drift corrections and reduction to relative Bouguer values. The gravity meter has software that compensate for diurnal variations due to earth tides as well as for sensor drift. Residual instrument drift is linear and can be removed on a time basis using the repeated readings at the base station. The drift corrected observed gravity values were adjusted for the effects of latitude and elevation variations along the profile to obtain relative Bouguer values:

- The rotation of the earth and the resulting equatorial bulge produce an increase of gravity with latitude. To compensate for this effect, latitude corrections were carried out on the data according to the formula  $8.17 \times 10^{-4} \sin(2\Phi) \text{ mgal.m}^{-1}$  where  $\Phi$  is the latitude of the study area. In this instance the reference latitude for Profile 1 was chosen around the centre of the 1997 part of the profile and corrections carried out relative to the zero station on Profile 1. The reference latitude was taken as  $33,55^\circ$  and the correction amounts to  $7,525 \times 10^{-4} \text{ mgal.m}^{-1}$ , this value being added/subtracted to every station gravity value according to its absolute distance north or south of the zero station. Although this correction is linear only over distances of less than 2 km, the effect of using only the one reference latitude is a slight regional trend, which in this case is negligible: The correction at the zero station latitude is  $7,532 \times 10^{-4} \text{ mgal.m}^{-1}$  and the correction at the last station latitude is  $7,519 \times 10^{-4} \text{ mgal.m}^{-1}$ . Over the 16 km profile surveyed in 1997 an error of 0,02 mgal would result, well within the relative accuracy of the survey itself. To ensure compatibility with the 1997 survey data the 2002 data as used in this report was also reduced according to the above description.
- Gravity varies inversely with the square of the distance from the earth's centre of mass, and it is therefore necessary to compensate for differences in elevations between stations. This correction is the free air correction and has the value of  $-0,3085 \text{ mgal.m}^{-1}$ . This correction is added to the observed data when the station is above the reference plane, and *vice versa*. The reference plane in this case was chosen as the zero station elevation on Profile 1.
- The free air correction does not take the gravitational effect of material between the reference and station planes into account. To compensate for this material the Bouguer correction is carried out. This correction assumes that the material between the stations is a slab of infinite horizontal extent with thickness equal to the elevation difference between the stations. This correction amounts to  $0,04188 \sigma \text{ mgal.m}^{-1}$ , where  $\sigma$  is the density of the material in  $\text{g.cm}^{-3}$ . This correction is subtracted when the station is above the datum plane, since the extra material has a positive gravity effect on the sensor.

For the study area a Bouguer density of  $2,3 \text{ g.cm}^{-3}$  was chosen, this being representative of the Uitenhage rocks. Tables 2 and 3 show the mean densities for rocks in the Oudtshoorn region.

**Table 2:** Cretaceous rock density values (from P.J. Smit)

Lithology	No. of samples	Range of density values ( $\text{g.cm}^{-3}$ )	Mean value ( $\text{g.cm}^{-3}$ )
Shale	4	2,28 – 2,31	2,30
Sandstone	8	2,12 – 2,47	2,27
Sandstone	18	2,13 – 2,52	2,34
Conglomerate	7	2,20 – 2,54	2,41

The data of the 1997 and 2002 surveys were adjusted to the same gravitation level. In the case of Profile 1 a smooth profile resulted. Note that the 2002 surveys did not use the same base for the gravity survey, but the tie-in work done with the profiles 2 and 3 enabled the data to be reduced to the same level.

The reduced gravity values are listed in Appendix A. Figures 8, 9 and 10 shows the reduced profiles, with the elevation trends.

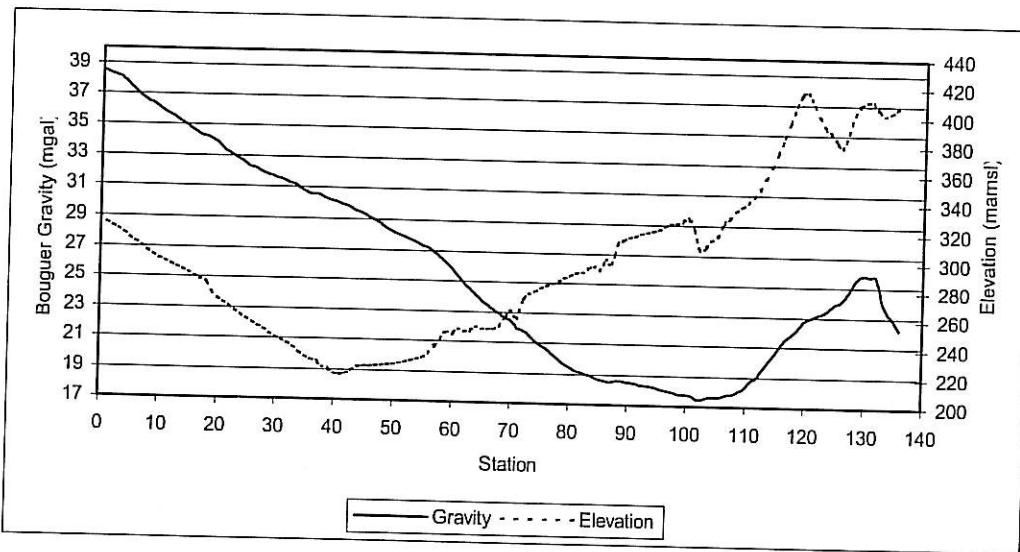


**Figure 8** Reduced Bouguer gravity values and relative elevations of stations for Profile 1. Bouguer density  $2,3 \text{ g} \cdot \text{cm}^{-3}$ , reference latitude  $33,55^\circ$ , elevation values meters above sea level.

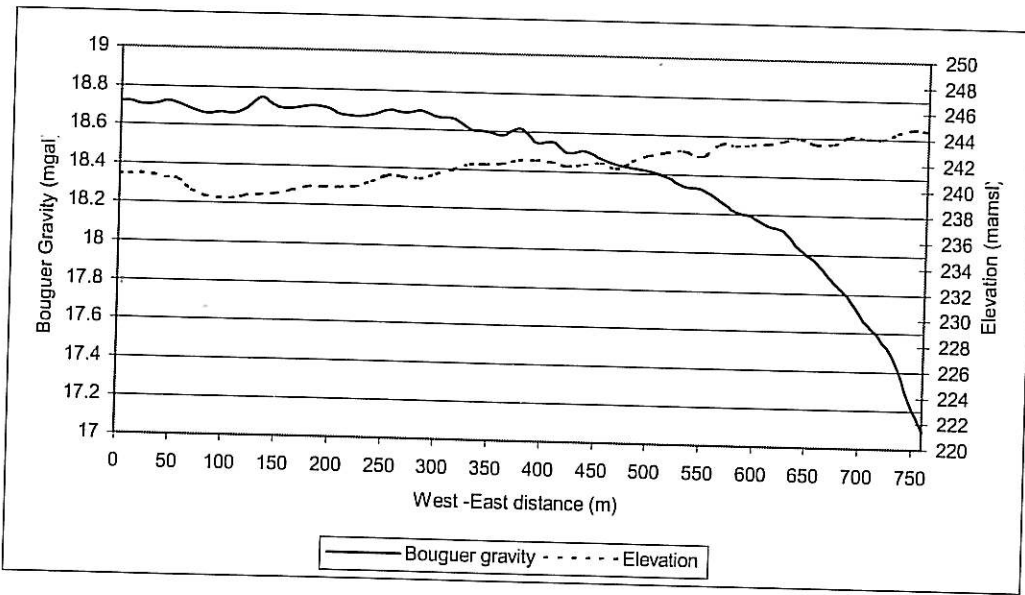


**Figure 9** Reduced Bouguer Gravity for Profile 2

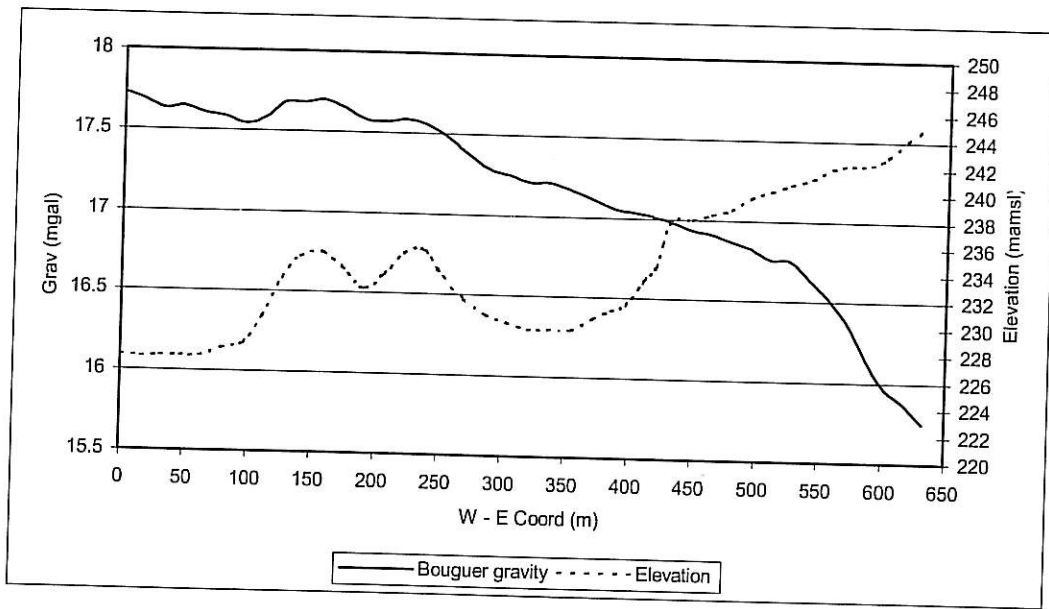


**Figure 10** Reduced Bouguer gravity for Profile 3

## 5. GRAVITY DATA INTERPRETATION AND MODEL

### 5.1 PROFILE 1

Profile 1 (Figure 8) closely approximates the results of Kleywelt (Figure 4), indicating that the basin structure is similar across its length. It is clear that the maximum gravity anomaly is not at the Cango fault (located around station 131, Figure 8) as the constant bedding dip model would suggest. In order to eliminate effects due to the winding of the profile, Figure 11 shows the gravity values plotted against true south - north distance for each station. Note that the resistivity pseudo-section from the CSIR report was not corrected for deviations in profile direction, so that the distance shown is not the true south - north distance, but rather the distances between the actual stations. Also note that the CSIR locality map only shows the old road between Calitzdorp and Oudtshoorn. The co-ordinates of the sounding positions are not known, leading to uncertainty in the positioning of the soundings relative to the gravity profile.

Two features are readily apparent on the Bouguer gravity profile (Figure 8):

1. The profile has a broad low gravity anomaly with peak around Station 102, this being caused by the lower density Uitenhage rocks.
2. At the position of the Cango fault (Station 131) a positive peak is present, followed immediately by a downward trend. This would seem to indicate a slice of higher density material present at the fault, with lower density material directly to the north.

Inspection of the Kleywelt profile as published indicates the same trend over the Cretaceous basin with a pronounced negative regional trend from south to north. Thus part of the gravitational drop-off north of the Cango fault can be accounted for by the regional trend.

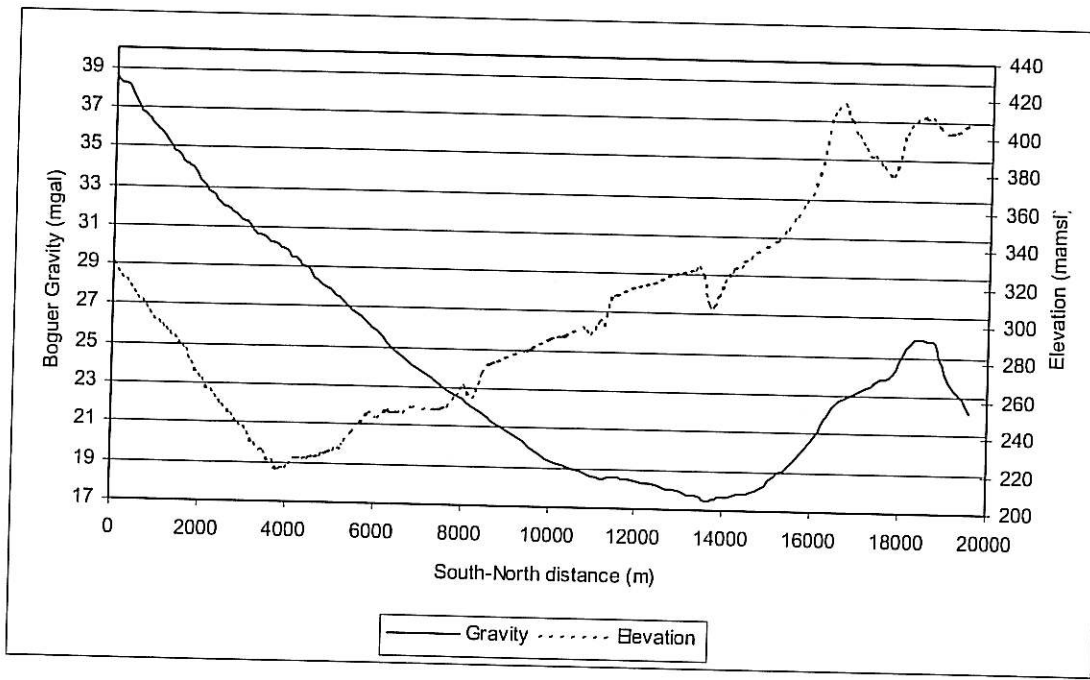


**Figure 11** Profile 1 Bouguer gravity and elevation values plotted against true south-north distance.

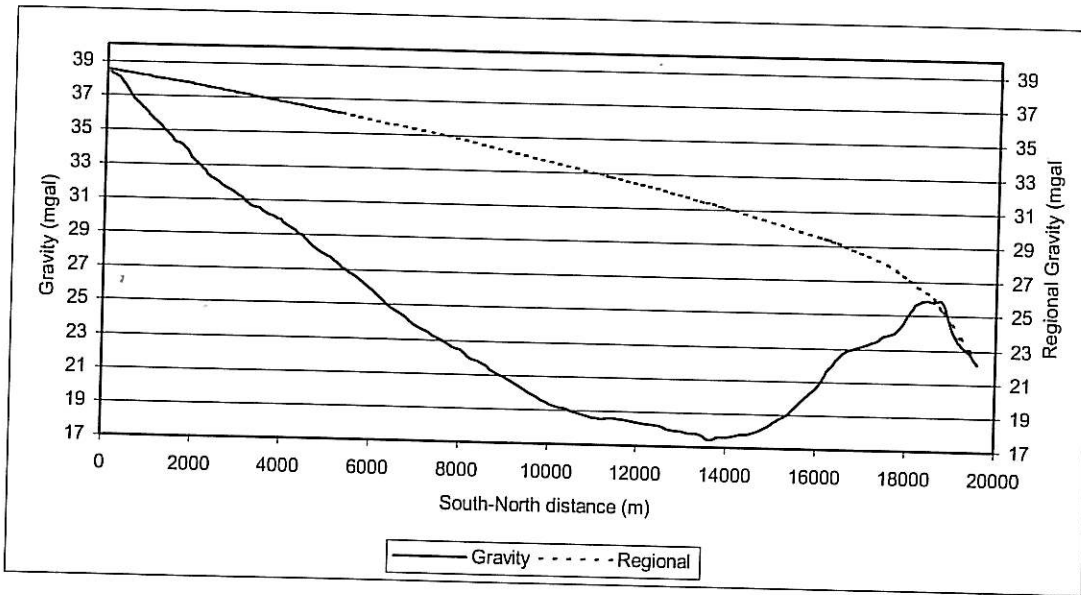


**Figure 12** Profile 1 Bouguer gravity shown alongside the interpolated regional gravity field. X-axis is plotted for true south-north distance. (Regional field interpolated from the 1997 Gravity Edition of the 1 : 1 000 000 scale geological map of South Africa.)

The regional gravity trend in the present study area was obtained from the 1997 edition of the 1:1 000 000 scale geological map of South Africa. It must be noted here that regional gravity data points in the northern part of the study area are sparse and the relevant map does not include the gravity work by Kleywegt. The residual gravity values presented here might therefore not be absolutely right. Choice of the regional trend is based on the assumption that Cape and Cango rocks form the basement of the basin, and therefore all gravity readings on these rocks must represent background or regional values (residual gravity = 0). The regional field is then interpolated between these points across the Cretaceous basin, aiming for a smooth curve. This trend is shown in Figure 12. The residual gravity values (Bouguer gravity - regional gravity) are plotted in Figure 13.

The residual gravity profile (Figure 13) indicates maximum thickness of the Cretaceous rocks in the region of station 11 000, with a gradual decrease in depth to the south, and a steep floor profile to the north. This steep floor slope would seem to indicate a normal fault situated around station 16 000.

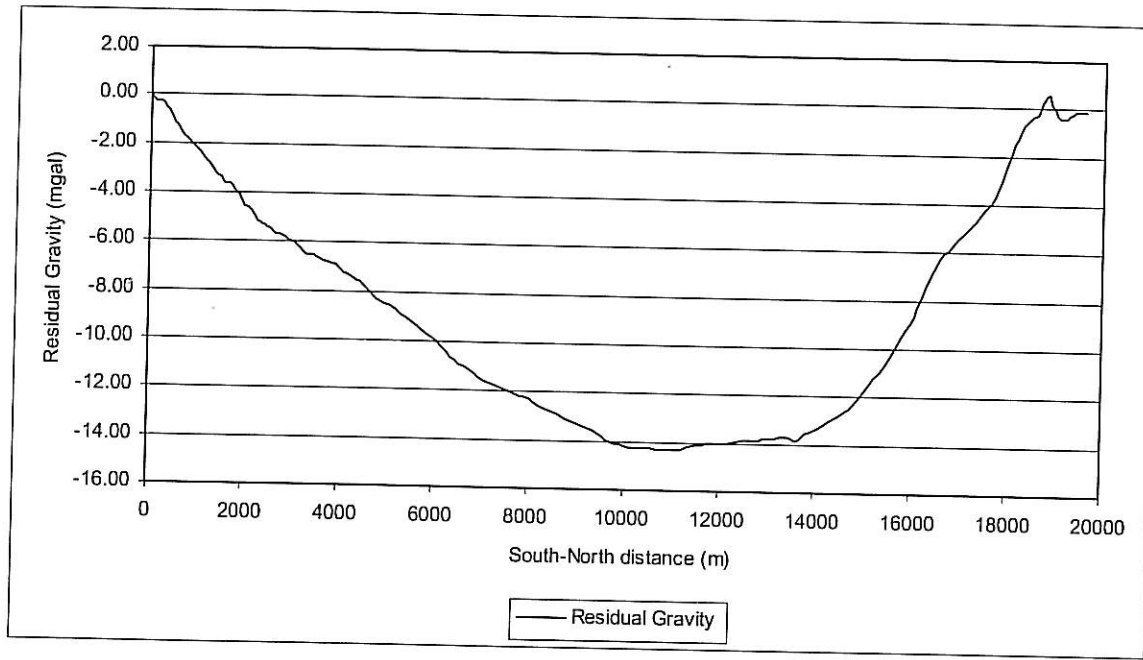


**Figure 13** Residual gravity values along Profile 1, plotted against true south-north distance.

The residual gravity values were modelled in the two-dimensional modelling software package *MAGIXXL*, using densities as published by Smit and Maree (Table 2, Table 3) as guide. The results of the CSIR resistivity interpretation were used for the starter model, and a simple model of Cretaceous sediments over TMS basement was set up. This model assumes a uniform floor rock type and density. The gravity model requires a slice of higher density material at the Cango Fault in order to fit the theoretical curve with the residual gravity. The shape of the Bouguer curve supports the existence of a higher density zone in this region. The first model (KK2) was set up using a density contrast of  $-0,27 \text{ g.cm}^{-3}$  between the Uitenhage and Cape rocks. This means that the average densities used are  $2,35 \text{ g.cm}^{-3}$  for the Uitenhage Rocks and  $2,62 \text{ g.cm}^{-3}$  for the TMS. A slice of higher density material was inserted at the inferred position of the Cango Fault, at the contact of the Cretaceous material and the TMS outcrops at the northern end of the profile. This density was chosen as  $4,5 \text{ g.cm}^{-3}$  (density contrast  $+1,88 \text{ g.cm}^{-3}$ ), and this material is interpreted to represent sulphide mineralisation along the fault plane. Results of exploration drilling in the Schoemanshoek area north of Oudtshoorn (Whittingham, GH 1501) indicated disseminated sulphides and pyrite cubes along a possible fault plane. At Toorwaterpoort a hot spring has resulted in thick deposits of manganese downslope from the spring, and inspection of Swartberg Fault outcrops reveal manganese nodules and -mineralisation along the fault plane. This mineralisation would add to a positive gravity anomaly in the fault area. The resulting model, obtained by inverse modelling of the residual gravity values, follows the same trend as the resistivity model, and is shown in Figure 14. As can be seen from the gravity model (Figure 14), a maximum thickness of 1500 m for the Cretaceous rocks is indicated at around station 10 000. The model derived by Kleywegt (Figure 5) follows the same trend, although the shallow area to the south of the Cango fault is wider. (Note that the model geometry will depend on the density contrast used. The contrast used is an estimate only, due to the lack of physical sample data from the profile area.)

**Table 3:** Density values of the pre-Cretaceous rocks in the study area (from P.J. Smit)

Lithology type	No. of samples	Range of density values (g.cm <sup>-3</sup> )	Mean value (g.cm <sup>-3</sup> )
Bokkeveld shale	3	2,66 - 2,67	2,67
Bokkeveld shale (borehole core)	8	2,72 - 2,74	2,73
Table Mountain Sandstone	22	2,54 - 2,66	2,64
Table Mountain Sandstone (Riversdale)	7	2,60 - 2,62	2,61
Cango Formation			2,86
Shale*	4	2,48 - 2,52	2,50
Sandstone*	8	2,66 - 3,02	2,74
Dolomite*	3	2,69 - 2,70	2,69
Limestone-schist*	4	2,72 - 2,79	2,75

\* These rocks were listed under "Malmesbury Formation", Oudtshoorn. It is possible that at the time of the determinations (1939 - 1948) some of the Cango Group rocks were still classified as belonging to the Malmesbury Group. These determinations are taken to mean Cango Rocks, since they refer to the Oudtshoorn locality as opposed to Cape Town for the Malmesbury hornfels mentioned by Smit and Maree. Note that the mean density given for the Cango is not concomitant with the rock densities listed.

A second model (KK1) was set up using the densities as published in the article by Kleywegt (density contrast -0,24 g.cm<sup>-3</sup>). A maximum depth of 1800 m for the basin results from this model, the same as found by Kleywegt on his profile. The model clearly indicates the half-graben structure of the basin, with down-throw to the south along synthetic faults, with associated antithetic faults in the southern part of the basin (Figure 15). Figure 16 shows the geological interpretation for these models. From the density determinations it is clear that the assumption of constant density for both the floor and basin is rather simplistic, and for a more accurate model varying densities will need to be built into the model. This is however not practical since the exact structure and composition of the floor and Cretaceous sediments are not known.

Both these models deviate from the depths obtained by the CSIR models for the study area. The depths obtained in the CSIR models (up to 2300 m) can only be replicated when a density contrast of -0,22 g.cm<sup>-3</sup> is used. The other mismatch between the gravity and resistivity models is the position of the faults. On the gravity model they are displaced to the north relative to the positions in the resistivity model.

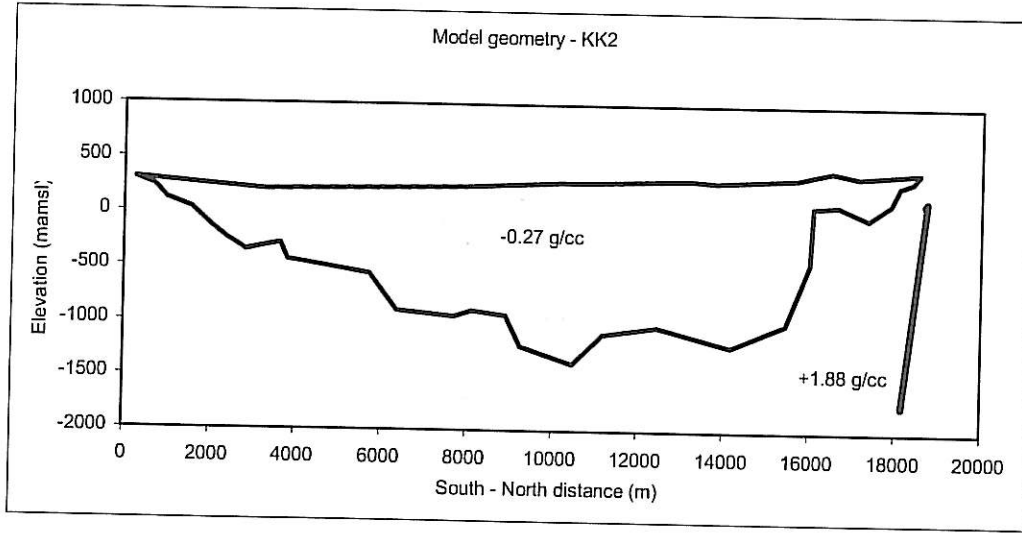
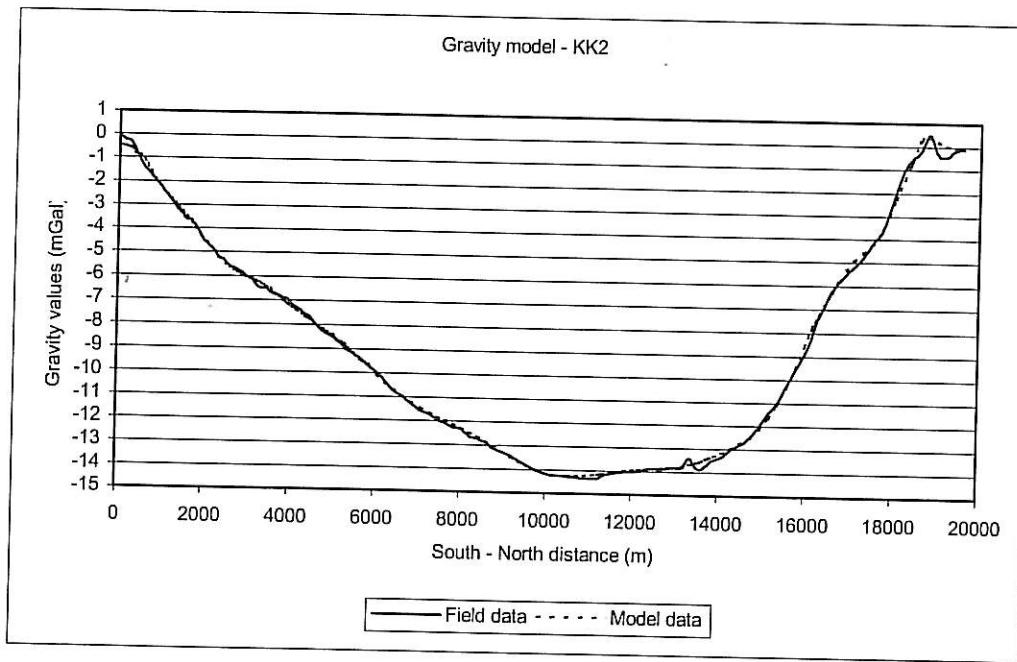


**Figure 14** Gravity model of the basin, using densities as published by Smit and Maree as starting guide. Vertical scale exaggerated.

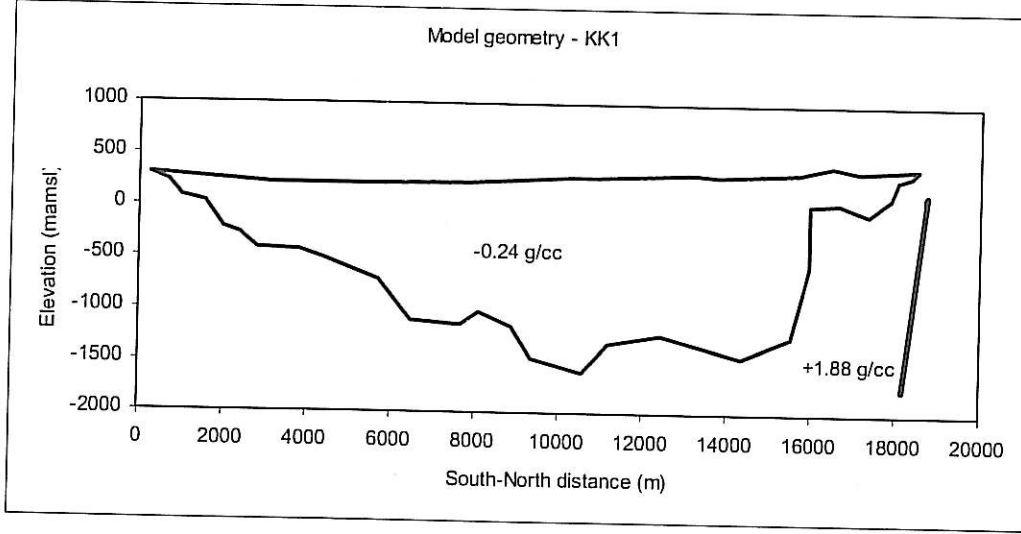
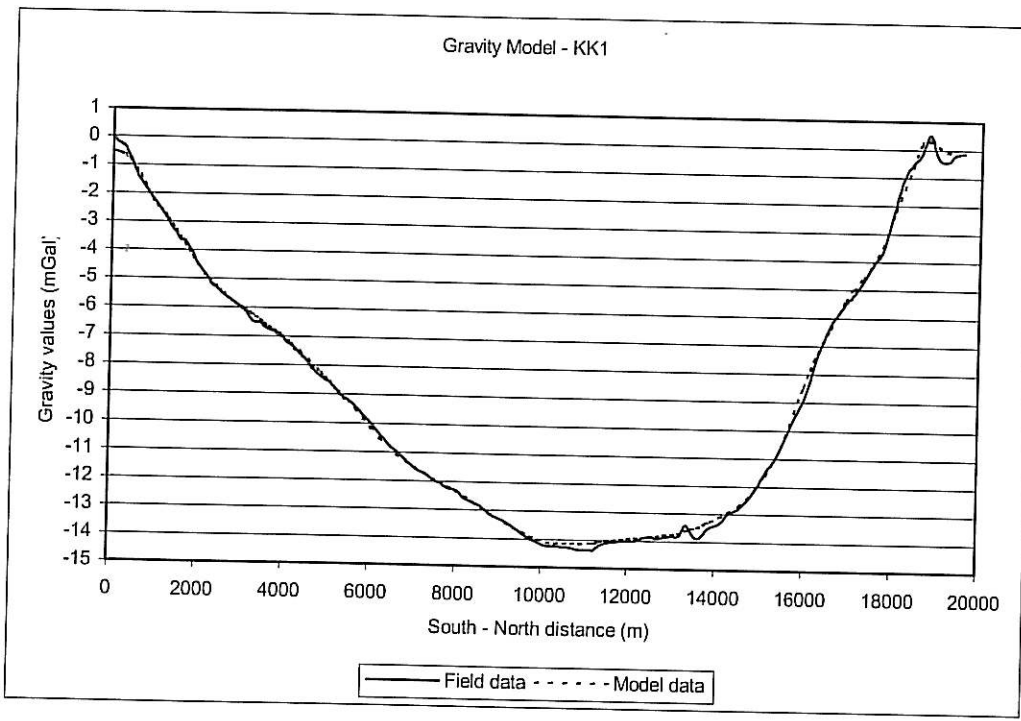


**Figure 15** Gravity model of the basin using densities from the Kleywegt report. Vertical scale exaggerated.

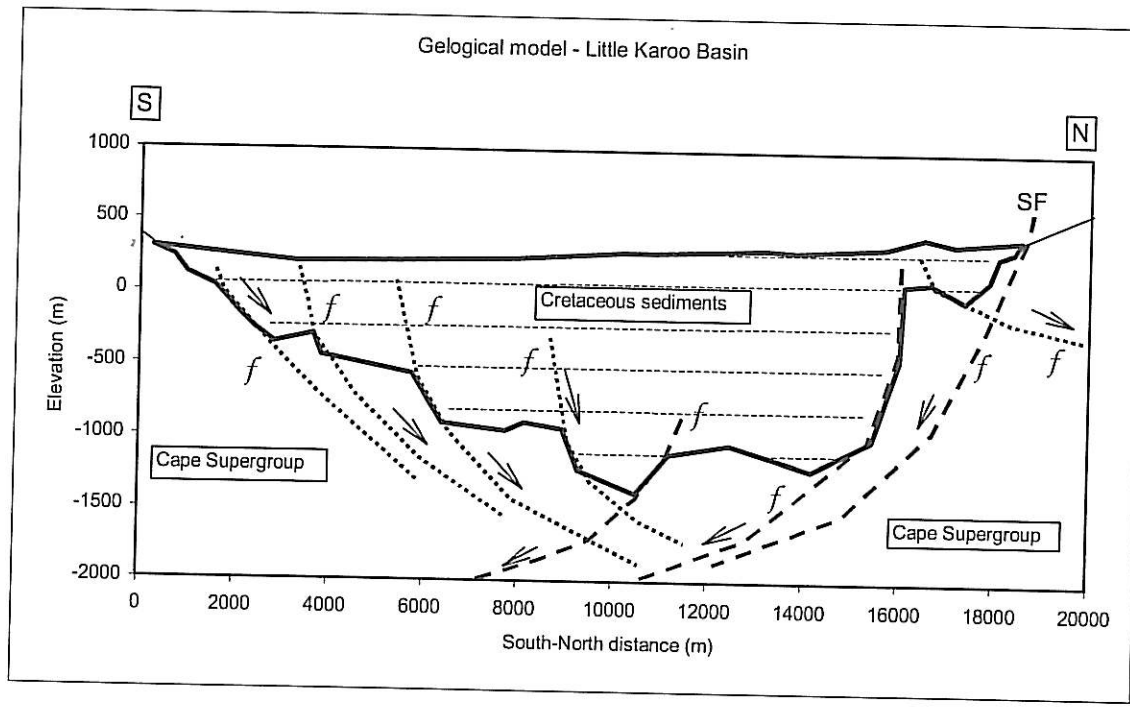


**Figure 16** Proposed geological model of the basin along the Profile 1. Vertical scale exaggerated. Sulphide mineralisation on Swartberg (Cango) fault (SF) not shown. Model geometry: KK2

## 5.2 PROFILES 2 AND 3

These profiles are oriented west-east, and were done in order to investigate the possible existence of a North-South trending normal fault terminating the western edge of the Cretaceous basin. The reduced data for Profiles 2 and 3 are given in Appendix A and are shown in Figures 17 and 18.

Modelling of the profiles however indicated that the data profiles are too short, and further work is required in this area. Due to insufficient data extent to the east, the models are quite simple, serving only as a rough indication of the possible floor geometry. Therefore the chosen regional is flat, to simulate the parallel-to-strike profile trend, and elevation data is not taken into account. In order to enable modelling, more data points were added to the east, but these data are estimates following the general basin trend only. On the model plots it will be noticed that the bulk of the model lies to the east of the available field data, but this is to be expected: The basin's influence on the regional gravity topography will result in depressed gravity values outside the basin margins. The models shown best follow the field data shape. The models are of little real value, and are presented in Figures 19 and 20. Inspection of the data profiles however shows a sharp decrease in gravity values near the end of the profiles, as would be expected if a normal fault with large down-throw to the east exists. The conceptual models (KK3 and KK4) indicate the possible existence of a listric-shaped normal fault with initial dip of  $74^\circ$ . Sediments of the Kirkwood formation west of Calitzdorp dips  $30^\circ$  in an easterly direction (refer to the section on structural geology), possibly indicating that the proposed fault was active until post-Cretaceous times.

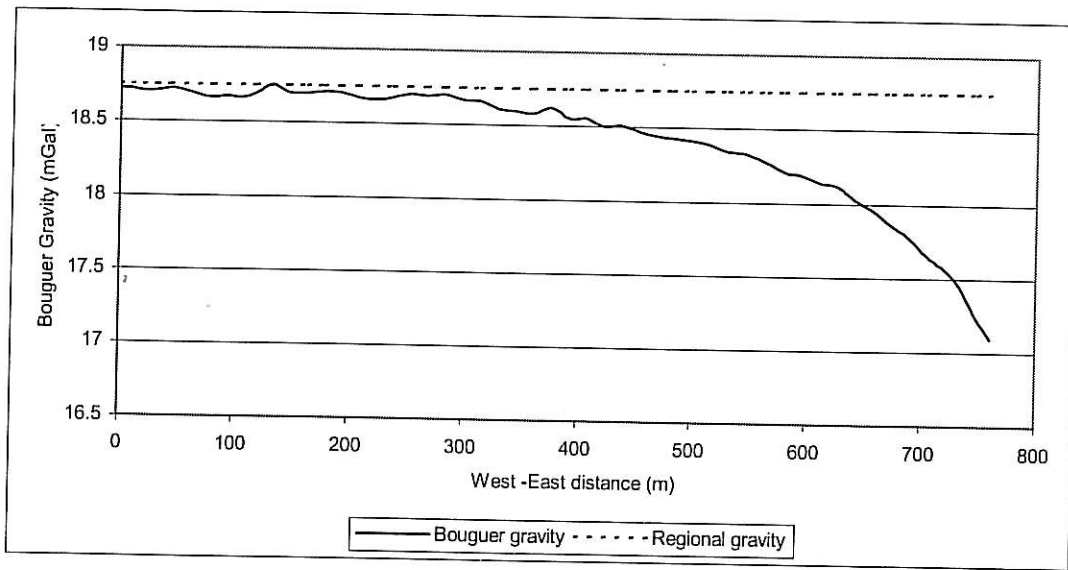


**Figure 17** Gravity values along Profile 2.

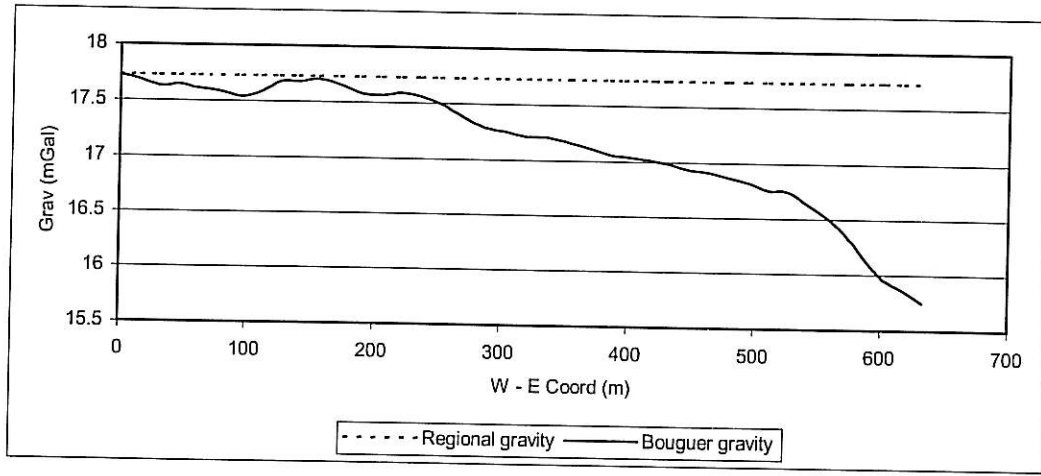


**Figure 18** Gravity values along Profile 3.

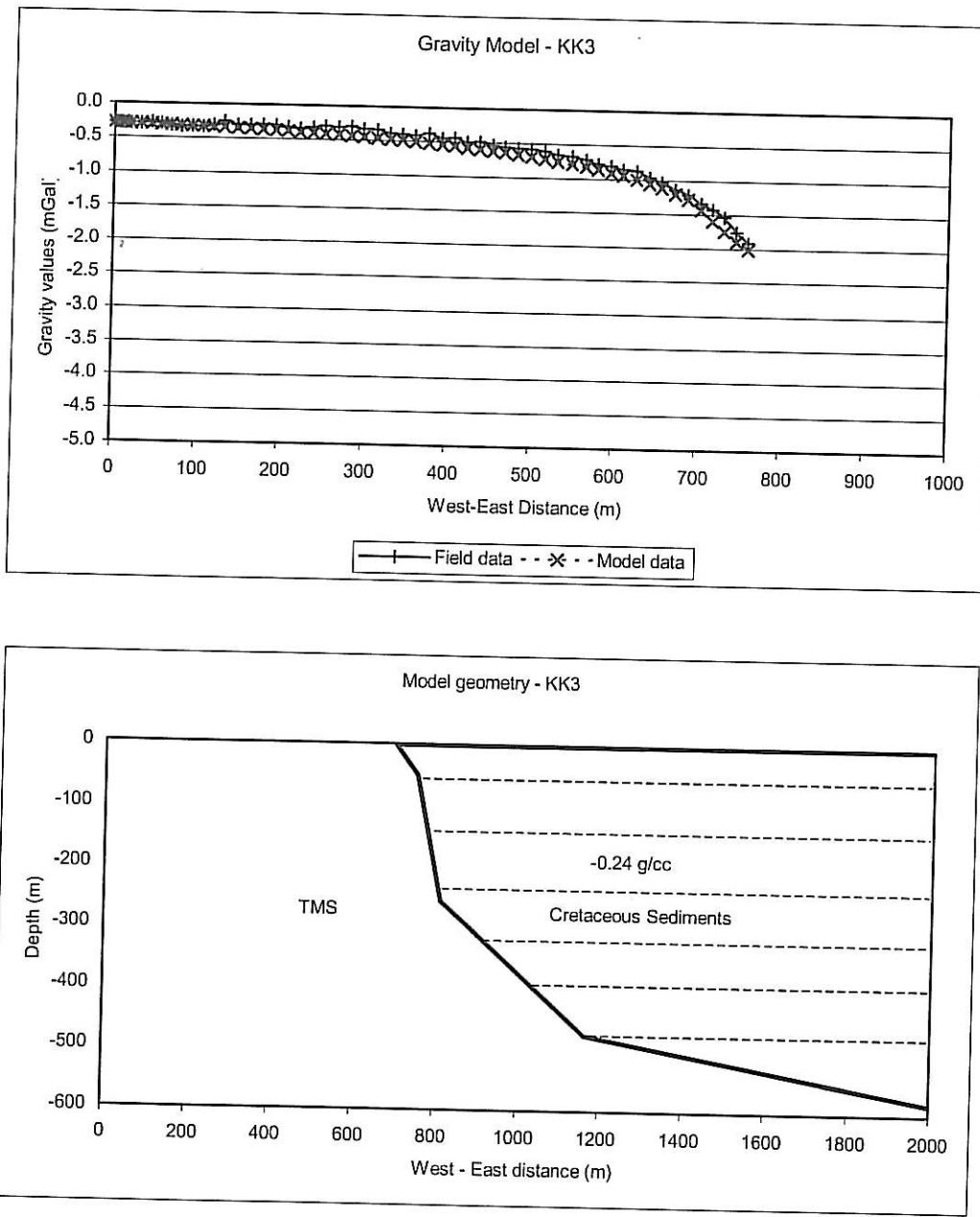


**Figure 19** Gravity model along Profile 2

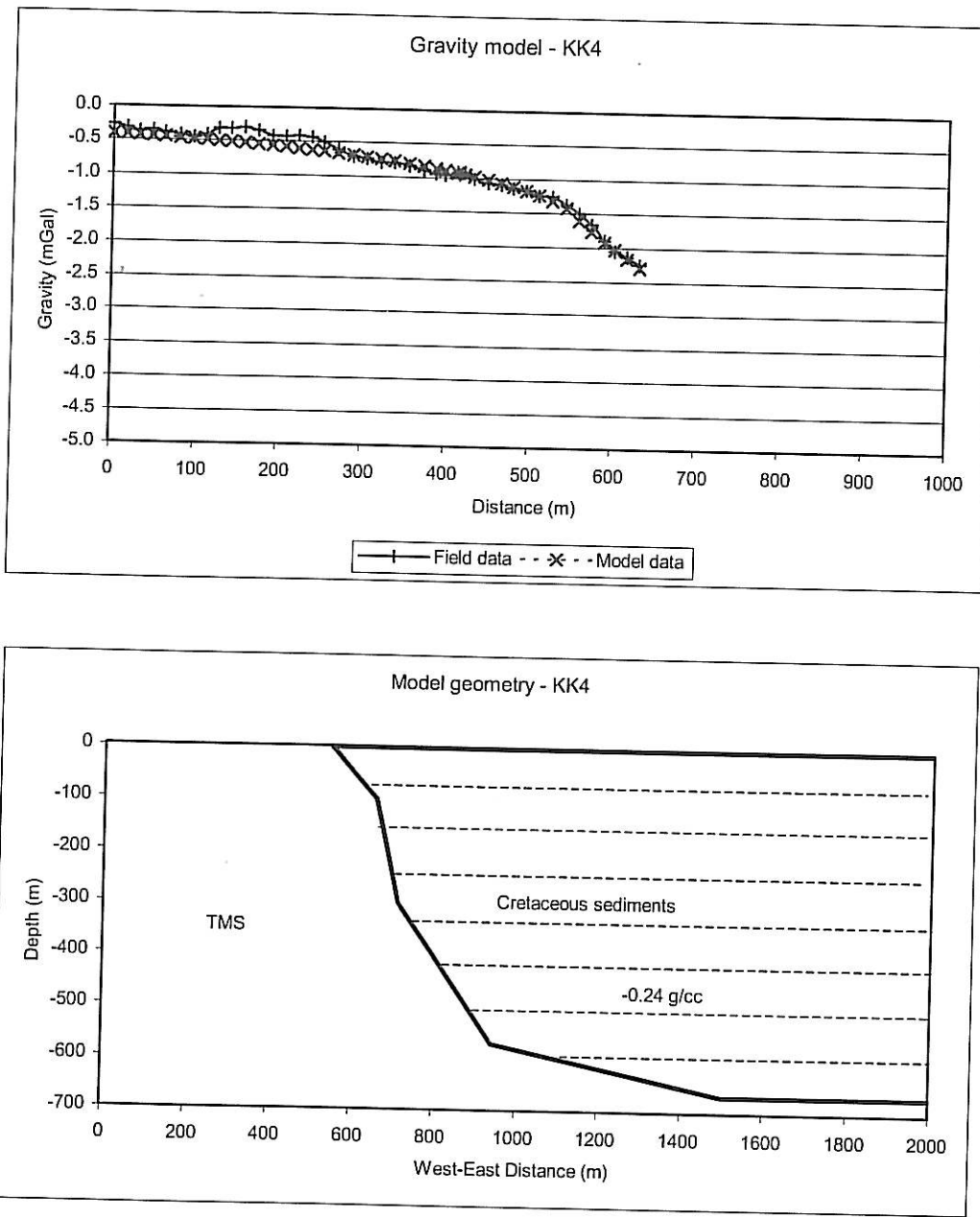


**Figure 20** Gravity model along Profile 3

### 5.3 SENSITIVITY OF THE GRAVITY METHOD FOR THIS SURVEY TYPE

In order to test the sensitivity of the gravity method in determining the position of the faults, synthetic models were used. In these models the fault position and dip was varied and compared to a base model response, and the difference between the gravity values were plotted. These models are shown in Appendix C. A base model (Model 1, TST1) was set up to resemble the situation encountered in the Little Karoo: A fault dipping  $67^\circ$ , with a down-throw of 1 200 m and covered by 300 m of overburden was used (Figure C1, Appendix C).

The first comparison (TST2) involved moving the fault position by 100 m. Comparison with the base model indicates a maximum deviation of around 0,45 mgal between the calculated responses. Compared to the base model curve, a readily observable shift in the response curve can be seen (Figure C2, Appendix C).

The next comparison (TST3) involved increasing the fault dip to  $80^\circ$ . The difference between the base and test models amount to around 0,5 mgal, and the difference in curves is again readily apparent (Figure C3, Appendix C).

The last comparison (TST4) in this series involved reducing the fault dip to  $60^\circ$ . A difference of around 0,33 mgal results, with a readily apparent difference in response curves (Figure C4, Appendix C).

Figure C5, Appendix C shows the comparisons for the Model 1 test series.

A second base model (Model 2, TST10) was set up with a fault of 1 000 m throw, dipping  $63^\circ$ , beneath 1 000 m of cover (Figure C6, Appendix C). Shifting the fault by 100 m (TST11) resulted in a deviation of up to 0,2 mgal in the response curves, but this difference was not readily apparent on the curves (Figure C7, Appendix C). A shift of 200 m (TST13) does indicate a visual difference between the base and test model anomalies (Figure C8 Appendix C). Figure C9, Appendix C shows the comparisons for the Model 2 test series.

## 6. DISCUSSION OF GEOPHYSICAL WORK

The model results indicate that the broad structure of the basin can successfully be resolved with the gravity method. The correlation between the gravity and resistivity models is good insofar the general trend of the basin geometry is concerned, but certain crucial differences exist. The position of the major faults is one area of contention. The synthetic gravity models indicate beyond doubt that the gravity method would successfully delineate the position of a major fault below 300 m of overburden. The difference in positions must thus be ascribed to the resistivity models. One problem is the absence of sounding co-ordinates in the CSIR report, making the positioning of the resistivity data difficult. Also note that the resistivity pseudo-section is based on only nine soundings spread across the valley: It is not possible to exactly position structures with these sparse data. To successfully map the structure of the basin deep resistivity or controlled source audio-frequency magnetotelluric (CSAMT) profiling would need to be done, but the logistics of such an operation precludes a study of this nature as first option. Another problem with the electrical methods is the volume of earth sampled in each sounding: To penetrate to a depth of three km, a chunk of earth measuring several cubic kilometer are included in the sample. The assumption is made that the sample volume has uniform electrical characteristics, but inspection of the pseudo-section indicates that this is not so: Resistivities as modelled vary considerably, for example from 10,2 ohm.m to 108 ohm.m for the Cretaceous rocks. Bear in mind that the sample volume is a three-dimensional half-space, and not merely a two-dimensional vertical slice directly below the sounding position. The exact position of structures can easily be swamped in the large sample volume.

The sensitivity tests carried out for the gravity method indicate the theoretical ability to resolve the fault position and dip to within 100 m and  $10^\circ$  respectively in the first test series (300 m overburden to top of fault). The models however show that it would be impossible to distinguish between a position or dip

variation, if no prior knowledge of one of the two is available. The second test series clearly confirms that the gravitational effect diminishes with increased distance from the source (1000 m overburden to top of fault). Increased overburden thickness reduces sensitivity, and only in the ideal case of uniform basin and floor densities and true two-dimensional structures would it be possible to confidently locate faults beneath 1000m of overburden to within 300 m. In this respect it can be stated that the gravity method can delineate the structure of the basin with good accuracy, but not accurately enough to enable the siting of deep boreholes to intersect fault planes at predetermined depths. The gravity method also "samples" a rather large volume of earth, but it is the recommended method for fast mapping of the basin structure: Profiles can easily and speedily be done along existing roads, data density will be good and such a regional survey will result in far more basin floor geometry information than the existing electrical soundings. The availability of real-time GPS systems with sufficient accuracy for gravity survey work extends the usefulness of the gravity method, enabling readings to be done "on the fly" at any location, and thus increasing data density where long profiles are not possible.

The indicated difference in basin depth between the resistivity and gravity models when using the densities as published would also seem to indicate that the Cretaceous succession have varying density both laterally and vertically. This can readily be understood in terms of facies differences and fluvial cycles. The assumption of constant floor rock density is also rather simplistic, and small variations in the gravity curve can easily result from differences in floor lithology and structure. This is however an unknown, and the reason for the exploration work in the first place. The only way to correlate the resistivity and gravity models is to assume that the density contrast between the Cretaceous and Cape rocks is smaller than the available literature suggests. The other alternative is that the basin is actually much shallower here than the resistivity model suggests: All the other profiles in the CSIR report indicate shallower floor conditions than the profile corresponding to the gravity profile position.

The model derived by Kleywegt indicates a maximum basin depth of 1800 m, with a density contrast assumed to be  $-0,24 \text{ g.cm}^{-3}$  (floor density:  $2,67 \text{ g.cm}^{-3}$ , basin density:  $2,43 \text{ g.cm}^{-3}$ ). This apparently agrees with both seismic refraction results in the basin and density determinations from boreholes for the upper 1 200 to 1 600 m of the Cretaceous rocks in the Algoa basin. No report on the seismic work was however located. Using this density contrast in the present study also results in a basin depth of 1 800 m at station 6 000 (Figure 15). It is thus assumed that the correct average density contrast for the basin is around  $-0,24 \text{ g.cm}^{-3}$  and that the basin depth is not as large here as the resistivity models suggest. Note that unique model solutions to the data do not exist: Model geometry depends on the input resistivity/density values, which are uncertainties.

The interpreted geological structure as derived from the gravity model KK2 is shown in Figure 16. This structure broadly agrees with that proposed by Kleywegt.

The existence of shallow TMS horsts or anticline structures in the floor remains unproven with the sparse data available. The envisaged structural evolution of the basin is based on the assumption of a relaxation phase after the Cape orogeny. The existence of any shallow TMS sub-outcrops (horsts) would then be subject to the evolution of the basin as a graben structure, and not as a result of the pre-existing TMS structures (anticlinal folds) as preserved around the valley today. The lack of Cretaceous material to the north of the Cango fault and the abrupt termination of the basin on the western and eastern edges suggest that basin formation proceeded with continued faulting to result in a basin much the same size and shape as which is preserved today. Near Calitzdorp the basin is reported to have a depth of around 1 200 m (CSIR report), yet the basin is truncated by TMS and Bokkeveld mountains 1 - 2,5 km to the west. This would seem to indicate that the western edge of the basin is truncated by north-south trending faults. Such faults would be good targets for future exploration. The resistivity models suggest that the basin floor does vary with depth from east to west, and it is thus proposed that the basin was formed by various interlinked graben and half-graben structures, giving rise to areas with more and less subsidence of the floor rocks. Tectonism continued after deposition of the basin sediments preserved today. One way to explain the present outcrop pattern and the surrounding topography is to postulate a renewed phase of faulting and subsidence after deposition of the Cretaceous material, with the remnant seen today surviving

erosion due to lower elevation than the surrounding areas. The existence of Uitenhage material to the south of the Cango fault at elevations higher than some rocks to the north of the fault fits this scenario, but gives rise to the question why no Uitenhage material is found to the north of the Cango Fault. A possible explanation is that any possible Cretaceous material has been removed by erosion after renewed uplift, leaving only the more resistant rocks to the north of the Cango fault.

Profiles 2 and 3 are too short to reliably show the geological structure at the western edge of the basin. These profiles need to be lengthened by two kilometers each, in order to have sufficient data to reliably model the basin geometry here. The available data however do point to the possible existence of a north-south trending normal fault with down-throw to the East.

## 7. STRUCTURAL GEOLOGY

### 7.1 STRUCTURAL CONSIDERATIONS

Compelling evidence of the half-graben nature of the valley exists. Signs of continued tectonic activity after basin formation and sedimentation are also present, and evidence of Recent faulting exists in the area. Seismic activity maps indicate the region to be active. Recent earthquakes in the Southern Cape indicate continued movement along the east-west trending fault lines. To better understand the structural history, structural measurements were carried out to collect data on the structural evolution of the basin through time, and to provide a background for future exploration.

Of note is the following:

- Kirkwood formation dips at around  $30^{\circ}$  east near Calitzdorp
- Cretaceous bedding is on average horizontal in the middle of the basin along Profile 1
- Cretaceous bedding dips in the order of  $20^{\circ}$  north in the vicinity of De Rust
- Cretaceous rocks dip in the order of  $20^{\circ}$  east to the east of Meiringspoort
- Cretaceous bedding show distinct differences in dip over short distances
- The presence of an Enon Formation erosional remnant against a TMG fault plane near Dysselsdorp
- Vertical joints exposed along road cuttings and visible in outcrops show east – west as well as north – south strikes.

Digital photographs of features of interest and measurement sites were taken, as well as handheld GPS coordinates. Where direct measurements were impossible, a Brunton compass was used to estimate apparent dip and strike direction. Examples of these features are shown in Appendix D, with photographs of some of the measured features discussed in paragraph 8. The accepted view of a constant average dip towards the north is overly simplistic, a more complex post-depositional history being suggested by the investigations. Ample evidence pointing to potential groundwater targets along possible large bedrock faults exist.

Time, personnel and budgetary constraints precluded the gathering of sufficient data, and more structural measurements and geological mapping is required to aid future exploration.

### 7.2 STRUCTURAL MEASUREMENTS

L.A. Smith, M.C. Smit and P. Smit carried out measurements of bedding planes and joints during February 2002 and September 2003. Time constraints precluded a full survey of the valley, and measurements were thus taken at easily accessible outcrops next to existing roads. Data collection was restricted to Cretaceous sediments, but ideally the TMG in the region should have been included in the study.

Measurements were carried out with a Breithaupt Kassel Coclà compass, with the declination set at  $0^{\circ}$ . The measurements were recorded as dip/azimuth for planes and surfaces suitable for the purpose. The

Cretaceous sediments are soft and measurements were restricted to harder surfaces in sandstone, mudstone and conglomerates. The mudstone typically is too soft to support uneroded surfaces, but several sandstone layers and lenses were available for measurements of dip and joint directions, as well as several hard joint planes in conglomerates. The measurements were corrected after the field phase for a magnetic declination of  $24^{\circ} 9'$  west, to reflect true azimuth. (Appendix E: Hermanus Magnetic Observatory, Pers. Comm.). The measurements were plotted using *SPHERISTAT* software. Data were plotted as poles-to-planes on lower hemisphere Schmidt nets, and rose diagrams showing dominant directions. It is deemed to be of no value to obtain an average for the whole bedding dip data set, since the measurements and physical evidence clearly indicate that a constant basin-wide dip/azimuth does not exist for the Cretaceous sediments, and the variation in joint strike directions also indicates separate fracture episodes.

Digital pictures of several worthwhile features were also obtained (Appendix D).

The structural measurements are listed in Appendix F, and the *Spheristat* plots are shown in Appendix G.

## 8. DISCUSSION OF STRUCTURAL MEASUREMENTS

### 8.1 Bedding

All the Kirkwood Formation bedding data were plotted as a set (Appendix G, Plot 1, Plot 2) to show the variations in dips measured. The plot indicates two groups of dip data distribution, suggesting a fold in the Cretaceous bedding, with fold axis striking  $343^{\circ}$  and plunging  $2^{\circ}$ .

#### 8.1.1 Calitzdorp: Kirkwood Formation bedding

The road cutting to the west of Calitzdorp on the Huisrivier road shows steeply dipping layers of Kirkwood Formation (Site 1). 13 Measurements were taken here on hard sandstone bedding planes. Kirkwood formation dips on average  $28^{\circ}$  in the direction  $69^{\circ}$ , strengthening the postulation of north-south striking normal faults at the western edge of the basin. These data suggest continued tectonic activity after Uitenhage deposition. Figure 21 shows a photograph of this area. (Appendix F, Site 1, Appendix G Plot 3, Plot 4)



**Figure 21** View of the steeply dipping Cretaceous sediments to the west of Calitzdorp. (Site 1)

#### 8.1.2 Mid-basin: Kirkwood Formation bedding

Measurements were taken along the gravity Profile 1 as well as along roads at suitable road cuttings throughout the basin (Appendix F, Sites 2, 3, 4, 7, 8, 9, 14, 15, 16, 18, 19, 20, 21). Dips measured vary from 2 to 24 degrees. These dips were measured on Kirkwood formation outcrops where hard sandstone/mudstone was present. The combined average dip for the 29 readings is 2.4° in the direction 312.3° (Appendix G, Plot 5, Plot 6). This indicates that on average the bedding is almost horizontal with a dip to the north-west. This average is a matter of interest only: The rose diagram shows that dip azimuths vary greatly and that a uniform dip trend is not present. It cannot be claimed that the average dip of the Uitenhage rocks in the basin is consistently to the north. Inspection of site-specific data indicates the following dip trends:

- northward dip for Sites 2, 4, 9, 15, 18,
- westward dip for Site 3,
- south-westwards dip for Site 7, 14,
- southwards dip for Site 8, 16,
- north-westwards for site 19, 20
- south-eastwards for site 21.

#### 8.1.3 Buffelskloof formation bedding

Only two readings of bedding in the Buffelskloof Formation were obtained, near the road cutting depicted in Figure 23 (Site 5). The data suggest an average dip of 7.9° in a direction of 155.8°. Other Buffelskloof Formation dips were estimated using a Brunton compass: These apparent dips vary from horizontal to 35° in a Northerly direction. The variation of dips seems to indicate that separate blocks were displaced, with dips varying over relatively short distances. (Appendix D)

## 8.2 Joints and faults

All the measured joint data were plotted as a combined set to show the variations in strike and dip for joints in all the Cretaceous strata (Appendix G, Plot 7, Plot 8). A wide variation of strike direction is evident from the rose diagram shown in Plot 8 (Appendix G). The histogram is based on 48 data points, calculated with a 15° class interval. The direction frequency distribution is shown in Figure 22.

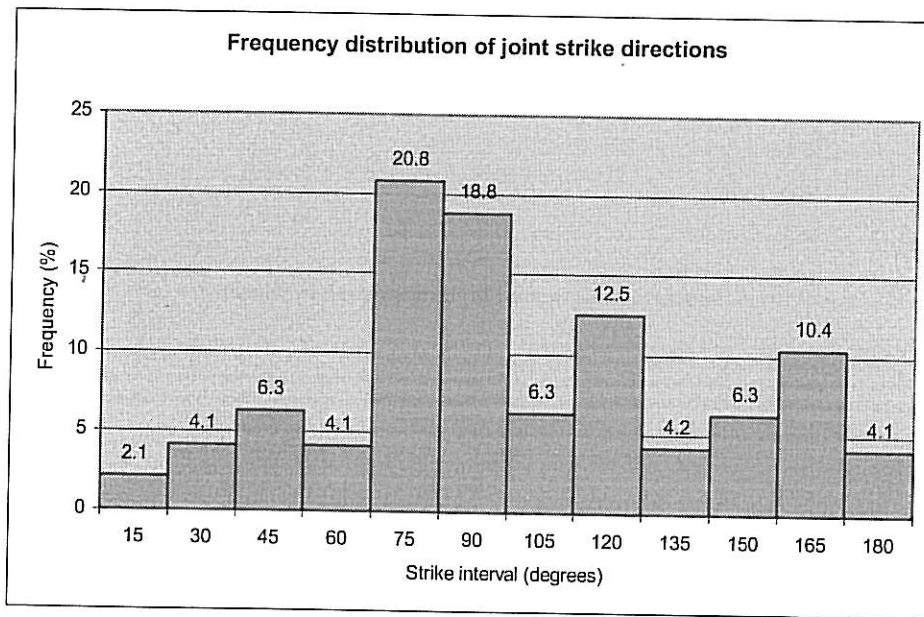


**Figure 22** Frequency distribution of strikes of joints for Cretaceous material in the Klein Karoo. Number of measurements: 48.

#### 8.2.1 Buffelskloof Formation

The distribution of joint directions in the Buffelskloof Formation is shown in Plot 9 and Plot 10, Appendix G. In the area near the end of Profile 1 joint faces with vertical striations are exposed in the Buffelskloof formation. These joints strike on average  $84^\circ$ . The presence of east-west striking vertical joints in the Uitenhage Group sediments is an indication of post Cretaceous tectonism along the earlier east west faulting of the floor. It is therefore likely that active faulting went on for an extensive period of time after the deposition of the sediments, leading to extensive erosion of the Cretaceous rocks, as well as potential targets for deep drilling. Figures 23 and 24 show photographs of these joints.



**Figure 23** Vertical joint in Buffelskloof conglomerate, strike  $82^\circ$ , dip  $82^\circ$  (near northern margin of basin on Kruisfontein road)

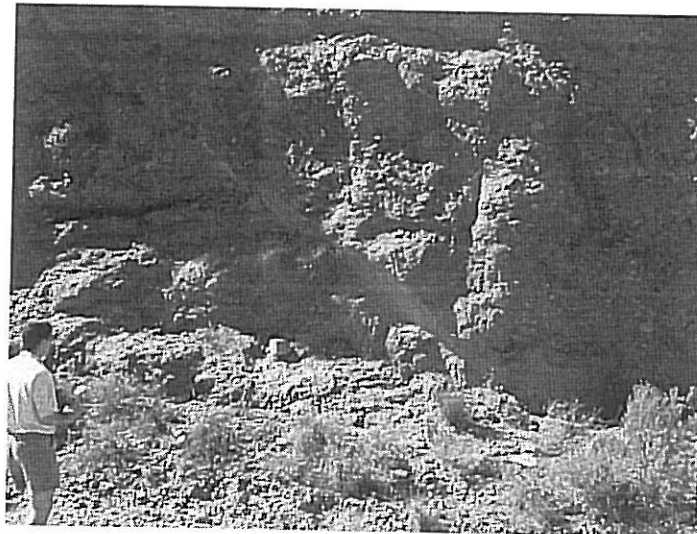


**Figure 24** Joint in Buffelskloof Formation, striking  $86^\circ$ , dipping  $61^\circ$ .

Seven measurements in the Buffelskloof Formation were taken along the Vergelegen road at three separate sites (sites 11, 12, 13). Figure 25 shows one of these joints in eroded Buffelskloof Formation. The average strike and dip for these joints in the Buffelskloof Formation are  $108^\circ$  and  $84^\circ$  respectively.



**Figure 25** Joint in eroded Buffelskloof Formation, Vergelegen Road ( $33^{\circ} 30' 51.7''$  S,  $022^{\circ} 22' 16.4''$  E) The conglomerate is eroded, but the joint surface is clearly identifiable. Strike is  $92^{\circ}$ , dip  $80^{\circ}$ .

Other joint strike directions estimated with Brunton Compass measurements are:

$99^{\circ}$  Buffelskloof Formation  
 $111^{\circ}$  Buffelskloof Formation  
 $103^{\circ}$  Buffelskloof Formation  
 $96^{\circ}$  Enon Formation  
(Average:  $102^{\circ}$ )

These strikes are for Buffelskloof Formation and Enon Formation on the northern edge and southern edge of the basin, indicating the pervasiveness of the joint pattern.

Inspection of Plot 10 shows that 15.4% of the measured Buffelskloof Formation joints strike in this direction. Adding these four approximate strikes to the data set increases this frequency to 35 %, equal in size to the  $75 - 90^{\circ}$  class interval: The dominant strike direction is on average east-west. Note that these statistics are approximate due to the small amount of data available, but the trends are reliable.

### 8.2.2 Kirkwood Formation

Appendix G, Plot 11 and Plot 12 shows the stereogram and rose diagram of all the joints measured in the Kirkwood Formation. The data set indicates the prominent strike direction to be around  $70^{\circ}$ . The next prominent direction is around  $157^{\circ}$ .

Figure 26 shows joints in the Kirkwood Formation along the tar road between Oudtshoorn and Calitzdorp near Kerkrand, striking  $73^{\circ}$ , an east - west trend. The absence of clear striations at this outcrop limits the value of the data in terms of structural history.



**Figure 26** Vertical joints, striking  $73^{\circ}$  showing cross bedding in the Kirkwood Formation mudstone.  
Middle of basin, on Oudtshoorn – Calitzdorp tar road near Kerkrand)

Measurements of joints in mudstone of the Kirkwood Formation along the Vergelegen Road (site 14) shows joint sets in two distinct dip directions of  $139.5^{\circ}$  and  $27.4^{\circ}$ , with dips of  $64.5^{\circ}$  and  $75^{\circ}$  respectively. The strikes of the two sets are  $49.5^{\circ}$  and  $117.4^{\circ}$ , with the included angle  $68^{\circ}$ . These joints are assumed to be conjugate, with a principal stress direction of  $80^{\circ}$ . The strike of the principal direction ( $80^{\circ}$ ) is in the same order as the majority of the joint directions listed thus far. The strike direction of the one set ( $117.4^{\circ}$ ) matches that of a fault measured at Dysselsdorp ( $105^{\circ}$ , Site 10). The other direction is similar to that of a fault measured at Calitzdorp ( $51^{\circ}$ , Site 22).

Another example of post-deposition activity is shown in Figure 27. This small “fault” in Kirkwood formation has footwall on the northern side, as is found at the fault in Varkieskloof near the Dysselsdorp purification works (see 8.2.3 below). The strike of the fault in Figure 27 approximates that of the fault measured at Calitzdorp (Site 22). The relationship seen above suggests continued normal faulting after lithification of the Uitenhage sediments.



**Figure 27** Joint with normal faulting displacement in Kirkwood Formation. (Site 15) The joint strikes  $69^{\circ}$  and dips  $65^{\circ}$ . The hangingwall is on the southern side. The bedding dip at this site was measured as  $24^{\circ}$  (azimuth  $355^{\circ}$ ) for the hangingwall side and  $15^{\circ}$  (azimuth  $8^{\circ}$ ) for the footwall side.

### 8.2.3 Measurements in the TMS and Bokkeveld Shale

#### 8.2.3.1 TMS

Faults and joints were measured in the TMS at Dysselsdorp and near Calitzdorp. The fault data set is plotted in Plot 13 and the joint data set in Plot 14, Appendix G. The measurements show some scatter, but the average strikes are  $50^{\circ}$  and  $105^{\circ}$  for the faults, and  $55^{\circ}$  for the joints. The faults are located on the two ends of the basin, and thus cannot be said to be a conjugate set in position terms, but the "included" angle is  $55^{\circ}$ , indicating a likely principal stress direction striking  $80^{\circ}$ . This direction matches that discussed in paragraph 8.2.2 for the Kirkwood Formation and is close to the prominent strike direction of all the joints measured in the Uitenhage material (Appendix G, Plot 7, Plot 8). The histogram shown in Figure 22 indicates almost 40% of the measured joints strike between 60 and 90 degrees, with a prominent peak at around  $75^{\circ}$ .

#### 8.2.3.2 Bokkeveld Shale

Two joints were measured in Bokkeveld Shale at the southern edge of the basin (Appendix F, Site 17). These joints strike on average  $164^{\circ}$  (Appendix G, Plot 18).

The combined plots for joints measured in the Cape Supergroup are shown in Plot 15, Plot 16, Plot 17 and Plot 18, Appendix G. Plot 17 and Plot 18 display the results of averaged directions for each locality (Sites 10, 17, 22) in order to remove data scatter and present the dominant directions. Plot 18 shows that the averaged joint directions are as follows:

TMS (Site 10):	$53^{\circ}$
TMS (Site 22):	$11^{\circ}$
Bokkeveld Shale (Site 17):	$164^{\circ}$

#### 8.2.4 Dysselsdorp

Near the Dysselsdorp water purification plant remnants of Cretaceous conglomerate is present on and next to TMS material. One remnant sits along a TMS cliff: The  $105^{\circ}$  strike and  $76^{\circ}$  S dip of this cliff face suggests it is a normal fault (Figure 29). A striation measured at the contact area dips at  $65^{\circ}$  along the face (azimuth  $122^{\circ}$ ). The striations indicate left-lateral strike-slip with dip-slip, an indication of East-West compressive stress during normal faulting. More work is needed here, to establish the relationship of the Cretaceous remnant to the TMS and to date the fault. In the next valley to the south (Varkieskloof) a piece of Cretaceous conglomerate is also present on a TMS hill, indicating extensive erosion of the Cretaceous sediments after deposition on rugged topography (Figure 28). From this remnant it would appear that the TMS here had much the same geomorphology at the time of deposition of the Cretaceous sediments as is presently exposed. These remnants are about 150 m above the present valley surface. (These remnants are not High Level Gravels – Enon conglomerate to the south-west of Dysselsdorp at Rooipuntjie attain an elevation of about 240 m above the valley, and Cretaceous conglomerates to the north of Dysselsdorp reach elevations of more than 400 m above the valley floor (Waboskop), indicating that extensive erosion of the Cretaceous sediments did indeed take place after deposition. High Level Gravels are seen higher up on TMS outcrops in the region.)

Figures 28 and 29 shows photographs of the features at Varkieskloof. Joints measured in the TMS at the site depicted in Figure 29 strike on average  $53.6^{\circ}$ , average dip  $45^{\circ}$  with azimuth  $143^{\circ}$ . This strike direction is similar to that of the fault measured at Calitzdorp, discussed below. It also follows the trend of some joints in the Cretaceous sediments (Appendix G, Plot 8, Plot 12).



**Figure 28** Small piece of Enon material on TMS outcrop at Varkieskloof, Dysselsdorp. (View from borehole DP 10 looking east)



**Figure 29**

Erosion remnant of Cretaceous material against a TMS cliff. Hill on left is TMS, block of Cretaceous conglomerate at right is shown with arrow (View is from Dysselsdorp purification works looking east)



**Figure 30**

Detail of contact in Figure 29 (Cretaceous conglomerate on the left). The contact plane has dip of  $76^\circ$  to the south and strikes  $105^\circ$ .

### 8.2.5 Calitzdorp

A prominent fault plane is present in the TMS near Borehole KG1. This fault strikes  $51^{\circ}$  and dips  $80^{\circ}$  in a north-westerly direction. Figures D10 (Appendix D) shows this fault plane. A prominent cliff face is also formed along a joint striking  $11^{\circ}$ , dipping  $84^{\circ}$  to the west. This plane may be related to a north – south striking normal fault in this area, the presence of which is suggested by the Kirkwood Formation bedding dip to the west of Calitzdorp (paragraph 8.1.1), as well as by the gravity survey (Profiles 2 and 3, paragraph 5). (The apparent differential tilting of Buffelskloof Formation discussed in Appendix D must also be along north – south striking lineaments, and the main river cuttings through the Swartberg (Gamkapoort and Meiringspoort) also follows a general north – south trend, as do a multitude of joints in the TMS, clearly visible on satellite pictures). Some Kirkwood Formation joint data (Appendix G, Plot 12) also show this strike direction.

Another prominent fault in this area is a thrust fault striking north-south, thrust from east to west, also indicating an east-west principal stress direction .

### 8.2.6 Discussion of structural considerations

Current thinking links the development of the Cretaceous basins to the break-up of Gondwana, specifically with the Agulhas Fracture Zone (AFZ), a right-lateral transform fault shear zone. This transform fault is accepted to have caused tension along the present coastline, resulting in the formation of sediment-filled grabens (Tankard, 1982, McCarthy, 2005). Figure 31 shows the AFZ and some of the sedimentary basins associated with the Gondwana break-up event. It is therefore expected to find structural evidence of this event in the study area. The age of these structures could render them unsuited to present-day exploration, but some joint/fault directions in the area are parallel to the present-day principal stress direction (north-south), and evidence points to continued activity along the east-west trending faults. Extended mapping of the surrounding area may enhance borehole placement on North-South trending faults/joints/shear zones coupled to anticlinal structures in the TMS.

Regionally, the Swartberg Fault (Cango Fault) trends east-west, and can be linked to the expected movements during and following the break-up of Gondwana. Inspection of the Southern Cape area shows this fault strike direction to be prevalent. Inspection of the *Google* image for Southern Africa shows a prominent structure on the Atlantic Ocean floor to the west of the sub-continent, lining up with the regional fault systems along the Cape Fold Belt. The fault plane shown in Figure 30 has striations as discussed in 8.2.4. At first glance the left-lateral shearing implied by the striation does not fit the right-lateral nature of the Agulhas Fracture Zone: Intuition would indicate the Swartberg fault system to be right-lateral as well. The structures measured however point to a more complicated picture: East-west compressive stresses were present in the area, not just north-south tension. This can be understood when looking at Figures 32 and 33. Figure 32 shows the strain ellipsoid for regional right-lateral shearing (as present along the AFZ). The Little Karoo Basin area would have experienced transtension during basin formation – the area was under north-south tension, forming the graben structures, as well as under east-west compression (forming the thrust faults at the western edge of the basin, the conjugate joint sets and the striations on the TMS fault face at Dysselsdorp). Transtension would result in anticlockwise rotation of the strain ellipsoid, as shown in Figure 33.

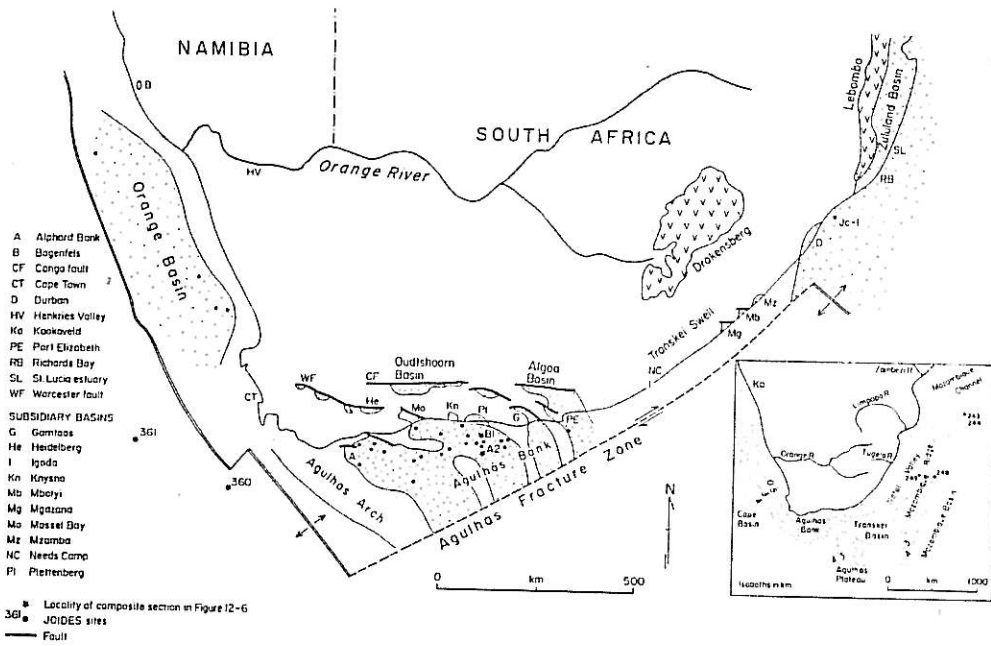


**Figure 12-2.** Locality map showing distribution of Mesozoic sedimentary basins. Inset shows major offshore physiographic features. The Outeniqua basin underlies the Agulhas Bank. [Sources: Dingle and Scruton (1974), Scruton and Dingle (1976), Du Toit (1979), McLachlan and McMillan (1979).]

**Figure 31.** The Agulhas Fracture Zone and associated sedimentary basins. (From "Crustal Evolution Of Southern Africa", Tankard *et al*)

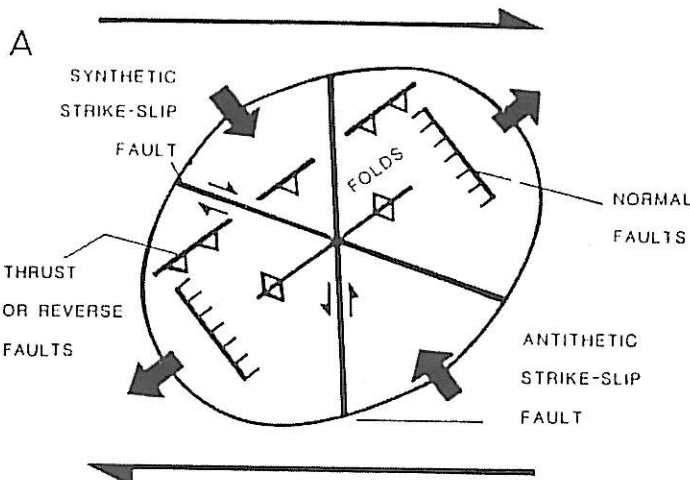


**Figure 32.** Strain ellipsoid showing the structures formed by a dextral simple shear couple (right-lateral fault zone).

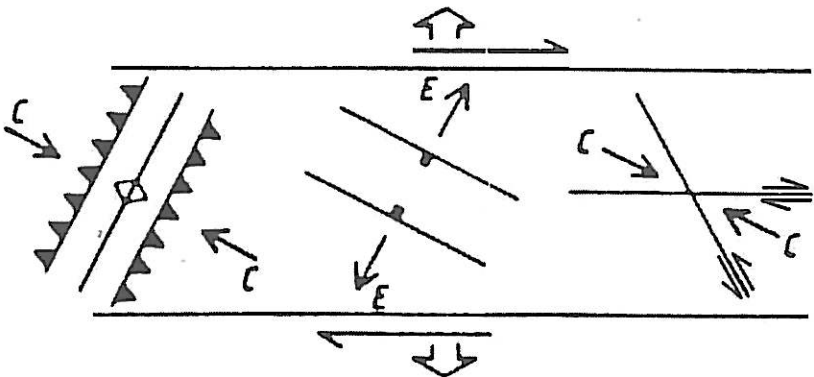


**Figure 33** Anti-clockwise rotation of structural elements shown in Figure 32 under transtension conditions.

Rotating Figure 33 to fit the situation in the Little Karoo basin is shown in Figure 34. If it is assumed that the AFZ influence extended northwards into the sub-continent, the study area would have experienced dextral shear conditions during the formation of the Cretaceous grabens, as shown in Figure 34. It is likely that the grabens only developed after the Falkland Plateau cleared the sub-continent. Replacing continental material (Falkland Plateau) with basaltic ocean floor (Indian ocean) south of the sub-continent might also have resulted in subsidence of the southern margin of the continent, previously elevated by the Cape Fold Belt, aiding the formation of east-west trending normal faulting, increasing the graben-forming tension condition. (The regionally extensive east-west trend of joints in the Karoo stratigraphy (Beaufort Group) extends further northwards than would be expected to have been caused by folding during formation of the Cape Fold Belt – could this be a possible result of continental margin subsidence coupled with the later uplift episodes of the sub-continent?) With the dextral shear couple aligned with the AFZ direction (Figure 34), the expected structures approximate those observed during the field measurements:

- Folding is observed in the Cretaceous sediments (Site 1), with the fold axis striking around  $340^{\circ}$
- Left-lateral faulting bearing  $105^{\circ}$  (Site 10)
- Conjugate joint sets with strikes around  $50^{\circ}$  and  $120^{\circ}$  (Site 14, Site 10, Plot 11 Appendix G)
- Principal stress direction of around  $85^{\circ}$  (Site 14, Site 10)
- Graben-forming east-west trending normal faults in the TMG
- North-south striking thrust faulting in the TMS observed near Calitzdorp.
- Normal faults trending east-west (Site 15, Site 6)
- Joints trending around  $75^{\circ}$  –  $80^{\circ}$  in Kirkwood Formation (Appendix G, Plot 12)

Inspection of the data plots in Appendix G indicates that this simplistic explanation is not self-evident when grouping all the lineament data together.

Some of the joint directions measured does not fit this scenario: The multitude of North-South trending joints in the TMS mountains, clearly visible in the drainage patterns, is a prominent feature throughout the region. This trend is also found in Bokkeveld Shale outcrops (Site 17, Appendix G, Plot 18). The small number of similar joint directions observed in the Cretaceous sediments (Appendix G, Plot 12) might indicate that these joint directions formed prior to the deposition of the Cretaceous sediments, with some re-activation after deposition.

The limited amount of structural data gathered during the field surveys are insufficient to unravel the structural history of the area, but the trends established suggests that this method will be of immense value during future investigations. The present-day principal stress direction is oriented around north-south, thus rendering joints/faults with this direction suitable groundwater targets. Note that the Cango cave system is developed along such a lineament.

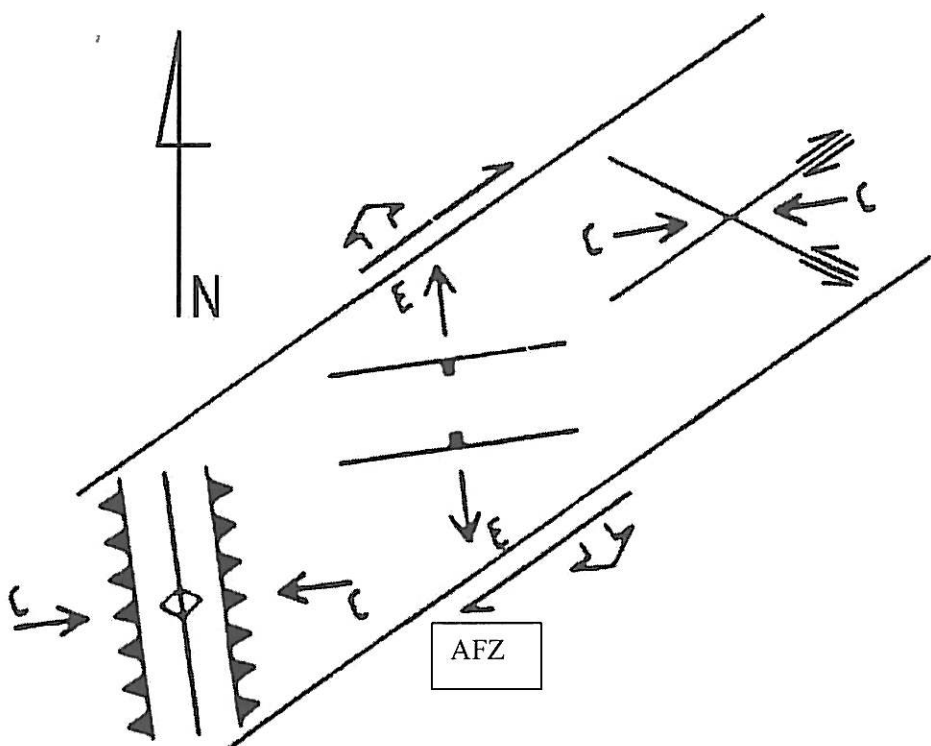


**Figure 34** Structures expected to develop under transtension right-lateral shear conditions in the sub-continent next to the AFZ. The structural measurement data show a close correlation to this structural picture.

## 9. CONCLUSIONS AND RECOMMENDATIONS

### 9.1 Geophysical work

The gravity Profile 1 clearly indicates the half-graben structure of the Cretaceous basin, and shows that the maximum thickness of Cretaceous rocks does not occur against the Cango fault (Figure 16). The Cretaceous rocks have maximum thickness around stations 10 500 m and 14 000 m. A large normal fault with down-throw in the order of 1 200 m occurs at station 16 000 m, with a basin depth of  $\approx$  1 600 m to the south of this fault. This is much shallower than suggested by previous workers who merely extrapolated the depth from the (non-existing) "constant dip" of the Uitenhage rocks. It is also clear that the basin is quite shallow directly south of the inferred Cango fault, as found by Whittingham and Kleywegt. It is clear that the Cango fault was not the only large normal fault active during the formation

of the basin, and might not have served as the northern termination of the basin. The drilling work carried out by Whittingham and the picture shown in Figure D2 (Appendix D) indicate the possibility that the sedimentation was not bounded only by faults at the northern edge, and that the basin was larger than preserved today - the erosional remnants near Dysselsdorp and the outcrop pattern of the Cretaceous rocks point to extensive post-depositional erosion.

It must be stressed that the gravity model results only hold for the densities and regional gravity field assumed in this report. The results are however indicative of the basin structure. The test series discussed (Section 5) indicates that large faults resulting in steps in the floor of the basin can be delineated, but cannot be pinpointed accurately enough to enable the drilling of boreholes to intersect them at a chosen depth. Boreholes can however be sited from the gravity results with enough precision to guarantee intersection of shallower target faults. Further to this the gravitational method has proved to be a fast tool for preliminary exploration work, and when combined with deep resistivity or CSAMT work should give a very good indication of the true subsurface structure. If the valley was formed by interlinked graben and half-graben structures, the existence of shallower TMS sub-outcrops is possible. The fastest way to test this is to extend the gravity survey to cover the entire valley with a pseudo-grid of stations, followed by CSAMT (Stratagem) soundings in areas where shallow floor conditions are delineated. (The results of the CSIR resistivity survey however points to the unlikelihood of finding shallow anticlinal sub-outcrops. The limitations of the CSIR survey are discussed in Section 5.)

A matter which should receive attention is the termination of the Cretaceous basin at the western edge near Calitzdorp: The indications are that the floor remains at a depth of more than 1 000 m in this area, with TMS and Bokkeveld outcrops close to the west. This might indicate hitherto unmapped north-south striking faults with down-throw to the east. This is borne out by the measured Cretaceous bedding dip at Calitzdorp (mean dip: 28°, dip direction 69°), which suggests post-lithification tilting along an axis striking NNW-SSE. Modelling of the two east-west gravity profiles south of Calitzdorp indicate a steep floor depth increase from west to east, as would be expected for a normal fault. This shallow fault may be a good target for exploration in this area and should be investigated.

## 9.2 Structural work

The primary bedding dip measurements for the Uitenhage Group clearly show random bedding dip in the area investigated, with an average dip for the Kirkwood Formation of only 3.5° in the direction 326°. This average merely shows the almost horizontal nature of the sediments. It does not fit Kleywegt's model of post-depositional faulting with block rotation, nor does it fit the literature description of the basin structure. The measured dip of the Buffelskloof formation is only 8° in the direction 156°. This southward dip is consistent with the northern provenance of the sediments. Detailed mapping and measurements may give an indication of any crustal tilting in post-Cretaceous times, as would be expected after the breakup of Gondwana and the removal of the stresses that caused the Cape Fold Belt. The photographs in Appendix D show varying dips for the Buffelskloof Formation, which might point to post-depositional block faulting and rotation, but the rest of the data precludes this as a basin-wide occurrence. The Buffelskloof-TMS contact shown in Figure D2 (Appendix D) might be a normal fault contact rotated to present day orientation, as this would indicate a shallow southward Buffelskloof Formation dip before tilting. The details of such tilting remain unclear, as faulting related to this should be evident, but is not seen. The drilling work by Whittingham (GH1501) showed the difficulty of pinpointing the Cango Fault as the major northern termination fault of the Cretaceous sediments.

The majority of the joint planes measured in the Cretaceous sediments strike around 80°, with an average dip of 74.1° south. This steeply dipping east-west orientation is consistent with continued post depositional fault activity along basin forming east-west trending normal faults (Seismic evidence indicates continued activity along the east-West Swartberg - Cango - Baviaanskloof fault line, extending to Ceres and Worcester). Joint plane measurements in Table Mountain Group sediments did not reflect this direction. It must however be stressed that measurements were restricted mainly to the Cretaceous

sediments, and that the survey needs to be extended to include the surrounding TMG outcrops – this is required to unravel the structural history of the region in order to facilitate groundwater exploration.

The present structural measurement dataset is too small to allow for reliable statistics and intensive interpretation, but the visible field relationships follow the measurements: The Cretaceous sediments do not dip consistently to the north, and the Cango Fault is not the major basin-forming fault as described in literature. Evidence of continued (Recent) faulting along east-west striking faults exists, and this is also mentioned in the report on the drilling work at Scoemanshoek (Whittingham, GH 1501). The extensive post depositional erosion and lack of Cretaceous material to the north of the Cango Fault line also indicates post-Cretaceous tectonism. The likely presence of north – south trending faults should not be ignored in future work, seeing as the present principal stress is along this direction (Andersen, 2003). The continued tectonism is of importance to future exploration efforts for groundwater sources below as well as around the present valley. It might be feasible to target younger fault zones in the Cape bedrock.

Due to the importance of the structural history of the basin in selecting targets in the region, detailed structural mapping and sedimentological investigation is needed, and should be seen as an essential complement to any further investigations of the area. The structural investigations to date indicate continued post-Cretaceous faulting of the region, and indications are that faulting is still active in this region. Detailed mapping and satellite image analysis, linked to geophysical work should be done to pinpoint exploration targets related to faults. As regards selection of drilling targets outside the basin, the same combination is recommended: TMS anticlines combined with north-south lineaments resulted in successful boreholes in the Steytlerville and Willowmore areas (Welman, Barnard, 2007, pers. comm.).

## 10. REFERENCES

Andersen, N., Antoine, L, Fereira, C. (2003) A short course in Structural Geology & Remote Sensing Analysis for Hydrogeologists for The Department of Water Affairs & Forestry. Unpublished notes, GeoScientific and Exploration Services, Southern Implants Office Park. 1 Albert Road, Irene, 0062, Pretoria. South Africa.

Davis G.H., Reynolds, S.J. (1996) Structural Geology of Rocks and Regions, Second Edition. John Wiley & Sons Inc.

Dobrin, M.B. (1976) Introduction to Geophysical Prospecting, Third Edition. McGraw-Hill.

Driscoll, F.G. (1986) Groundwater and Wells, Second Edition. Johnson Division.

Duvenhage, A.W.A., Meyer, R. (1992) The reinterpretation of Schlumberger deep resistivity soundings from the Oudtshoorn Cretaceous Basin and an evaluation of the applicability of other geoelectrical techniques to identify target areas in the Table Mountain Group for ground water exploration. CSIR report No. EMA-C-92023.

Duvenhage, A.W.A., Meyer, R., Raath, C.J. (1993) A geoelectrical survey in the Oudtshoorn area to identify potential drilling targets for ground water. CSIR report No. EMAP-C-93042.

Hobbs B.E., Means W.D., Williams P.F. (1976) An Outline Of Structural Geology. John Wiley & Sons Inc.

Hurlbut, C.S., Klein, C. (1977) Manual of Mineralogy, 19<sup>th</sup> Edition. John Wiley & Sons.

Kleywelt, R.J. (1972) Interpretation of a gravity profile across the Oudtshoorn Cretaceous Basin. Ann. Geol. Surv. S. Afr., 9,p.125 - 128.

McCarthy, T., Rubidge, B. (2005) The Story of Earth and Life – A southern African perspective on a 4.6-billion-year journey. Struik Publishers.

Meyer, P.S. (1999) An Explanation of the 1:500 000 General Hydrogeological Map: Oudtshoorn 3320 (DWAF)

Meyer, P.S. (1999) 1:500 000 General Hydrogeological Map: Oudtshoorn 3320 (DWAF)

Norman, N., Whitfield G. (2006) Geological Journeys – A Traveller's guide to South Africa's rocks and landforms. Struik Publishers.

Park C.F, MacDiarmid R.A. (1975) Ore Deposits, Third Edition. W.H. Freeman and Company.

Pettijohn, E.J. (1975) Sedimentary Rocks, Third Edition. Harper & Row, Publishers.

Smit, P.J., Maree, B.D., (1966) Densities of South African Rocks for the Interpretation of Gravity Anomalies. Bulletin 48, Council for Geoscience, Government Printer, South Africa.

Söngle, A.P.G. and Hälbich, I.W. (1983) Geodynamics of the Cape Fold Belt. Special publication No. 12, The Geological Society of South Africa.

South African Committee for Stratigraphy (SACS), (1980) Stratigraphy of South Africa. Part 1: Lithostratigraphy of the Republic of South Africa, South West Africa/Namibia, and the Republics of Bophuthatswana, Transkei and Venda. Geological Survey of South Africa.

Tankard, A.J., Jackson, M.P.A., Eriksson, K.A., Hobday, D.K., Hunter, D.R. and Minter, W.E.L. (1982) Crustal evolution of Southern Africa. Springer-Verlag.

Telford, W. M., Geldart, L. P., Sheriff, R. E., and Keys, D. A., (1976) Applied geophysics. Cambridge Univ. Press.

Thornbury W.D. (1969) Principles of Geomorphology, Second Edition. John Wiley & Sons Inc.

Truswell, J.F. (1977) The Geological Evolution of South Africa. Purnell.

Van Der Ventel, Michelle, Hermanus Magnetic Observatory, 06 August 2003, Pers. Comm.

Welman P.I., Barnard H.C., (June 2007) Willowmore Bulk Water Supply - Hydrogeological Investigation. Report Bav.06/048, GCS (Pty) Ltd

Whittingham, J.K. (1970) Exploratory drilling for ground water in the Cango Fault zone at Schoemanshoek, Oudtshoorn District. Report No. 1501, Directorate Geohydrology, DWAF.

Whittingham, J.K. (1972) Water supply investigations for Oudtshoorn Municipality: Cape Province. Report No. GH 1800, Directorate Geohydrology, DWAF.

Whittingham, J.K. (1971) Geology of the Cretaceous rocks of Oudtshoorn Area, Cape Province, with an outline of the Geological structure of the Oudtshoorn Basin. Report No. 1591, Directorate Geohydrology, DWAF.

Whittingham, J.K. (1974?) Borehole G.26325 (D.W.A. No. 116105/3) at Minwater near Volmoed, Oudtshoorn District. Unpublished borehole report, DWAF.

## 11. LIST OF FIGURES AND TABLES

	<i>PAGE</i>
Figure 1 Simplified Geology map of the study area	4
Figure 2 Simplified geology map showing the positions of the deep resistivity soundings carried out by the CSIR	6
Table 1 Resistivities of lithologies in the study area	7
Figure 3 The interpretation given by the CSIR for the deep sounding data along their Profile B – B'	7
Figure 4 Regional gravity profile of data as presented by Kleywelt	8
Figure 5 Model of the residual gravity anomaly caused by the Cretaceous rocks along the gravity profile of Kleywelt	8
Figure 6 The structure of the Little Karoo cretaceous basin as envisaged by Kleywelt	9
Figure 7 Position of the gravity profiles done in 1997 and 2002	10
Table 2 Cretaceous rock density values	11
Figure 8 Reduced Bouguer gravity values and relative elevations of stations for Profile 1	12
Figure 9 Reduced Bouguer Gravity for Profile 2	12
Figure 10 Reduced Bouguer gravity for Profile 3	13
Figure 11 Profile 1 Bouguer gravity and elevation values	14
Figure 12 Profile 1 Bouguer gravity shown alongside the interpolated regional gravity field	14
Figure 13 Residual gravity values along Profile 1	15
Table 3 Density values of the pre-Cretaceous rocks	16
Figure 14 Gravity model of the basin, using densities as published by Smit and Maree	17
Figure 15 Gravity model of the basin using densities from the Kleywelt report	18
Figure 16 Proposed geological model of the basin along the Profile 1	19
Figure 17 Gravity values along Profile 2	20
Figure 18 Gravity values along Profile 3	20

Figure 19 Gravity model along Profile 2	21
Figure 20 Gravity model along Profile 3	22
Figure 21 View of the steeply dipping Cretaceous sediments west of Calitzdorp. (Site 1)	
26	
Figure 22 Frequency distribution of strikes of joints for Cretaceous material in the Klein Karoo	27
Figure 23 Vertical joint in Buffelskloof conglomerate	28
Figure 24 Joint in Buffelskloof Formation	
28	
Figure 25 Joint in eroded Buffelskloof Formation, Vergelegen Road	29
Figure 26 Vertical joints showing cross bedding in Kirkwood Formation Mudstone	30
Figure 27 Joint with normal faulting displacement in Kirkwood Formation	31
Figure 28 Small piece of Enon material on TMG outcrop	32
Figure 29 Erosion remnant of Cretaceous material against a TMS cliff	33
Figure 30 Detail of contact in Figure 29	33
Figure 3 The Agulhas Fracture Zone and associated sedimentary basins	35
Figure 32 Strain ellipsoid showing the structures formed by a dextral simple shear couple	35
Figure 33 Anti-clockwise rotation of structural elements shown in Figure 32 under transtension conditions.	
36	
Figure 34 Structures expected to develop under transtension right-lateral shear conditions in the sub-continent next to the AFZ.	
37	

## 12. ACKNOWLEDGEMENTS

The study was carried out over an extended period of time, necessitating the involvement of various people during different phases. The survey was initiated by Dziem Dziembowski, on the premise that shallow TMS anticlines/ horst ridges may be present under the Cretaceous sediments. This idea was inspired by the ridge of TMS outcrops directly to the north of the Cango fault, wedged between the fault and the Cango Group outcrops.

Gravity data acquisition was carried out by Fabian Anke, Danie Brink, Lucas Smith, Jacques Groenewald and Paul Smit.

Structural data acquisition was carried out by Lucas Smith, Cornè Smit, Heine Barnard and Paul Smit. (Paul Smit was a paraplegic confined to a wheelchair during the later phases of the field survey, and is indebted to the people doing the climbing-work to measure structures.)

Geological information of the TMS aquifers was supplied by Heine Barnard and Pete Welman of GCS. To further understanding of these aquifers DWA personnel, in conjunction with GCS personnel, were active in gravity method testing on the TMS aquifers in the Willowmore and Steytlerville areas, as part of the bulk water supply wellfield extensions for these towns.

General aquifer information was obtained during the Little Karoo wellfield rehabilitation carried out by DWA personnel. Of special mention here is the work by Cecil Less, Barry Venter and Lucas Smith. Re-equipping boreholes with better casing and screens enabled Borehole Television and geophysical logging of the TMS itself, and pumping tests added valuable information on aquifer characteristics.

GHP3949

## APPENDIX A

## Geophysical Data Listing

### **Observed Gravity data (Instrument Dump files)**

### Observed Gravity: Profile 1

Profile 1 North: Running from station 0 to 16000 (stations numbered in Meters, at 200 m intervals, profile direction South – North).

Profile 1 South: Running from station 0 to 57, (station interval of 100 m, profile direction South - North).

Profile 1 South Station 57 close to Profile 1 North Station 0. Tie-in work was carried out to link the two data sets.

### Observed Gravity: Profile 1 North

Station	Grav.	SD.	Tilt x	Tilt y	Temp.	E.T.C.	Dur	# Rej	Time
0. 3974.975*	0.072	-1.	-2.	0.04	-0.047	60	0	10:28:23	
0. 3974.970*	0.052	-3.	1.	0.03	-0.045	60	0	10:31:22	
0. 3975.000*	0.054	1.	-1.	0.10	0.016	60	0	13:12:50	
200. 3973.460*	0.072	-5.	-6.	0.02	-0.043	60	0	10:35:39	
400. 3971.950*	0.054	-7.	-1.	0.02	-0.042	60	0	10:39:01	
600. 3970.380*	0.064	1.	-4.	0.02	-0.040	60	0	10:42:17	
800. 3970.150*	0.051	-1.	4.	0.03	-0.039	60	0	10:45:27	
1000. 3968.735*	0.057	3.	-9.	0.04	-0.038	60	0	10:48:22	
1200. 3968.460*	0.055	1.	-9.	0.04	-0.036	60	0	10:51:39	
1400. 3967.845*	0.076	-1.	-5.	0.05	-0.035	60	0	10:54:36	
1600. 3966.690*	0.062	12.	-6.	0.05	-0.033	60	0	10:59:20	
1800. 3966.380*	0.066	-2.	-12.	0.07	-0.031	60	0	11:02:49	
2000. 3966.030*	0.075	4.	-3.	0.06	-0.029	60	0	11:06:30	

Observed Gravity: Profile 1 North continued

2200.3965.550*	0.054	-10.	9.	0.06	-0.028	60	0	11:10:14
2400.3964.675*	0.056	-10.	-5.	0.06	-0.026	60	0	11:13:31
2600.3963.110*	0.066	-2.	6.	0.05	-0.025	60	0	11:17:20
2800.3961.775*	0.052	-9.	4.	0.05	-0.023	60	0	11:20:36
3000.3962.335*	0.045	3.	-5.	0.05	-0.020	60	0	11:25:33
3200.3959.160*	0.055	-5.	-3.	0.06	-0.019	60	1	11:29:45
3200.3959.175*	0.062	-2.	1.	0.10	0.015	60	0	13:04:57
3400.3957.845*	0.058	-1.	7.	0.05	-0.017	60	0	11:33:13
3600.3956.970*	0.071	-1.	9.	0.06	-0.015	60	0	11:36:45
3800.3956.055*	0.059	1.	-7.	0.06	-0.014	60	0	11:40:11
4000.3955.240*	0.060	4.	-1.	0.06	-0.013	60	0	11:43:11
4200.3954.390*	0.048	-25.	18.	0.05	-0.012	2	0	11:45:42
4200.3954.455*	0.068	-2.	-6.	0.07	-0.011	60	0	11:46:21
4400.3953.765*	0.072	-5.	-5.	0.07	-0.010	60	0	11:49:47
4600.3952.645*	0.069	-11.	3.	0.07	-0.009	60	0	11:52:47
4800.3951.890*	0.062	6.	13.	0.07	-0.007	60	0	11:56:07
5000.3951.125*	0.067	-8.	-6.	0.07	-0.006	60	0	11:58:53
5200.3950.785*	0.071	-0.	-7.	0.09	-0.005	60	0	12:02:06
5400.3949.840*	0.071	0.	-1.	0.09	-0.003	60	0	12:06:36
5600.3949.210*	0.059	4.	-8.	0.09	-0.002	60	0	12:09:47
5800.3949.465*	0.053	1.	1.	0.09	-0.001	60	0	12:12:46
6000.3947.755*	0.057	-10.	-7.	0.09	0.001	60	0	12:16:25
6000.3947.765*	0.057	2.	-7.	0.08	0.013	60	0	12:58:17
6200.3948.095*	0.058	-0.	-0.	0.09	0.002	60	0	12:21:17
6400.3945.125*	0.058	2.	1.	0.08	0.004	60	0	12:24:38
6600.3944.535*	0.071	4.	-6.	0.07	0.005	60	0	12:28:42
6800.3943.925*	0.070	-1.	0.	0.08	0.006	60	0	12:32:31
7000.3943.505*	0.056	1.	-3.	0.08	0.008	60	0	12:36:41
7200.3942.965*	0.051	6.	-14.	0.09	0.008	60	0	12:40:12
7400.3942.570*	0.059	-4.	-1.	0.08	0.009	60	0	12:43:09
7600.3942.175*	0.055	4.	-3.	0.09	0.010	60	0	12:46:17
7800.3941.705*	0.069	-10.	7.	0.07	0.012	60	0	12:51:35

### Observed Gravity: Profile 1 North continued

SCINTREX V4.1      AUTOGRAV / Field Mode      R4.4  
 Line: 1.1 Grid: 1. Job: 1. Date: 97/04/11 Operator: 2.  
 GREF.: 0. mGals      Tilt x sensit.: 248.7  
 GCAL.1: , 6233.479      Tilt y sensit.: 249.2  
 GCAL.2: 0.      Deg.Latitude: -33.5  
 TEMPCO.: -0.1287 mGal/mK      Deg.Longitude: -21.75  
 Drift const.: 0.86      GMT Difference: -1.45hr  
 Drift Correction Start Time: 09:16:52      Cal.after x samples: 12  
 Date: 97/04/01      On-Line Tilt Corrected = "\*\*\*"

Station	Grav.	SD.	Tilt x	Tilt y	Temp.	E.T.C.	Dur	# Rej	Time
0.	3975.105*	0.074	-0.	1.	0.02	-0.047	60	0	08:09:50
0.	3975.135*	0.056	-0.	-3.	0.13	-0.039	60	0	11:20:59
7800.	3941.825*	0.074	-1.	-3.	-0.02	-0.052	60	0	08:27:10
8000.	3941.110*	0.094	2.	1.	-0.03	-0.053	60	0	08:30:41
8200.	3940.545*	0.087	-4.	4.	-0.02	-0.054	60	0	08:33:51
8400.	3940.235*	0.079	5.	-7.	-0.01	-0.054	60	0	08:36:59
8600.	3939.720*	0.086	-5.	-1.	-0.00	-0.055	60	0	08:39:41
8800.	3939.120*	0.072	-4.	1.	0.01	-0.055	60	0	08:42:46
8800.	3939.140*	0.084	2.	-4.	0.11	-0.043	60	0	11:08:53
9000.	3940.060*	0.080	6.	4.	0.01	-0.056	60	0	08:45:50
9200.	3943.040*	0.092	3.	-3.	0.02	-0.056	60	0	08:49:03
9400.	3942.785*	0.079	-0.	-2.	0.02	-0.057	60	0	08:52:05
9600.	3941.725*	0.112	-1.	2.	0.02	-0.057	60	0	08:55:01
9800.	3941.015*	0.091	2.	1.	0.03	-0.058	60	0	08:58:11
10000.	3938.995*	0.081	8.	-7.	0.03	-0.058	60	0	09:01:01
10200.	3938.255*	0.077	5.	2.	0.04	-0.058	60	0	09:04:35
10400.	3937.240*	0.074	-5.	-4.	0.04	-0.059	60	0	09:07:46
10600.	3936.655*	0.068	-0.	0.	0.04	-0.059	60	0	09:11:05
10800.	3936.035*	0.071	1.	4.	0.03	-0.059	60	0	09:14:10
11000.	3935.420*	0.072	2.	-6.	0.03	-0.059	60	0	09:17:07
11200.	3934.435*	0.068	2.	-4.	0.03	-0.059	60	0	09:19:54
11400.	3933.340*	0.082	0.	-5.	0.03	-0.059	60	0	09:23:12
11600.	3931.965*	0.084	-3.	1.	0.02	-0.059	60	0	09:26:15
11800.	3930.400*	0.078	5.	-10.	0.03	-0.059	60	0	09:29:06
12000.	3928.345*	0.064	-3.	-1.	0.03	-0.059	60	0	09:32:19
12200.	3926.560*	0.058	2.	9.	0.02	-0.059	60	0	09:35:44
12400.	3922.490*	0.000	0.	0.	0.00	-0.059	1	0	09:38:21
12400.	3924.330*	0.066	0.	5.	0.04	-0.059	60	1	09:39:33
12400.	3924.330*	0.084	1.	-4.	0.08	-0.045	60	1	11:00:46
12600.	3923.075*	0.064	-1.	-4.	0.04	-0.059	60	0	09:42:23
12800.	3923.090*	0.053	-1.	2.	0.05	-0.059	60	1	09:45:22

Observed Gravity: Profile 1 North continued

13000.3924.985* 0.063	2.	4.	0.04	-0.059	60	0	09:47:57
13200.3926.610* 0.069	-0.	3.	0.05	-0.058	60	0	09:50:58
13400.3928.265* 0.062	-4.	1.	0.07	-0.058	60	1	09:53:46
13600.3929.160* 0.056	-4.	5.	0.05	-0.058	60	0	09:56:32
13800.3930.500* 0.060	6.	-6.	0.05	-0.058	60	0	09:59:11
14000.3931.360* 0.049	-1.	-2.	0.06	-0.057	60	1	10:02:12
14200.3929.575* 0.057	-6.	-1.	0.07	-0.057	60	0	10:05:36
14400.3927.475* 0.060	2.	-5.	0.07	-0.056	60	0	10:08:31
14600.3926.445* 0.069	0.	-3.	0.07	-0.056	60	0	10:11:28
14800.3926.005* 0.077	-4.	-0.	0.07	-0.055	60	0	10:14:38
15000.3925.940* 0.069	-3.	1.	0.07	-0.055	60	0	10:17:53
15200.3926.935* 0.071	-1.	4.	0.07	-0.047	60	0	10:53:13
15400.3925.875* 0.055	-1.	8.	0.08	-0.048	60	0	10:48:35
15600.3924.680* 0.059	-1.	3.	0.08	-0.049	60	0	10:45:17
15800.3923.335* 0.060	4.	-4.	0.08	-0.050	60	0	10:42:05
16000.3921.810* 0.064	-7.	14.	0.06	-0.051	60	0	10:38:27

### Observed Gravity: Profile 1 South

Station	Grav.	SD.	Tilt x	Tilt y	Temp.	E.T.C.	Dur	# Rej	Time
-9998.	5028.530*	0.128	-1.	-2.	-1.65	-0.042	60	1	08:32:30
-9998.	5028.540*	0.130	1.	-2.	-1.64	-0.043	60	0	08:34:34
-9998.	5028.540*	0.118	8.	0.	-1.49	-0.033	60	0	14:02:23
-9998.	5028.540*	0.109	5.	-0.	-1.47	-0.032	60	0	14:04:28
0.	5041.365*	0.129	-3.	-7.	-1.58	-0.067	60	0	10:02:16
1.	5042.070*	0.129	2.	-7.	-1.55	-0.067	60	0	10:05:36
2.	5042.455*	0.100	4.	-10.	-1.53	-0.068	60	0	10:08:54
3.	5042.605*	0.090	3.	-12.	-1.55	-0.068	60	0	10:12:08
4.	5042.765*	0.137	3.	-9.	-1.56	-0.068	60	0	10:15:52
5.	5043.005*	0.103	2.	-13.	-1.57	-0.068	60	0	10:19:24
6.	5043.160*	0.106	1.	-9.	-1.57	-0.068	60	0	10:23:08
7.	5043.385*	0.110	-2.	-20.	-1.58	-0.069	60	0	10:26:16
8.	5043.715*	0.101	4.	-5.	-1.59	-0.069	60	0	10:29:26
9.	5044.010*	0.104	-5.	-7.	-1.59	-0.069	60	0	10:33:11
10.	5044.295*	0.084	-3.	-5.	-1.59	-0.069	60	0	10:36:47
11.	5044.365*	0.119	-0.	-8.	-1.59	-0.068	60	0	10:40:08
12.	5044.475*	0.090	-4.	-6.	-1.59	-0.068	60	0	10:44:11
13.	5044.620*	0.114	-0.	-7.	-1.60	-0.068	60	0	10:48:09
14.	5044.585*	0.121	2.	-11.	-1.59	-0.068	60	0	10:51:25
15.	5044.675*	0.138	4.	-4.	-1.59	-0.068	60	0	10:54:40
16.	5044.945*	0.093	-6.	-3.	-1.58	-0.067	60	0	10:58:27
17.	5045.135*	0.102	10.	-7.	-1.58	-0.067	60	0	11:01:51
18.	5045.330*	0.116	-0.	-1.	-1.58	-0.067	60	0	11:05:58
19.	5046.635*	0.092	6.	-7.	-1.57	-0.066	60	0	11:09:15
20.	5047.135*	0.123	1.	-7.	-1.57	-0.066	60	0	11:12:28
21.	5047.215*	0.093	7.	-8.	-1.58	-0.066	60	0	11:15:20
22.	5047.450*	0.073	3.	-7.	-1.58	-0.065	60	0	11:18:26
23.	5047.785*	0.089	1.	-9.	-1.58	-0.065	60	0	11:21:33
24.	5048.090*	0.165	-2.	-9.	-1.58	-0.064	60	0	11:24:45

Observed Gravity: Profile 1 South continued

25. 5048.300* 0.097	4.	-6.	-1.58	-0.064	60	0	11:27:57
26. 5048.620* 0.091	1.	-6.	-1.57	-0.063	60	0	11:31:14
27. 5048.940* 0.104	2.	-6.	-1.57	-0.063	60	0	11:34:14
28. 5049.185* 0.103	-2.	-6.	-1.57	-0.062	60	0	11:37:21
29. 5049.540* 0.130	2.	-10.	-1.57	-0.062	60	0	11:40:25
30. 5049.825* 0.099	8.	-7.	-1.57	-0.061	60	0	11:43:35
31. 5050.100* 0.087	1.	-0.	-1.57	-0.061	60	0	11:47:13
32. 5050.275* 0.090	-3.	-7.	-1.57	-0.060	60	0	11:50:23
33. 5050.560* 0.090	4.	-8.	-1.56	-0.059	60	0	11:53:30
34. 5051.090* 0.117	-8.	-7.	-1.56	-0.059	60	0	11:56:44
35. 5051.385* 0.111	-4.	-6.	-1.56	-0.058	60	0	12:00:28
36. 5051.650* 0.122	1.	-7.	-1.55	-0.057	60	0	12:04:25
37. 5051.865* 0.101	5.	6.	-1.64	-0.053	60	0	12:22:35
38. 5052.370* 0.108	7.	-10.	-1.63	-0.052	60	0	12:25:41
39. 5052.400* 0.112	-6.	-6.	-1.61	-0.052	60	0	12:28:47
40. 5052.805* 0.097	0.	-7.	-1.59	-0.051	60	0	12:32:01
41. 5052.850* 0.121	1.	-9.	-1.58	-0.050	60	0	12:35:24
42. 5052.470* 0.121	0.	-8.	-1.57	-0.049	60	0	12:38:27
43. 5051.695* 0.111	-1.	4.	-1.56	-0.049	60	0	12:41:32
44. 5050.885* 0.105	-7.	-14.	-1.57	-0.048	60	0	12:44:35
45. 5050.585* 0.130	0.	-8.	-1.56	-0.047	60	0	12:47:54
46. 5050.245* 0.117	-8.	10.	-1.56	-0.046	60	0	12:51:45
47. 5049.965* 0.108	-2.	-14.	-1.56	-0.046	60	0	12:55:07
48. 5049.525* 0.122	-8.	-5.	-1.55	-0.045	60	0	12:58:20
49. 5049.130* 0.106	2.	-4.	-1.54	-0.044	60	0	13:01:46
50. 5048.715* 0.095	-1.	-9.	-1.53	-0.043	60	0	13:06:13
51. 5048.330* 0.126	5.	-2.	-1.54	-0.042	60	0	13:10:01
52. 5047.895* 0.105	7.	-7.	-1.54	-0.042	60	0	13:13:21
53. 5047.460* 0.086	3.	-7.	-1.53	-0.041	60	0	13:17:06
54. 5046.900* 0.132	2.	-4.	-1.53	-0.040	60	0	13:20:22
55. 5046.495* 0.086	0.	-8.	-1.52	-0.040	60	0	13:24:08
56. 5045.920* 0.115	-3.	-3.	-1.52	-0.039	60	0	13:27:20
57. 5045.470* 0.098	3.	-2.	-1.53	-0.038	60	0	13:30:42

### Observed Gravity: Profiles 2 and 3

## Profile 2 (Stations 0 – 52)

### Profile 3 (Stations 54 -105).

### Tie-in between Profile 1 North and 1 South (Stations 106 – 111).

Station	Grav.	SD.	Tilt x	Tilt y	Temp.	E.T.C.	Dur	# Rej	Time
-9997.	5006.530*	0.121	-1.	-1.	-0.76	-0.023	60	0	08:02:33
-9997.	5006.525*	0.113	2.	-2.	-0.77	-0.024	60	0	08:05:48
-9997.	5006.525*	0.100	2.	-3.	-0.78	-0.025	60	0	08:07:49
-9997.	5006.445*	0.098	2.	6.	-0.60	0.003	60	0	14:32:16
-9997.	5006.440*	0.097	2.	1.	-0.58	0.005	60	0	14:37:22
0.	5016.580*	0.092	-1.	0.	-0.86	-0.031	60	0	08:27:27
1.	5016.580*	0.087	-3.	1.	-0.86	-0.031	60	0	08:29:12
2.	5016.545*	0.102	-2.	4.	-0.86	-0.032	60	0	08:31:18
3.	5016.570*	0.149	5.	-0.	-0.89	-0.033	60	0	08:35:11
4.	5016.630*	0.088	6.	2.	-0.90	-0.034	60	0	08:37:14
5.	5016.635*	0.106	0.	5.	-0.91	-0.035	60	0	08:39:08
6.	5016.780*	0.088	0.	4.	-0.91	-0.035	60	0	08:41:08
7.	5016.870*	0.125	5.	6.	-0.91	-0.036	60	0	08:43:00
8.	5016.900*	0.112	2.	-4.	-0.91	-0.037	60	0	08:44:56
9.	5016.895*	0.089	-3.	5.	-0.91	-0.037	60	0	08:46:49
10.	5016.880*	0.082	9.	-2.	-0.91	-0.038	60	0	08:48:42
11.	5016.920*	0.115	4.	7.	-0.91	-0.039	60	0	08:50:31
12.	5016.850*	0.078	-10.	32.	-0.91	-0.039	60	0	08:52:21
13.	5016.785*	0.104	5.	-2.	-0.91	-0.039	60	0	08:54:17
14.	5016.735*	0.100	3.	3.	-0.92	-0.040	60	0	08:56:14
15.	5016.730*	0.088	4.	9.	-0.91	-0.041	60	0	08:58:05
16.	5016.700*	0.109	-9.	24.	-0.92	-0.041	60	0	09:00:05
17.	5016.670*	0.086	-27.	48.	-0.92	-0.042	60	0	09:01:58
18.	5016.600*	0.097	4.	2.	-0.92	-0.042	60	0	09:03:52
19.	5016.520*	0.099	4.	7.	-0.92	-0.043	60	0	09:05:51
20.	5016.530*	0.093	-0.	9.	-0.92	-0.044	60	0	09:07:43

Observed Gravity: Profile 2 and 3 continued

21. 5016.565* 0.120	1.	15.	-0.92	-0.044	60	0	09:09:32
22. 5016.450* 0.100	-6.	-1.	-0.91	-0.045	60	0	09:11:28
23. 5016.360* 0.104	4.	3.	-0.91	-0.045	60	0	09:13:21
24. 5016.225* 0.095	8.	14.	-0.91	-0.045	60	0	09:15:13
25. 5016.215* 0.102	6.	-1.	-0.91	-0.046	60	0	09:17:03
26. 5016.180* 0.118	9.	-0.	-0.91	-0.046	60	0	09:18:47
27. 5016.155* 0.119	10.	0.	-0.91	-0.047	60	0	09:20:38
28. 5016.085* 0.144	-10.	27.	-0.90	-0.047	60	0	09:22:28
29. 5016.115* 0.098	4.	13.	-0.91	-0.048	60	0	09:24:20
30. 5016.125* 0.101	7.	2.	-0.90	-0.048	60	0	09:26:10
31. 5016.095* 0.115	13.	5.	-0.90	-0.049	60	0	09:28:05
32. 5016.035* 0.104	1.	0.	-0.90	-0.049	60	0	09:29:56
33. 5016.095* 0.122	8.	-5.	-0.90	-0.049	60	0	09:31:45
34. 5015.955* 0.114	14.	-0.	-0.90	-0.050	60	0	09:33:37
35. 5015.835* 0.103	11.	-0.	-0.89	-0.050	60	0	09:35:24
36. 5015.750* 0.088	10.	2.	-0.89	-0.051	60	0	09:37:09
37. 5015.685* 0.119	-6.	24.	-0.88	-0.051	60	0	09:38:59
38. 5015.755* 0.103	8.	8.	-0.88	-0.051	60	0	09:40:53
39. 5015.490* 0.131	20.	2.	-0.88	-0.052	60	0	09:42:46
40. 5015.455* 0.101	-2.	17.	-0.88	-0.052	60	0	09:44:40
41. 5015.415* 0.103	-6.	23.	-0.87	-0.052	60	0	09:46:32
42. 5015.345* 0.110	4.	-1.	-0.87	-0.053	60	0	09:48:16
43. 5015.260* 0.104	18.	5.	-0.87	-0.053	60	0	09:50:02
44. 5015.150* 0.108	10.	-6.	-0.87	-0.053	60	0	09:51:56
45. 5015.175* 0.089	5.	6.	-0.87	-0.054	60	0	09:53:53
46. 5015.055* 0.123	6.	9.	-0.87	-0.054	60	0	09:55:41
47. 5014.850* 0.090	1.	-7.	-0.87	-0.054	60	0	09:57:23
48. 5014.770* 0.097	-4.	16.	-0.87	-0.054	60	0	09:59:16
49. 5014.695* 0.093	9.	-12.	-0.87	-0.055	60	0	10:01:18
50. 5014.480* 0.090	-1.	3.	-0.87	-0.055	60	0	10:03:04
51. 5014.200* 0.120	-0.	-14.	-0.88	-0.055	60	0	10:05:54
52. 5014.065* 0.113	-33.	-36.	-0.88	-0.055	60	0	10:07:58
54. 5011.740* 0.101	-3.	4.	-0.76	-0.049	60	0	12:01:58
55. 5012.110* 0.098	-4.	-14.	-0.76	-0.049	60	0	11:59:54
56. 5012.450* 0.092	10.	9.	-0.76	-0.049	60	0	11:57:52
57. 5012.725* 0.113	-1.	15.	-0.76	-0.050	60	0	11:55:59
58. 5012.975* 0.123	-9.	20.	-0.75	-0.050	60	0	11:54:08
59. 5013.180* 0.105	-8.	0.	-0.75	-0.051	60	0	11:52:16
60. 5013.475* 0.115	-7.	5.	-0.74	-0.051	60	0	11:50:26
61. 5013.710* 0.095	5.	-6.	-0.73	-0.051	60	0	11:48:39
62. 5013.825* 0.100	23.	11.	-0.72	-0.052	60	0	11:46:52
63. 5014.005* 0.083	-15.	10.	-0.72	-0.052	60	0	11:45:05
64. 5014.235* 0.097	6.	-29.	-0.72	-0.052	60	0	11:43:11

Observed Gravity: Profile 2 and 3 continued

65. 5014.365* 0.110	-4.	-1.	-0.72	-0.053	60	0	11:41:26
66. 5014.475* 0.080	-15.	-7.	-0.73	-0.053	60	0	11:39:41
67. 5014.570* 0.092	-7.	15.	-0.73	-0.053	60	0	11:37:55
68. 5014.650* 0.103	-1.	-21.	-0.72	-0.054	60	0	11:36:05
69. 5014.775* 0.096	2.	0.	-0.73	-0.054	60	0	11:34:16
70. 5014.890* 0.091	-1.	-1.	-0.73	-0.054	60	0	11:32:29
71. 5014.990* 0.094	-11.	13.	-0.72	-0.054	60	0	11:30:43
72. 5015.120* 0.102	2.	4.	-0.73	-0.055	60	0	11:28:56
73. 5015.260* 0.113	-7.	7.	-0.73	-0.055	60	0	11:27:12
74. 5015.400* 0.075	6.	-5.	-0.73	-0.055	60	0	11:25:30
75. 5015.255* 0.100	5.	7.	-0.74	-0.055	60	0	11:23:44
76. 5015.365* 0.103	-10.	-16.	-0.75	-0.055	60	0	11:21:52
77. 5015.565* 0.119	-34.	-38.	-0.75	-0.056	60	0	11:20:02
78. 5015.690* 0.133	-3.	7.	-0.76	-0.056	60	0	11:18:14
79. 5015.765* 0.093	-2.	2.	-0.77	-0.056	60	2	11:16:22
80. 5015.830* 0.091	-10.	-4.	-0.78	-0.056	60	0	11:14:32
81. 5015.945* 0.101	-2.	6.	-0.78	-0.056	60	0	11:12:17
82. 5016.115* 0.094	-15.	5.	-0.78	-0.057	60	0	11:09:50
83. 5016.360* 0.080	-5.	6.	-0.79	-0.057	60	0	11:08:00
84. 5016.410* 0.117	-14.	36.	-0.78	-0.057	60	0	11:06:12
85. 5016.410* 0.088	6.	3.	-0.79	-0.057	60	0	11:04:23
86. 5016.350* 0.074	-10.	35.	-0.79	-0.057	60	0	11:02:30
87. 5016.280* 0.108	4.	-9.	-0.78	-0.057	60	0	11:00:44
88. 5016.120* 0.111	10.	-6.	-0.79	-0.057	60	0	10:58:58
89. 5015.890* 0.127	1.	11.	-0.79	-0.057	60	0	10:57:16
90. 5015.530* 0.126	9.	-4.	-0.79	-0.057	60	0	10:55:29
91. 5015.625* 0.104	-6.	9.	-0.79	-0.057	60	0	10:53:41
92. 5015.950* 0.103	-8.	-12.	-0.79	-0.057	60	0	10:51:57
93. 5016.195* 0.086	-0.	2.	-0.79	-0.058	60	0	10:50:08
94. 5015.930* 0.099	6.	-8.	-0.79	-0.058	60	0	10:48:18
95. 5015.745* 0.093	-13.	12.	-0.79	-0.058	60	0	10:46:18
96. 5015.815* 0.108	14.	-3.	-0.79	-0.058	60	0	10:44:16
97. 5016.155* 0.108	2.	-5.	-0.79	-0.058	60	0	10:42:25
98. 5016.680* 0.071	7.	-6.	-0.80	-0.058	60	0	10:40:25
99. 5017.065* 0.086	-15.	-25.	-0.80	-0.057	60	0	10:38:29
100. 5017.195* 0.114	-0.	10.	-0.80	-0.057	60	0	10:36:43
101. 5017.350* 0.098	2.	7.	-0.81	-0.057	60	0	10:34:53
102. 5017.390* 0.107	15.	1.	-0.81	-0.057	60	0	10:33:09
103. 5017.375* 0.087	-50.	-73.	-0.83	-0.057	60	0	10:31:17
104. 5017.450* 0.092	-3.	16.	-0.84	-0.057	60	0	10:29:24
105. 5017.475* 0.108	-5.	-8.	-0.86	-0.057	60	0	10:27:38

Observed Gravity: Profile 1 South and 1 North tie-in

106. 5031.295* 0.138	1.	-4.	-0.67	-0.033	60	0	12:56:10
107. 5032.300* 0.128	6.	4.	-0.66	-0.032	60	0	13:00:36
108. 5031.555* 0.126	3.	-10.	-0.67	-0.030	60	0	13:04:06
109. 5031.880* 0.136	16.	-9.	-0.67	-0.029	60	0	13:07:13
110. 5028.275* 0.107	-16.	4.	-0.66	-0.020	60	0	13:32:15
111. 5030.405* 0.126	-11.	12.	-0.64	-0.019	60	0	13:35:25

## Elevation and Coordinate Data

### Elevations: Profile 1 North - Field book data

Elevation data are relative to Station 1. (Data listing format: Line number, Station number, back reading, front reading, elevation difference between back and front readings, reduced elevation (relative to Station 0) - Elevation data was corrected to absolute elevation during tie-in work with the GPS system. The corrected elevations were used in the Bouguer gravity reductions and gravity model)

ELEV.ST 1000

LINE STATION BACK FRONT DIFF RED.ELEV

1	0	4709			1000.000
1	cp	3741	88	4.621	1004.621
1	200	3291	3291	0.450	1005.071
1	cp	4721	140	3.151	1008.222
1	400	2838	2838	1.883	1010.105
1	cp	3892	108	2.730	1012.835
1	600	1809	1809	2.083	1014.918
1	800	3671	3329	-1.520	1013.398
1	cp	392	68	3.603	1017.001
1	1000	279	279	0.113	1017.114
1	1200	582	1868	-1.589	1015.525
1	cp	3741	188	0.394	1015.919
1	1400	3500	3500	0.241	1016.160
1	1600	812	712	2.788	1018.948
1	1800	1584	1969	-1.157	1017.791
1	2000	3303	1892	-0.308	1017.483
1	2200	3578	3149	0.154	1017.637
1	2400	3981	1171	2.407	1020.044
1	cp	4942	192	3.789	1023.833
1	2600	3372	3372	1.570	1025.403
1	cp	1931	159	3.213	1028.616
1	2800	428	428	1.503	1030.119
1	cp	2518	4508	-4.080	1026.039
1	3000	3725	3725	-1.207	1024.832
1	cp	3881	304	3.421	1028.253
1	cp	3817	101	3.780	1032.033
1	cp	3883	292	3.525	1035.558
1	3200	4699	1353	2.530	1038.088
1	cp	2792	453	4.246	1042.334
1	3400	2791	2791	0.001	1042.335
1	3600	2374	1084	1.707	1044.042
1	cp	2603	241	2.133	1046.175

Elevations: Profile 1 North continued

1	3800	2332	2332	0.271	1046.446
1	4000	2782	393	1.939	1048.385
1	4200	2382	900	1.882	1050.267
1	4400	1601	1601	0.781	1051.048
1	cp	4109	252	1.349	1052.397
1	4600	2269	2269	1.840	1054.237
1	4800	2578	532	1.737	1055.974
1	5000	1471	672	1.906	1057.880
1	5200	3653	1121	0.350	1058.230
1	5400	2548	619	3.034	1061.264
1	5600	721	887	1.661	1062.925
1	5800	4822	3383	-2.662	1060.263
1	cp	3257	149	4.673	1064.936
1	6000	938	938	2.319	1067.255
1	6200	3819	3401	-2.463	1064.792
1	cp	3833	163	3.656	1068.448
1	cp	3729	183	3.650	1072.098
1	cp	3877	161	3.568	1075.666
1	6400	3301	840	3.037	1078.703
1	6600	2891	1104	2.197	1080.900
1	6800	2002	942	1.949	1082.849
1	7000	2484	877	1.125	1083.974
1	7200	2149	932	1.552	1085.526
1	7400	2109	1134	1.015	1086.541
1	7600	2499	1032	1.077	1087.618
1	7800		1191	1.308	1088.926
1	7800	1758		0.000	1088.926
1	cp	2131	1182	0.576	1089.502
1	8000	2002	730	1.401	1090.903
1	cp	2132	1161	0.841	1091.744
1	8200	1874	1212	0.920	1092.664
1	cp	2045	1304	0.570	1093.234
1	8400	248	2101	-0.056	1093.178
1	cp	2995	387	-0.139	1093.039
1	8600	2641	1617	1.378	1094.417
1	cp	1962	1098	1.543	1095.960
1	8800	1773	1260	0.702	1096.662
1	cp	26	2059	-0.286	1096.376
1	cp	25	3549	-3.523	1092.853
1	9000	273	1577	-1.552	1091.301
1	cp	165	3319	-3.046	1088.255
1	cp	172	3992	-3.827	1084.428
1	cp	23	3891	-3.719	1080.709

Elevations: Profile 1 North continued

1	cp	12	3744	-3.721	1076.988
1	9200	1261	1261	-1.249	1075.739
1	cp	3598	2583	-1.322	1074.417
1	9400	2127	1260	2.338	1076.755
1	cp	4623	982	1.145	1077.900
1	9600	1239	608	4.015	1081.915
1	cp	3654	371	0.868	1082.783
1	9800	3041	1425	2.229	1085.012
1	cp	4588	28	3.013	1088.025
1	cp	4671	678	3.910	1091.935
1	10000	2618	2618	2.053	1093.988
1	cp	2371	581	2.037	1096.025
1	10200	2380	940	1.431	1097.456
1	cp	2784	432	1.948	1099.404
1	10400	2553	553	2.231	1101.635
1	cp	2661	1122	1.431	1103.066
1	10600	2668	1155	1.506	1104.572
1	cp	3852	200	2.468	1107.040
1	10800	2840	2840	1.012	1108.052
1	cp	4052	1059	1.781	1109.833
1	11000	1671	1671	2.381	1112.214
1	cp	4043	100	1.571	1113.785
1	11200	3987	392	3.651	1117.436
1	cp	4288	667	3.320	1120.756
1	11400	3768	577	3.711	1124.467
1	cp	4127	34	3.734	1128.201
1	cp	4562	477	3.650	1131.851
1	11600	3707	3707	0.855	1132.706
1	cp	4861	49	3.658	1136.364
1	cp	3921	173	4.688	1141.052
1	11800	3237	3237	0.684	1141.736
1	cp	4768	42	3.195	1144.931
1	cp	4982	74	4.694	1149.625
1	12000	3870	1143	3.839	1153.464
1	cp	4803	207	3.663	1157.127
1	cp	3328	174	4.629	1161.756
1	12200	4298	1452	1.876	1163.632
1	cp	4561	238	4.060	1167.692
1	cp	3745	603	3.958	1171.650
1	cp	2621	33	3.712	1175.362
1	12400	2682	2682	-0.061	1175.301
1	cp	4998	182	2.500	1177.801
1	cp	3321	41	4.957	1182.758

Elevations: Profile 1 North continued

1	12600	3301	3301	0.020	1182.778
1	cp	2422	44	3.257	1186.035
1	cp	229	3528	-1.106	1184.929
1	12800	1023	1023	-0.794	1184.135
1	cp	438	3449	-2.426	1181.709
1	cp	888	3823	-3.385	1178.324
1	cp	273	2775	-1.887	1176.437
1	13000	1167	1167	-0.894	1175.543
1	cp	609	2502	-1.335	1174.208
1	cp	132	3539	-2.930	1171.278
1	13200	614	3339	-3.207	1168.071
1	cp	400	3595	-2.981	1165.090
1	cp	235	3477	-3.077	1162.013
1	13400	1855	1855	-1.620	1160.393
1	cp	950	3335	-1.480	1158.913
1	cp	1202	3453	-2.503	1156.410
1	13600	807	1145	0.057	1156.467
1	cp	662	3000	-2.193	1154.274
1	cp	264	3292	-2.630	1151.644
1	13800	918	918	-0.654	1150.990
1	cp	394	3382	-2.464	1148.526
1	14000	3753	1998	-1.604	1146.922
1	cp	3748	100	3.653	1150.575
1	cp	3872	13	3.735	1154.310
1	14200	1245	1245	2.627	1156.937
1	cp	4659	220	1.025	1157.962
1	cp	3928	52	4.607	1162.569
1	cp	3952	419	3.509	1166.078
1	14400	4880	599	3.353	1169.431
1	cp	4155	778	4.102	1173.533
1	14600	2463	1253	2.902	1176.435
1	cp	2542	1138	1.325	1177.760
1	14800	1672	1672	0.870	1178.630
1	cp	1342	1017	0.655	1179.285
1	15000	802	2709	-1.367	1177.918
1	cp	605	2680	-1.878	1176.040
1	cp	311	2502	-1.897	1174.143
1	15200	2050	2050	-1.739	1172.404
1	cp	478	3067	-1.017	1171.387
1	cp	1123	2381	-1.903	1169.484
1	15400	1279	1279	-0.156	1169.328
1	cp	2675	935	0.344	1169.672
1	15600	2128	2128	0.547	1170.219

Elevations: Profile 1 North continued

1	cp	4155	324	1.804	1172.023
1	15800	2493	2493	1.662	1173.685
1	cp	2847	519	1.974	1175.659
1	16000		1533	1.314	1176.973

2

Coordinates: Profile 1 North

Coordinates scaled from the relevant 1 : 50 000 Topographical sheets ( 3321 DB Vleirivier Second Edition, 3321 BD Kruisrivier First Edition).  
(Central Meridian 21° East, Clarke 1880 Spheroid)

Station	Longitude (m)	Latitude (m)
0	-83549	3721686
200	-83473	3721506
400	-83397	3721326
600	-83383	3721136
800	-83431	3720936
1000	-83479	3720736
1200	-83527	3720536
1400	-83575	3720336
1600	-83571	3720126
1800	-83515	3719906
2000	-83459	3719686
2200	-83443	3719506
2400	-83427	3719326
2600	-83397	3719140
2800	-83353	3718949
3000	-83309	3718757
3200	-83265	3718566
3400	-83221	3718375
3600	-83177	3718183
3800	-83133	3717992
4000	-83089	3717800
4200	-83045	3717609
4400	-83001	3717417
4600	-82957	3717226
4800	-82913	3717035
5000	-82869	3716843
5200	-82825	3716652
5400	-82781	3716460
5600	-82737	3716269
5800	-82693	3716077
6000	-82649	3715886
6200	-82449	3715761
6400	-82249	3715636
6600	-82149	3715469
6800	-82049	3715303
7000	-81949	3715136
7200	-81849	3714969
7400	-81749	3714803

Coordinates: Profile 1 North\_continued

7600	-81649	3714636
7800	-81549	3714469
8000	-81449	3714303
8200	-81349	3714136
8400	-81249	3713969
8600	-81149	3713803
8800	-81049	3713636
9000	-81182	3713503
9200	-81316	3713369
9400	-81449	3713236
9600	-81649	3713169
9800	-81699	3713061
10000	-81655	3712881
10200	-81667	3712671
10400	-81679	3712461
10600	-81691	3712251
10800	-81703	3712041
11000	-81715	3711831
11200	-81727	3711621
11400	-81739	3711411
11600	-81751	3711201
11800	-81763	3710991
12000	-81682	3710844
12200	-81509	3710761
12400	-81336	3710678
12600	-81196	3710553
12800	-81091	3710386
13000	-80985	3710219
13200	-80880	3710053
13400	-80774	3709886
13600	-80766	3709669
13800	-80757	3709453
14000	-80749	3709236
14200	-80894	3709086
14400	-81039	3708936
14600	-81098	3708749
14800	-81157	3708561
15000	-81215	3708374
15200	-81274	3708186
15400	-81318	3707986
15600	-81362	3707786
15800	-81405	3707586
16000	-81449	3707386

### Coordinates and Elevations: Profile 1 South

Data obtained with Sokkia Differential GPS system  
(Longitude (m), Latitude (m), Station number, Elevation (mamsl))

82472	-3726985.9	0	325.7	-32.56
82508.4	-3726891.9	1	321.1	-32.71
82545.9	-3726798.9	2	318.4	-32.79
82583.4	-3726705.8	3	316.7	-32.91
82623.2	-3726612.6	4	314.1	-33.21
82659.6	-3726519.2	5	310.9	-33.53
82698.3	-3726426.4	6	308.1	-33.87
82735.5	-3726332.6	7	305.4	-34.1
82773	-3726238.8	8	302.4	-34.3
82811	-3726145.9	9	299.6	-34.5
82849.3	-3726052	10	296.8	-34.7
82888.5	-3725958.9	11	294.9	-34.94
82925	-3725866.7	12	293	-35.15
82964.1	-3725772.7	13	290.8	-35.37
83002.1	-3725679.1	14	289.4	-35.61
83039.9	-3725584.7	15	287.4	-35.84
83078	-3725491.4	16	284.7	-36.06
83115.2	-3725397.7	17	282.3	-36.26
83152.9	-3725303.3	18	280.7	-36.32
83191.6	-3725209.7	19	273.1	-36.46
83229.8	-3725117.1	20	269.2	-36.67
83268	-3725023.7	21	266.7	-37.01
83305.2	-3724930.2	22	264.2	-37.21
83343.8	-3724837.5	23	261.2	-37.4
83381.7	-3724743.9	24	258.4	-37.6
83419.9	-3724650.3	25	255.7	-37.84
83458	-3724556.9	26	253.2	-37.97
83495.8	-3724463.7	27	250.5	-38.11
83534	-3724370.4	28	248.2	-38.25
83572	-3724277.1	29	245.6	-38.35
83609.8	-3724183.7	30	243.2	-38.48
83648	-3724090.1	31	240.9	-38.59
83686.1	-3723996.8	32	239	-38.71
83724.4	-3723903.9	33	236.7	-38.83
83763.2	-3723810.6	34	232.7	-39.03
83801.5	-3723717.7	35	230	-39.19
83839.3	-3723623.9	36	227.9	-39.28
83862.1	-3723525.4	37	226.3	-39.31
83869.8	-3723424.8	38	222.6	-39.47
83876.9	-3723324.4	39	221.4	-39.61
83882.7	-3723223.5	40	218.7	-39.67

Coordinates and Elevations: Profile 1 South continued

83890.8	-3723123.8	41	217.4	-39.8
83898.2	-3723023.1	42	218.4	-39.91
83910.1	-3722922.1	43	220.5	-40.18
83917.7	-3722821.8	44	223.2	-40.38
83919.8	-3722720.8	45	223.5	-40.55
83922.1	-3722619.6	46	223.7	-40.77
83924.8	-3722518.9	47	223.9	-40.94
83927.3	-3722418.1	48	224.4	-41.2
83930.6	-3722316.8	49	224.7	-41.45
83932.1	-3722216	50	225.3	-41.67
83935.5	-3722115.4	51	226	-41.85
83938.5	-3722014.5	52	227	-42
83939.9	-3721912.9	53	228	-42.17
83943.6	-3721812.5	54	229.3	-42.39
83945.2	-3721711.3	55	229.9	-42.59
83948.5	-3721610.3	56	231.2	-42.84
83949.5	-3721540.7	57	232.2	-43.04

### Coordinates and Elevations: Profile 2

Elevation data obtained with Sokkia Differential GPS system  
(Longitude (m), Latitude (m), Station number, Elevation (mamsl))

62064.8	-3714516	0	240.1	-50.93
62055.2	-3714516.3	1	240.1	-50.93
62045.1	-3714518	2	240.2	-50.95
62033	-3714520	3	240.1	-50.95
62020.7	-3714522.1	4	239.9	-50.93
62009	-3714525.5	5	239.8	-50.95
61996.7	-3714527.8	6	239	-50.96
61984	-3714530	7	238.5	-50.96
61971.8	-3714532	8	238.4	-50.95
61959.2	-3714534	9	238.4	-50.95
61946.3	-3714535.8	10	238.6	-50.93
61932.7	-3714538.5	11	238.7	-50.87
61917.8	-3714541.2	12	238.8	-50.93
61902.1	-3714543.4	13	239.1	-50.92
61887.2	-3714546.5	14	239.4	-50.92
61872.1	-3714549.1	15	239.4	-50.93
61857.7	-3714551	16	239.4	-50.95
61842.7	-3714554	17	239.5	-50.95
61827.5	-3714555.7	18	239.9	-50.96
61812.6	-3714559.2	19	240.4	-50.94
61797.4	-3714562	20	240.3	-50.94
61781.9	-3714564.5	21	240.2	-50.94
61766.6	-3714567	22	240.6	-50.97
61750.8	-3714570.2	23	241	-50.97
61735.3	-3714573.1	24	241.4	-51.04
61720.3	-3714575.8	25	241.4	-51.05
61705	-3714578.5	26	241.5	-51.07
61688.9	-3714581.1	27	241.8	-51.03
61673	-3714584.1	28	241.8	-51.1
61658.2	-3714587.2	29	241.7	-51.09
61643.1	-3714589.7	30	241.4	-51.14
61627.5	-3714592.4	31	241.6	-51.12
61611.9	-3714594.9	32	241.7	-51.17
61597.4	-3714598.2	33	241.3	-51.19
61582.1	-3714601.5	34	241.9	-51.21
61566	-3714604.5	35	242.4	-51.23
61550	-3714607.1	36	242.7	-51.26
61534.3	-3714610.2	37	242.8	-51.3
61517	-3714613.3	38	242.4	-51.32

Coordinates and Elevations: Profile 2 continued

61500.1	-3714616.5	39	243.4	-51.39
61484.8	-3714619.4	40	243.3	-51.43
61469.5	-3714621.9	41	243.4	-51.47
61454.3	-3714624.6	42	243.5	-51.51
61438.6	-3714627.9	43	243.8	-51.54
61423.2	-3714631.3	44	243.9	-51.63
61408.4	-3714634.8	45	243.5	-51.69
61392.1	-3714637.8	46	243.6	-51.78
61377	-3714641.1	47	244.2	-51.88
61361.3	-3714643.3	48	244	-51.99
61347.4	-3714653.9	49	244	-52.08
61333	-3714660	50	244.5	-52.19
61318	-3714661.4	51	244.8	-52.41
61304.3	-3714665.5	52	244.7	-52.57

Coordinates and Elevations: Profile 3

Elevation data obtained with Sokkia Differential GPS system  
(Longitude (m), Latitude (m), Station number, Elevation (mamsl))

61602.8	-3713391	105	227.1	-51.72
61586.8	-3713388.8	104	227	-51.76
61571.6	-3713387.2	103	227.1	-51.81
61555.8	-3713384.6	102	227.1	-51.78
61540.7	-3713381.4	101	227.1	-51.83
61522.9	-3713380	100	227.7	-51.86
61506.6	-3713376.3	99	228.1	-51.91
61491.1	-3713371.5	98	230.1	-51.88
61476.5	-3713368.7	97	233	-51.84
61461.8	-3713366	96	234.6	-51.85
61445.6	-3713363.9	95	235	-51.84
61429.3	-3713362.1	94	233.9	-51.88
61412.6	-3713360	93	232.3	-51.91
61396.4	-3713358.1	92	233.4	-51.94
61380.7	-3713355.3	91	235	-51.95
61365.4	-3713352.9	90	235.3	-51.98
61350.3	-3713351.1	89	233.3	-52.03
61333.8	-3713349.8	88	231.7	-52.11
61315.8	-3713349	87	230.5	-52.19
61299.6	-3713350.4	86	230	-52.21
61282.5	-3713349.4	85	229.5	-52.26
61266.7	-3713350	84	229.5	-52.26
61248.1	-3713348.8	83	229.5	-52.31

Coordinates and Elevations: Profile 3 continued

61231.2	-3713350	82	230.4	-52.37
61216.9	-3713357.3	81	231	-52.43
61205.4	-3713368.9	80	231.5	-52.45
61200.2	-3713383.1	79	232.2	-52.38
61198.6	-3713399	78	232.8	-52.35
61190.6	-3713412.2	77	233.4	-52.36
61181.6	-3713425.1	76	234.4	-52.38
61175.4	-3713439	75	234.8	-52.42
61187	-3713452.9	74	234.2	-52.41
61194.9	-3713466.8	73	234.8	-52.44
61195.4	-3713483.2	72	235.4	-52.47
61195.7	-3713500	71	236	-52.5
61196.3	-3713516.7	70	236.6	-52.48
61194.2	-3713532.2	69	237.3	-52.48
61180.4	-3713542.3	68	237.6	-52.54
61170.7	-3713554.6	67	237.8	-52.6
61153.5	-3713555.5	66	238	-52.66
61138	-3713551.8	65	238.4	-52.69
61123.1	-3713551	64	238.8	-52.72
61107.8	-3713552.3	63	239.7	-52.78
61092.1	-3713550.2	62	240.2	-52.85
61076.4	-3713547.5	61	240.7	-52.87
61059.4	-3713544	60	241.2	-53
61043.7	-3713541.6	59	242	-53.13
61028.5	-3713541.9	58	242.2	-53.31
61013	-3713544	57	242.3	-53.52
61000.4	-3713550.4	56	242.9	-53.69
60985.7	-3713552.2	55	244.1	-53.79
60970.2	-3713558.5	54	245.3	-53.92

Coordinates and Elevations: Tie in between Profile 1 North and Profile 1 South

Elevation data obtained with Sokkia Differential GPS system  
(Longitude (m), Latitude (m), Station number, Elevation (mamsl))

83948.8	-3721547.5	106	232.3	-42.86	(Station 57 Profile 1 South)
83945	-3721711.3	107	229.9	-42.45	(Station 55 Profile 1 South)
83806.6	-3721577.1	108	232.2	-42.63	
83549.1	-3721685.7	109	233.1	-42.21	(Station 00 Profile 1 North)
83461.7	-3721509.1	110	237.5	-44.82	
83398.4	-3721233.3	111	244.4	-41.1	

### Reduced Gravity values

#### Reduced gravity: Profile 1

Station	Long	Lat	Elevation (mamsl)	Bouguer gravity (mgal)	Regional gravity (mgal)	Residual gravity (mgal)
0	-82472	3726985.9	325.7	38.55	38.55	0.00
1	-82508.4	3726891.9	321.1	38.35	38.51	-0.17
2	-82545.9	3726798.9	318.4	38.23	38.48	-0.25
3	-82583.4	3726705.8	316.7	38.09	38.44	-0.35
4	-82623.2	3726612.6	314.1	37.77	38.40	-0.64
5	-82659.6	3726519.2	310.9	37.40	38.37	-0.97
6	-82698.3	3726426.4	308.1	37.03	38.33	-1.30
7	-82735.5	3726332.6	305.4	36.75	38.29	-1.54
8	-82773	3726238.8	302.4	36.51	38.26	-1.74
9	-82811	3726145.9	299.6	36.28	38.22	-1.94
10	-82849.3	3726052	296.8	36.05	38.18	-2.14
11	-82888.5	3725958.9	294.9	35.78	38.14	-2.36
12	-82925	3725866.7	293	35.56	38.11	-2.55
13	-82964.1	3725772.7	290.8	35.31	38.07	-2.76
14	-83002.1	3725679.1	289.4	35.04	38.03	-2.98
15	-83039.9	3725584.7	287.4	34.78	37.99	-3.21
16	-83078	3725491.4	284.7	34.55	37.95	-3.40
17	-83115.2	3725397.7	282.3	34.30	37.91	-3.62
18	-83152.9	3725303.3	280.7	34.23	37.88	-3.65
19	-83191.6	3725209.7	273.1	33.99	37.84	-3.85
20	-83229.8	3725117.1	269.2	33.73	37.80	-4.07
21	-83268	3725023.7	266.7	33.35	37.76	-4.41
22	-83305.2	3724930.2	264.2	33.12	37.71	-4.59
23	-83343.8	3724837.5	261.2	32.89	37.67	-4.78
24	-83381.7	3724743.9	258.4	32.67	37.62	-4.95
25	-83419.9	3724650.3	255.7	32.38	37.58	-5.20
26	-83458	3724556.9	253.2	32.24	37.53	-5.29
27	-83495.8	3724463.7	250.5	32.06	37.49	-5.43
28	-83534	3724370.4	248.2	31.88	37.44	-5.56
29	-83572	3724277.1	245.6	31.76	37.40	-5.64
30	-83609.8	3724183.7	243.2	31.60	37.36	-5.75
31	-83648	3724090.1	240.9	31.46	37.31	-5.85
32	-83686.1	3723996.8	239	31.30	37.27	-5.97
33	-83724.4	3723903.9	236.7	31.17	37.22	-6.06
34	-83763.2	3723810.6	232.7	30.92	37.18	-6.26
35	-83801.5	3723717.7	230	30.71	37.13	-6.42
36	-83839.3	3723623.9	227.9	30.60	37.09	-6.49
37	-83862.1	3723525.4	226.3	30.55	37.04	-6.50

Reduced gravity: Profile 1 continued

38	-83869.8	3723424.8	222.6	30.34	37.00	-6.66
39	-83876.9	3723324.4	221.4	30.19	36.95	-6.76
40	-83882.7	3723223.5	218.7	30.10	36.90	-6.80
41	-83890.8	3723123.8	217.4	29.95	36.86	-6.91
42	-83898.2	3723023.1	218.4	29.85	36.81	-6.96
43	-83910.1	3722922.1	220.5	29.60	36.76	-7.16
44	-83917.7	3722821.8	223.2	29.44	36.71	-7.27
45	-83919.8	3722720.8	223.5	29.28	36.67	-7.39
46	-83922.1	3722619.6	223.7	29.06	36.62	-7.56
47	-83924.8	3722518.9	223.9	28.90	36.57	-7.68
48	-83927.3	3722418.1	224.4	28.64	36.52	-7.89
49	-83930.6	3722316.8	224.7	28.38	36.48	-8.09
50	-83932.1	3722216	225.3	28.17	36.43	-8.26
51	-83935.5	3722115.4	226	28.01	36.38	-8.37
52	-83938.5	3722014.5	227	27.86	36.33	-8.47
53	-83939.9	3721912.9	228	27.72	36.29	-8.57
54	-83943.6	3721812.5	229.3	27.51	36.24	-8.73
55	-83945.2	3721711.3	229.9	27.31	36.19	-8.88
56	-83948.5	3721610.3	231.2	27.08		
57	-83949.5	3721540.7	232.2	26.90		
0	-83549	3721686	233.1	27.20	36.17	-8.97
200	-83473	3721506	238.2	26.90	36.06	-9.16
400	-83397	3721326	243.2	26.59	35.96	-9.36
600	-83383	3721136	248.0	26.19	35.85	-9.66
800	-83431	3720936	246.5	25.78	35.74	-9.96
1000	-83479	3720736	250.2	25.31	35.63	-10.33
1200	-83527	3720536	248.6	24.85	35.53	-10.68
1400	-83575	3720336	249.3	24.52	35.42	-10.91
1600	-83571	3720126	252.0	24.11	35.31	-11.20
1800	-83515	3719906	250.9	23.72	35.21	-11.49
2000	-83459	3719686	250.6	23.47	35.10	-11.63
2200	-83443	3719506	250.7	23.16	34.99	-11.84
2400	-83427	3719326	253.1	22.93	34.89	-11.96
2600	-83397	3719140	258.5	22.64	34.78	-12.14
2800	-83353	3718949	263.2	22.45	34.67	-12.22
3000	-83309	3718757	257.9	22.03	34.56	-12.54
3200	-83265	3718566	271.2	21.81	34.46	-12.65
3400	-83221	3718375	275.4	21.54	34.35	-12.81
3600	-83177	3718183	277.1	21.17	34.24	-13.07
3800	-83133	3717992	279.5	20.91	34.14	-13.23
4000	-83089	3717800	281.5	20.65	34.03	-13.38
4200	-83045	3717609	283.4	20.34	33.92	-13.58
4400	-83001	3717417	284.1	20.03	33.81	-13.79

Reduced gravity: Profile 1 continued

4600	-82957	3717226	287.3	19.73	33.71	-13.98
4800	-82913	3717035	289.1	19.48	33.60	-14.12
5000	-82869	3716843	291.0	19.27	33.49	-14.22
5200	-82825	3716652	291.3	19.15	33.37	-14.23
5400	-82781	3716460	294.4	18.99	33.26	-14.27
5600	-82737	3716269	296.0	18.85	33.15	-14.29
5800	-82693	3716077	293.4	18.69	33.04	-14.35
6000	-82649	3715886	300.4	18.61	32.92	-14.32
6200	-82449	3715761	297.9	18.52	32.81	-14.29
6400	-82249	3715636	311.8	18.59	32.70	-14.10
6600	-82149	3715469	314.0	18.59	32.58	-13.99
6800	-82049	3715303	315.9	18.52	32.47	-13.95
7000	-81949	3715136	317.1	18.47	32.36	-13.89
7200	-81849	3714969	318.6	18.38	32.25	-13.87
7400	-81749	3714803	319.6	18.32	32.13	-13.81
7600	-81649	3714636	320.7	18.28	32.02	-13.74
7800	-81549	3714469	322.0	18.22	31.91	-13.68
8000	-81449	3714303	324.0	18.05	31.79	-13.74
8200	-81349	3714136	325.8	17.99	31.68	-13.69
8400	-81249	3713969	326.3	17.91	31.57	-13.66
8600	-81149	3713803	327.5	17.78	31.45	-13.67
8800	-81049	3713636	329.8	17.79	31.34	-13.56
9000	-81182	3713503	324.4	17.69	31.23	-13.54
9200	-81316	3713369	308.8	17.46	31.12	-13.65
9400	-81449	3713236	309.9	17.52	31.00	-13.48
9600	-81649	3713169	315.0	17.61	30.89	-13.28
9800	-81699	3713061	318.1	17.64	30.78	-13.14
10000	-81655	3712881	327.1	17.66	30.66	-13.01
10200	-81667	3712671	330.6	17.81	30.55	-12.74
10400	-81679	3712461	334.7	17.84	30.44	-12.60
10600	-81691	3712251	337.7	18.04	30.33	-12.29
10800	-81703	3712041	341.2	18.31	30.21	-11.90
11000	-81715	3711831	345.3	18.74	30.10	-11.36
11200	-81727	3711621	350.5	19.02	29.96	-10.94
11400	-81739	3711411	357.6	19.58	29.83	-10.25
11600	-81751	3711201	365.8	20.11	29.69	-9.58
11800	-81763	3710991	374.8	20.62	29.55	-8.93
12000	-81682	3710844	386.6	21.16	29.41	-8.25
12200	-81509	3710761	396.7	21.60	29.26	-7.67
12400	-81336	3710678	408.4	21.91	29.12	-7.21
12600	-81196	3710553	415.9	22.33	28.95	-6.62
12800	-81091	3710386	417.2	22.76	28.81	-6.05
13000	-80985	3710219	408.6	22.96	28.67	-5.71
13200	-80880	3710053	401.2	23.12	28.47	-5.35

Reduced gravity: Profile 1 continued

13400	-80774	3709886	393.5	23.27	28.28	-5.01
13600	-80766	3709669	389.6	23.49	28.10	-4.60
13800	-80757	3709453	384.1	23.83	27.91	-4.08
14000	-80749	3709236	380.0	23.99	27.68	-3.69
14200	-80894	3709086	390.0	24.45	27.36	-2.91
14400	-81039	3708936	402.5	25.11	27.10	-1.99
14600	-81098	3708749	409.5	25.71	26.73	-1.02
14800	-81157	3708561	411.7	25.88	26.40	-0.52
15000	-81215	3708374	411.0	25.80	25.97	-0.17
15200	-81274	3708186	405.5	25.76	25.24	0.52
15400	-81318	3707986	402.4	24.20	24.51	-0.31
15600	-81362	3707786	403.3	23.34	23.77	-0.43
15800	-81405	3707586	406.8	22.89	23.04	-0.16
16000	-81449	3707386	410.1	22.21	22.31	-0.10

Reduced gravity: Profile 2

Station	Long	Lat	Elevation (mamsl)	Bouguer gravity (mgal)	Regional gravity (mgal)	Residual gravity (mgal)
0	-62064.8	3714516	240.1	18.72	19.00	-0.28
1	-62055.2	3714516.3	240.1	18.72	19.01	-0.28
2	-62045.1	3714518	240.2	18.71	19.01	-0.29
3	-62033	3714520	240.1	18.71	19.02	-0.29
4	-62020.7	3714522.1	239.9	18.72	19.02	-0.28
5	-62009	3714525.5	239.8	18.71	19.03	-0.29
6	-61996.7	3714527.8	239	18.68	19.03	-0.32
7	-61984	3714530	238.5	18.66	19.04	-0.34
8	-61971.8	3714532	238.4	18.67	19.05	-0.33
9	-61959.2	3714534	238.4	18.66	19.05	-0.34
10	-61946.3	3714535.8	238.6	18.69	19.06	-0.31
11	-61932.7	3714538.5	238.7	18.75	19.06	-0.25
12	-61917.8	3714541.2	238.8	18.70	19.07	-0.30
13	-61902.1	3714543.4	239.1	18.70	19.08	-0.30
14	-61887.2	3714546.5	239.4	18.71	19.08	-0.29
15	-61872.1	3714549.1	239.4	18.70	19.09	-0.30
16	-61857.7	3714551	239.4	18.67	19.09	-0.33
17	-61842.7	3714554	239.5	18.66	19.10	-0.34

Reduced gravity: Profile 2 continued

18	-61827.5	3714555.7	239.9	18.68	19.10	-0.32
19	-61812.6	3714559.2	240.4	18.70	19.11	-0.30
20	-61797.4	3714562	240.3	18.69	19.12	-0.31
21	-61781.9	3714564.5	240.2	18.70	19.12	-0.30
22	-61766.6	3714567	240.6	18.67	19.13	-0.33
23	-61750.8	3714570.2	241	18.66	19.13	-0.34
24	-61735.3	3714573.1	241.4	18.61	19.14	-0.39
25	-61720.3	3714575.8	241.4	18.60	19.14	-0.40
26	-61705	3714578.5	241.5	18.58	19.15	-0.42
27	-61688.9	3714581.1	241.8	18.62	19.16	-0.38
28	-61673	3714584.1	241.8	18.55	19.16	-0.45
29	-61658.2	3714587.2	241.7	18.55	19.17	-0.45
30	-61643.1	3714589.7	241.4	18.50	19.17	-0.50
31	-61627.5	3714592.4	241.6	18.51	19.18	-0.49
32	-61611.9	3714594.9	241.7	18.47	19.18	-0.53
33	-61597.4	3714598.2	241.3	18.44	19.19	-0.56
34	-61582.1	3714601.5	241.9	18.43	19.20	-0.57
35	-61566	3714604.5	242.4	18.41	19.20	-0.59
36	-61550	3714607.1	242.7	18.39	19.21	-0.61
37	-61534.3	3714610.2	242.8	18.34	19.21	-0.66
38	-61517	3714613.3	242.4	18.33	19.22	-0.67
39	-61500.1	3714616.5	243.4	18.27	19.23	-0.73
40	-61484.8	3714619.4	243.3	18.21	19.23	-0.79
41	-61469.5	3714621.9	243.4	18.19	19.24	-0.81
42	-61454.3	3714624.6	243.5	18.14	19.24	-0.86
43	-61438.6	3714627.9	243.8	18.12	19.25	-0.88
44	-61423.2	3714631.3	243.9	18.03	19.25	-0.97
45	-61408.4	3714634.8	243.5	17.97	19.26	-1.03
46	-61392.1	3714637.8	243.6	17.87	19.27	-1.13
47	-61377	3714641.1	244.2	17.79	19.27	-1.21
48	-61361.3	3714643.3	244	17.66	19.28	-1.34
49	-61347.4	3714653.9	244	17.58	19.28	-1.42
50	-61333	3714660	244.5	17.47	19.29	-1.53
51	-61318	3714661.4	244.8	17.25	19.29	-1.75
52	-61304.3	3714665.5	244.7	17.09	19.30	-1.91

Reduced Gravity: Profile 3

Station	Long	Lat	Elevation (mamsl)	Bouguer gravity (mgal)	Regional gravity (mgal)	Residual gravity (mgal)
54	-60970.2	3713558.5	245.3	15.75	18.0	-2.25
55	-60985.7	3713552.2	244.1	15.87	18.0	-2.13
56	-61000.4	3713550.4	242.9	15.96	18.0	-2.04
57	-61013	3713544	242.3	16.11	18.0	-1.89
58	-61028.5	3713541.9	242.2	16.34	18.0	-1.66
59	-61043.7	3713541.6	242	16.50	18.0	-1.5
60	-61059.4	3713544	241.2	16.62	18.0	-1.38
61	-61076.4	3713547.5	240.7	16.75	18.0	-1.25
62	-61092.1	3713550.2	240.2	16.76	18.0	-1.24
63	-61107.8	3713552.3	239.7	16.83	18.0	-1.17
64	-61123.1	3713551	238.8	16.87	18.0	-1.13
65	-61138	3713551.8	238.4	16.91	18.0	-1.09
66	-61153.5	3713555.5	238	16.93	18.0	-1.07
67	-61170.7	3713554.6	237.8	16.99	18.0	-1.01
68	-61180.4	3713542.3	237.6	17.01	18.0	-0.97
69	-61194.2	3713532.2	237.3	17.10	18.0	-0.90
70	-61196.3	3713516.7	236.6	17.08	18.0	-0.92
71	-61195.7	3713500	236	17.06	18.0	-0.94
72	-61195.4	3713483.2	235.4	17.08	18.0	-0.92
73	-61194.9	3713466.8	234.8	17.10	18.0	-0.90
74	-61187	3713452.9	234.2	17.13	18.0	-0.87
75	-61175.4	3713439	234.8	17.12	18.0	-0.88
76	-61181.6	3713425.1	234.4	17.15	18.0	-0.85
77	-61190.6	3713412.2	233.45	17.15	18.0	-0.85
78	-61198.6	3713399	232.8	17.16	18.0	-0.84
79	-61200.2	3713383.1	232.2	17.12	18.0	-0.88
80	-61205.4	3713368.9	231.53	17.04	18.0	-0.96
81	-61216.9	3713357.3	231	17.06	18.0	-0.94
82	-61231.2	3713350	230.4	17.11	18.0	-0.89
83	-61248.1	3713348.8	229.5	17.16	18.0	-0.84
84	-61266.7	3713350	229.5	17.21	18.0	-0.79
85	-61282.5	3713349.4	229.5	17.21	18.0	-0.79
86	-61299.6	3713350.4	230	17.26	18.0	-0.74
87	-61315.8	3713349	230.5	17.29	18.0	-0.71
88	-61333.8	3713349.8	231.7	17.39	18.0	-0.61
89	-61350.3	3713351.1	233.3	17.50	18.0	-0.5
90	-61365.4	3713352.9	235.3	17.56	18.0	-0.44
91	-61380.7	3713355.3	235	17.59	18.0	-0.41
92	-61396.4	3713358.1	233.4	17.57	18.0	-0.43

Reduced gravity: Profile 3 continued

93	-61412.6	3713360	232.3	17.58	18.0	-0.42
94	-61429.3	3713362.1	233.9	17.65	18.0	-0.35
95	-61445.6	3713363.9	235	17.70	18.0	-0.3
96	-61461.8	3713366	234.6	17.68	18.0	-0.32
97	-61476.5	3713368.7	233	17.68	18.0	-0.32
98	-61491.1	3713371.5	230.1	17.59	18.0	-0.41
99	-61506.6	3713376.3	228.1	17.54	18.0	-0.46
100	-61522.9	3713380	227.7	17.59	18.0	-0.41
101	-61540.7	3713381.4	227.1	17.61	18.0	-0.39
102	-61555.8	3713384.6	227.1	17.65	18.0	-0.35
103	-61571.6	3713387.2	227.1	17.63	18.0	-0.37
104	-61586.8	3713388.8	227	17.68	18.0	-0.32
105	-61602.8	3713391	227.1	17.73	18.0	-0.27

Reduced Gravity: Profile 1 South – 1 North Tie-in

Profile	Station	Long	Lat	Elevation (mamsl)	Bouguer gravity (mgal)
1 South	57	-83948.8	3721547.5	232.3	26.56
1 South	55	-83945	3721711.3	229.9	26.93
		-83806.6	3721577.1	232.2	26.78
1 North	0	-83549.1	3721685.7	233.1	27.22
1 North	200	-83461.7	3721509.1	237.5	24.68
1 North	600	-83398.4	3721233.3	244.4	28.49

## GHP3949

### APPENDIX B

#### Gravity model: Input data listing

The gravity data used in the models (Appendix C) is the residual gravity obtained from the relevant Bouguer gravity data and regional gravity as chosen (Appendix A).

##### Profile 1

The regional field was chosen so that the residual gravity is zero at the start of the profile (TMS/Bokkeveld) as well as at the end of the profile (Cango). The overlapping stations at the join of the South and North parts of the profile is omitted. The first station (0) is the southernmost station of the profile, profile runs north. The station values are meters along a true South – North projection of the profile.

Station (m)	Elevation (mamsl)	Bouguer gravity (mgal)	Regional gravity (mgal)	Residual gravity (mgal)
0	325.7	38.55	38.55	0.00
94	321.1	38.35	38.51	-0.17
187	318.4	38.23	38.48	-0.25
280	316.7	38.09	38.44	-0.35
373	314.1	37.77	38.40	-0.64
466	310.9	37.40	38.37	-0.97
559	308.1	37.03	38.33	-1.30
653	305.4	36.75	38.29	-1.54
747	302.4	36.51	38.26	-1.74
840	299.6	36.28	38.22	-1.94
933	296.8	36.05	38.18	-2.14
1027	294.9	35.78	38.14	-2.36
1119	293	35.56	38.11	-2.55
1213	290.8	35.31	38.07	-2.76
1306	289.4	35.04	38.03	-2.98
1401	287.4	34.78	37.99	-3.21
1494	284.7	34.55	37.95	-3.40
1588	282.3	34.30	37.91	-3.62
1682	280.7	34.23	37.88	-3.65
1776	273.1	33.99	37.84	-3.85
1868	269.2	33.73	37.80	-4.07
1962	266.7	33.35	37.76	-4.41
2055	264.2	33.12	37.71	-4.59
2148	261.2	32.89	37.67	-4.78
2242	258.4	32.67	37.62	-4.95

Gravity model: Input data listing Profile 1 (Continued)

Station (m)	Elevation (mamsl)	Bouguer gravity (mgal)	Regional gravity (mgal)	Residual gravity (mgal)
2335	255.7	32.38	37.58	-5.20
2429	253.2	32.24	37.53	-5.29
2522	250.5	32.06	37.49	-5.43
2615	248.2	31.88	37.44	-5.56
2708	245.6	31.76	37.40	-5.64
2802	243.2	31.60	37.36	-5.75
2895	240.9	31.46	37.31	-5.85
2989	239	31.30	37.27	-5.97
3082	236.7	31.17	37.22	-6.06
3175	232.7	30.92	37.18	-6.26
3268	230	30.71	37.13	-6.42
3362	227.9	30.60	37.09	-6.49
3460	226.3	30.55	37.04	-6.50
3561	222.6	30.34	37.00	-6.66
3661	221.4	30.19	36.95	-6.76
3762	218.7	30.10	36.90	-6.80
3862	217.4	29.95	36.86	-6.91
3962	218.4	29.85	36.81	-6.96
4063	220.5	29.60	36.76	-7.16
4164	223.2	29.44	36.71	-7.27
4265	223.5	29.28	36.67	-7.39
4366	223.7	29.06	36.62	-7.56
4467	223.9	28.90	36.57	-7.68
4567	224.4	28.64	36.52	-7.89
4669	224.7	28.38	36.48	-8.09
4769	225.3	28.17	36.43	-8.26
4870	226	28.01	36.38	-8.37
4971	227	27.86	36.33	-8.47
5073	228	27.72	36.29	-8.57
5173	229.3	27.51	36.24	-8.73
5274	229.9	27.31	36.19	-8.88
5299	233.1	27.20	36.17	-8.97
5479	238.2	26.90	36.07	-9.17
5659	243.2	26.59	35.97	-9.38
5849	248.0	26.19	35.88	-9.69
6049	246.5	25.78	35.78	-9.99
6249	250.2	25.31	35.68	-10.37
6449	248.6	24.85	35.58	-10.73
6649	249.3	24.52	35.48	-10.97
6859	252.0	24.11	35.38	-11.27
7079	250.9	23.72	35.29	-11.57

Gravity model: Input data listing Profile 1 (Continued)

Station (m)	Elevation (mamsl)	Bouguer gravity (mgal)	Regional gravity (mgal)	Residual gravity (mgal)
7299	250.6	23.47	35.19	-11.72
7479	250.7	23.16	35.09	-11.93
7659	253.1	22.93	34.99	-12.06
7845	258.5	22.64	34.87	-12.24
8037	263.2	22.45	34.76	-12.31
8228	257.9	22.03	34.64	-12.61
8419	271.2	21.81	34.53	-12.72
8611	275.4	21.54	34.41	-12.87
8802	277.1	21.17	34.30	-13.12
8994	279.5	20.91	34.18	-13.27
9185	281.5	20.65	34.07	-13.41
9377	283.4	20.34	33.95	-13.61
9568	284.1	20.03	33.83	-13.81
9759	287.3	19.73	33.72	-13.99
9951	289.1	19.48	33.60	-14.12
10142	291.0	19.27	33.49	-14.22
10334	291.3	19.15	33.37	-14.23
10525	294.4	18.99	33.26	-14.27
10717	296.0	18.85	33.15	-14.29
10908	293.4	18.69	33.04	-14.35
11099	300.4	18.61	32.95	-14.35
11224	297.9	18.52	32.87	-14.35
11349	311.8	18.59	32.78	-14.19
11516	314.0	18.59	32.70	-14.11
11683	315.9	18.52	32.59	-14.07
11849	317.1	18.47	32.50	-14.03
12016	318.6	18.38	32.40	-14.02
12183	319.6	18.32	32.31	-13.99
12349	320.7	18.28	32.20	-13.91
12516	322.0	18.22	32.08	-13.86
12683	324.0	18.05	31.96	-13.91
12849	325.8	17.99	31.84	-13.86
13016	326.3	17.91	31.73	-13.82
13183	327.5	17.78	31.61	-13.82
13349	329.8	17.79	31.51	-13.72
13483	324.4	17.69	31.40	-13.72
13616	308.8	17.46	31.35	-13.89
13749	309.9	17.52	31.24	-13.72
13816	315.0	17.61	31.20	-13.59

Gravity model: Input data listing Profile 1 (Continued)

Station (m)	Elevation (mamsl)	Bouguer gravity (mgal)	Regional gravity (mgal)	Residual gravity (mgal)
13924	318.1	17.64	31.10	-13.46
14104	327.1	17.66	31.01	-13.35
14314	330.6	17.81	30.82	-13.01
14524	334.7	17.84	30.67	-12.83
14734	337.7	18.04	30.52	-12.48
14944	341.2	18.31	30.37	-12.06
15154	345.3	18.74	30.21	-11.47
15364	350.5	19.02	30.04	-11.02
15574	357.6	19.58	29.88	-10.30
15784	365.8	20.11	29.71	-9.61
15994	374.8	20.62	29.55	-8.93
16141	386.6	21.16	29.46	-8.30
16224	396.7	21.60	29.38	-7.78
16308	408.4	21.91	29.29	-7.38
16433	415.9	22.33	29.20	-6.87
16599	417.2	22.76	29.02	-6.26
16766	408.6	22.96	28.83	-5.88
16933	401.2	23.12	28.65	-5.53
17099	393.5	23.27	28.50	-5.23
17316	389.6	23.49	28.25	-4.76
17533	384.1	23.83	28.00	-4.17
17749	380.0	23.99	27.68	-3.69
17899	390.0	24.45	27.36	-2.91
18049	402.5	25.11	27.10	-1.99
18237	409.5	25.71	26.73	-1.02
18424	411.7	25.88	26.40	-0.52
18612	411.0	25.80	25.97	-0.17
18799	405.5	25.76	25.24	0.52
18999	402.4	24.20	24.51	-0.31
19199	403.3	23.34	23.77	-0.43
19399	406.8	22.89	23.04	-0.16
19599	410.1	22.21	22.31	-0.10

Cango Fault line at Station 18612  
Profile ends on TMS

## Gravity model: Input data listing Profile 2

The regional field was initially chosen to be flat from west to east along the profile direction, but modelling indicated that a regional gradient was required to attain acceptable model fit. Station values are meters along a West – East projection of the profile, with duplicate positions removed.

Station (m)	Elevation (mamsl)	Bouguer gravity (mgal)	Regional gravity (mgal)	Residual gravity (mgal)
0	240.1	18.72	19.00	-0.28
9.6	240.1	18.72	19.01	-0.28
19.7	240.2	18.71	19.01	-0.29
31.8	240.1	18.71	19.02	-0.29
44.1	239.9	18.72	19.02	-0.28
55.8	239.8	18.71	19.03	-0.29
68.1	239	18.68	19.03	-0.32
80.8	238.5	18.66	19.04	-0.34
93	238.4	18.67	19.05	-0.33
105.6	238.4	18.66	19.05	-0.34
118.5	238.6	18.69	19.06	-0.31
132.1	238.7	18.75	19.06	-0.25
147	238.8	18.70	19.07	-0.30
162.7	239.1	18.70	19.08	-0.30
177.6	239.4	18.71	19.08	-0.29
192.7	239.4	18.70	19.09	-0.30
207.1	239.4	18.67	19.09	-0.33
222.1	239.5	18.66	19.10	-0.34
237.3	239.9	18.68	19.10	-0.32
252.2	240.4	18.70	19.11	-0.30
267.4	240.3	18.69	19.12	-0.31
282.9	240.2	18.70	19.12	-0.30
298.2	240.6	18.67	19.13	-0.33
314	241	18.66	19.13	-0.34
329.5	241.4	18.61	19.14	-0.39
344.5	241.4	18.60	19.14	-0.40
359.8	241.5	18.58	19.15	-0.42
375.9	241.8	18.62	19.16	-0.38
391.8	241.8	18.55	19.16	-0.45
406.6	241.7	18.55	19.17	-0.45
421.7	241.4	18.50	19.17	-0.50
437.3	241.6	18.51	19.18	-0.49
452.9	241.7	18.47	19.18	-0.53
467.4	241.3	18.44	19.19	-0.56
482.7	241.9	18.43	19.20	-0.57

Gravity model: Input data listing Profile 2 (Continued)

Station (m)	Elevation (mamsl)	Bouguer gravity (mgal)	Regional gravity (mgal)	Residual gravity (mgal)
498.8	242.4	18.41	19.20	-0.59
514.8	242.7	18.39	19.21	-0.61
530.5	242.8	18.34	19.21	-0.66
547.8	242.4	18.33	19.22	-0.67
564.7	243.4	18.27	19.23	-0.73
580	243.3	18.21	19.23	-0.79
595.3	243.4	18.19	19.24	-0.81
610.5	243.5	18.14	19.24	-0.86
626.2	243.8	18.12	19.25	-0.88
641.6	243.9	18.03	19.25	-0.97
656.4	243.5	17.97	19.26	-1.03
672.7	243.6	17.87	19.27	-1.13
687.8	244.2	17.79	19.27	-1.21
703.5	244	17.66	19.28	-1.34
717.4	244	17.58	19.28	-1.42
731.8	244.5	17.47	19.29	-1.53
746.8	244.8	17.25	19.29	-1.75
760.5	244.7	17.09	19.30	-1.91

### Gravity model: Input data listing Profile 3

The regional field was chosen to be flat from west to east along the profile direction. Station values are meters along a West -East projection of the profile, with duplicate positions removed.

Station (m)	Elevation (mamsl)	Bouguer gravity (mgal)	Regional gravity (mgal)	Residual gravity (mgal)
0	227.1	17.73	18	-0.27
16	227	17.68	18	-0.32
31.2	227.1	17.63	18	-0.37
47	227.1	17.65	18	-0.35
62.1	227.1	17.61	18	-0.39
79.9	227.7	17.59	18	-0.41
96.2	228.1	17.54	18	-0.46
111.7	230.1	17.59	18	-0.41
126.3	233	17.68	18	-0.32
141	234.6	17.68	18	-0.32
157.2	235	17.70	18	-0.30
173.5	233.9	17.65	18	-0.35
190.2	232.3	17.58	18	-0.42
206.4	233.4	17.57	18	-0.43
222.1	235	17.59	18	-0.41
237.4	235.3	17.56	18	-0.44
252.5	233.3	17.50	18	-0.50
269	231.7	17.39	18	-0.61
287	230.5	17.29	18	-0.71
303.2	230	17.26	18	-0.74
320.3	229.5	17.21	18	-0.79
336.1	229.5	17.21	18	-0.79
354.7	229.5	17.16	18	-0.84
371.6	230.4	17.11	18	-0.89
385.9	231	17.06	18	-0.94
397.4	231.5	17.04	18	-0.96
412.2	233.4	17.03	18	-0.92
421.2	234.4	17.01	18	-0.92
432.1	237.8	16.99	18	-1.01
449.3	238	16.93	18	-1.07
464.8	238.4	16.91	18	-1.09
479.7	238.8	16.87	18	-1.13
495	239.7	16.83	18	-1.17
510.7	240.2	16.76	18	-1.24
526.4	240.7	16.75	18	-1.25
543.4	241.2	16.62	18	-1.38

Gravity model: Input data listing Profile 3 (Continued)

Station (m)	Elevation (mamsl)	Bouguer gravity (mgal)	Regional gravity (mgal)	Residual gravity (mgal)
559.1	242	16.50	18	-1.50
574.3	242.2	16.34	18	-1.66
589.8	242.3	16.11	18	-1.89
602.4	242.9	15.96	18	-2.04
617.1	244.1	15.87	18	-2.13
632.6	245.3	15.75	18	-2.25

## GHP3949

### APPENDIX C

#### Synthetic Gravity Models

This appendix contains data listings for the MAGIXXL software program, as well as the relevant plots of model geometry and gravity model curves. The Vertices listed are the corners of the relevant body modeled. X-Loc indicates the horizontal position of the vertex in meters, Z-Loc indicates the elevation of the vertex, in meters. Negative values of Z indicate elevations above sea/ground level, while positive values of Z indicate elevations below sea/ground level. Densities refer to the density contrast of the relevant body to the background density – e.g. (KK1) TMS background with an assumed density of 2.62 g/cc (Density contrast 0), Cretaceous basin (Body 1) with assumed density of 2.38 g/cc: Density Contrast -0.24 g/cc, Sulphide mineralisation on the Swartberg Fault (Body 2), assumed density 4.5 g/cc, Density Contrast: 1.88 g/cc. Bodies are modeled as two-dimensional structures with finite strike length.

#### I Gravity models of Profile data

##### Profile 1

Two models are presented, with different density contrasts for the Cretaceous sediments.

##### Model KK1

Densities:      TMS: 2.62 g/cc  
                    Cretaceous 2.38 g/cc  
                    Sulphides on Swartberg Fault 4.5 g/cc

MAGIXXL Gravity Model Data

KK1 Model Date 31/10/2005

Sulphides on Swartberg Fault

Data Set :            KK1.MGX

Location:      Calitzdorp                      Profile: Profile 1  
County:          Klein Karoo                      X-units              m  
Project:        Grav                              Z-units m

Start point of profile

X (grid easting)	0.00 m
Y Grid northing)	0.00m
Distance value at start	0.00m

Gravity models      **KK1 (Continued)**

Profile is oriented      0.000 deg east of true north  
 Strike direction is      90.00 deg east of true north  
 Grid north is      0.000 deg east of true north

Base line intersects profile at      0.000 m

All angles are measured clockwise from true north

Gravity Field      milligals  
 Density units      g/cc  
 Fitting error      0.156 units

There are no regional values

Body: Background      Layer: Yes  
 Density: 0      Free parameter: No  
 Background is 2-dimensional

Body: 1      38 Vertices      0 free parameters      Layer: No  
 Density: -0.24      Free Parameter: No  
 Symmetric Body; Strike length:      10000.000 m  
 Body Direction:      CW

Internal Coordinate Positions:

Vertex No	X-Loc	Z-Loc	Vertex No	X-Loc	Z-Loc
1	241.85	-304.30	20	15533.88	1257.66
2	3258.91	-207.02	21	14351.76	1447.32
3	5364.53	-219.70	22	12417.26	1228.66
4	7899.28	-240.74	23	11184.89	1315.72
5	10167.60	-286.58	24	10566.64	1604.73
6	10791.86	-287.11	25	9352.24	1472.80
7	13167.74	-312.97	26	8863.62	1158.41
8	13798.53	-298.53	27	8105.93	1012.94
9	15683.45	-334.56	28	7634.52	1146.83
10	16483.48	-407.62	29	6478.02	1105.08
11	17130.80	-357.22	30	5697.50	721.63
12	18535.72	-398.43	31	4423.73	523.12
13	18369.14	-316.41	32	3811.13	422.09
14	18059.98	-277.65	33	2835.25	402.21
15	17866.73	-112.04	34	2377.80	276.34
16	17344.04	58.23	35	1981.03	209.08

Gravity models      **KK1 (Continued)**

17	16630.63	-54.90	36	1548.43	-32.51
18	15971.72	-42.84	37	987.51	-97.23
19	15972.81	559.56	38	680.02	-239.17

Body: 2      4 Vertices      8 free parameters      Layer: No  
 Density:      1.88      Free Parameter: No  
 Symmetric Body; Strike length:      10000.000 m  
 Body Direction:      CW

Internal Coordinate Positions:

Vertex No	X-Loc	Z-Loc	Vertex No	X-Loc	Z-Loc
1	18676.945	-114.856	3	18167.881	1755.377
2	18726.387	-142.934	4	18171.883	1735.853

Station No	Distance (m)	Elevation (m)	Data	Gravity (mgal) Synthetic	Difference
1	0	325.7	0.00	-0.50	-0.50
2	94	321.1	-0.17	-0.53	-0.36
3	187	318.3	-0.25	-0.58	-0.33
4	280	316.7	-0.35	-0.67	-0.32
5	373	314.1	-0.64	-0.82	-0.18
6	466	310.8	-0.97	-0.98	-0.01
7	559	308.1	-1.30	-1.15	0.15
8	653	305.3	-1.54	-1.36	0.18
9	747	302.3	-1.74	-1.65	0.09
10	840	299.6	-1.94	-1.94	0.00
11	933	296.7	-2.14	-2.20	-0.06
12	1027	294.8	-2.36	-2.41	-0.05
13	1119	293.0	-2.55	-2.59	-0.04
14	1213	290.7	-2.76	-2.76	0.00
15	1306	289.3	-2.98	-2.92	0.06
16	1401	287.3	-3.21	-3.11	0.10
17	1494	284.7	-3.40	-3.31	0.09
18	1588	282.2	-3.62	-3.53	0.09
19	1682	280.7	-3.65	-3.77	-0.12
20	1776	273.1	-3.85	-4.01	-0.16
21	1868	269.2	-4.07	-4.23	-0.16
22	1962	266.7	-4.41	-4.45	-0.04
23	2055	264.2	-4.59	-4.64	-0.05
24	2148	261.2	-4.78	-4.82	-0.04

Gravity models      **KK1 (Continued)**

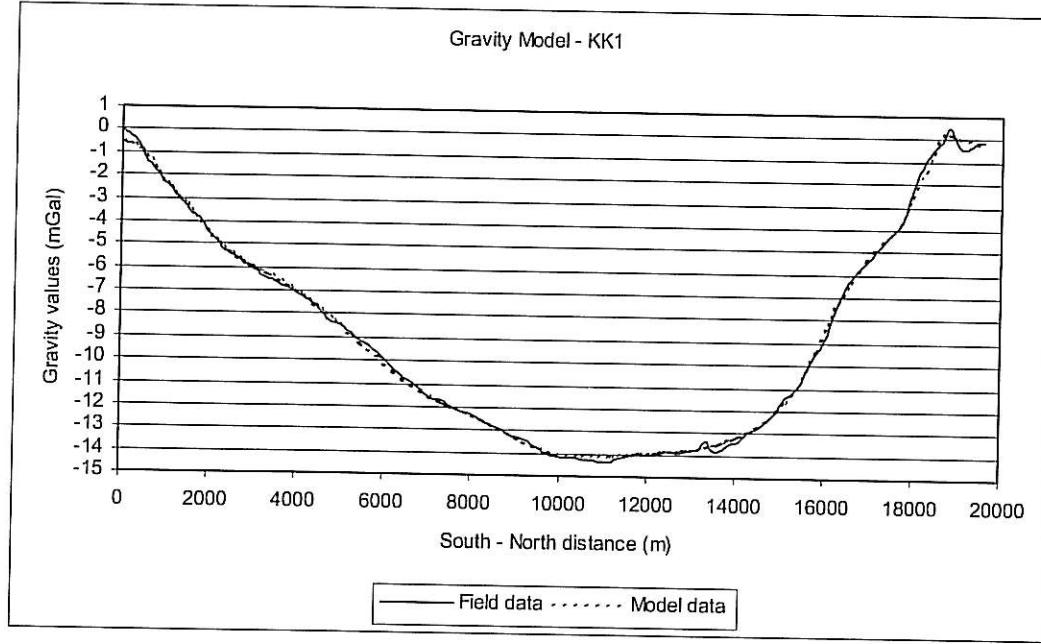
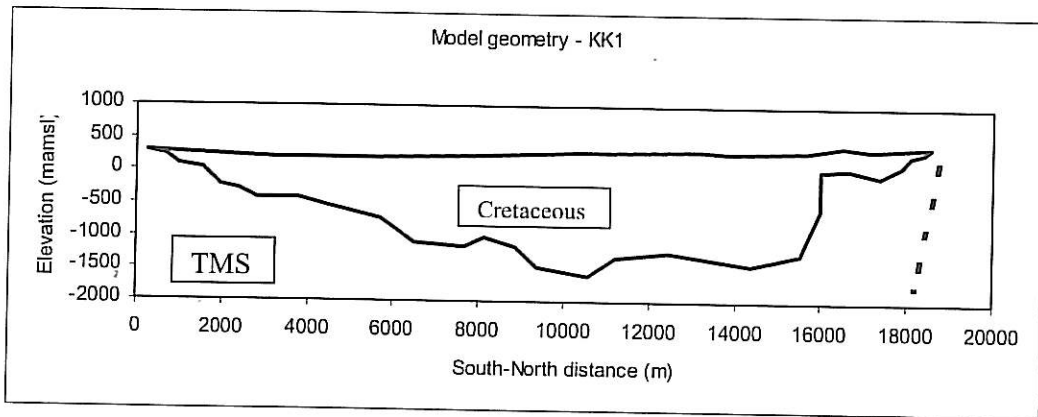
Station No	Distance (m)	Elevation (m)	Data	Gravity (mgal) Synthetic	Difference
25	2242	258.3	-4.95	-4.99	-0.04
26	2335	255.7	-5.20	-5.14	0.06
27	2429	253.2	-5.29	-5.28	0.01
28	2522	250.5	-5.43	-5.41	0.02
29	2615	248.2	-5.56	-5.53	0.03
30	2708	245.6	-5.64	-5.65	-0.01
31	2802	243.2	-5.75	-5.75	0.00
32	2895	240.8	-5.85	-5.85	0.00
33	2989	239.0	-5.97	-5.94	0.03
34	3082	236.7	-6.06	-6.02	0.04
35	3175	232.7	-6.26	-6.10	0.16
36	3268	230.0	-6.42	-6.19	0.23
37	3362	227.8	-6.49	-6.29	0.20
38	3460	226.3	-6.50	-6.39	0.11
39	3561	222.6	-6.66	-6.51	0.15
40	3661	221.3	-6.76	-6.62	0.14
41	3762	218.7	-6.80	-6.74	0.06
42	3862	217.3	-6.91	-6.86	0.05
43	3962	218.3	-6.96	-6.99	-0.03
44	4063	220.5	-7.16	-7.11	0.05
45	4164	223.2	-7.27	-7.25	0.02
46	4265	223.5	-7.39	-7.39	0.00
47	4366	223.7	-7.56	-7.53	0.03
48	4467	223.8	-7.68	-7.67	0.01
49	4567	224.3	-7.89	-7.82	0.07
50	4669	224.7	-8.09	-7.97	0.12
51	4769	225.3	-8.26	-8.12	0.14
52	4870	226.0	-8.37	-8.27	0.10
53	4971	227.0	-8.47	-8.43	0.04
54	5073	228.0	-8.57	-8.59	-0.02
55	5173	229.3	-8.73	-8.74	-0.01
56	5274	229.8	-8.88	-8.91	-0.03
57	5299	233.1	-8.97	-8.94	0.03
58	5479	238.2	-9.17	-9.23	-0.06
59	5659	243.2	-9.38	-9.53	-0.15
60	5849	248.0	-9.69	-9.84	-0.15
61	6049	246.5	-9.99	-10.17	-0.18
62	6249	250.2	-10.37	-10.48	-0.11
63	6449	248.6	-10.73	-10.77	-0.04
64	6649	249.3	-10.97	-11.04	-0.07
65	6859	252.0	-11.27	-11.28	-0.01

Gravity models      **KK1 (Continued)**

Station No	Distance (m)	Elevation (m)	Data	Gravity (mgal) Synthetic	Difference
66	7079	250.8	-11.57	-11.52	0.05
67	7299	250.6	-11.72	-11.73	-0.01
68	7479	250.7	-11.93	-11.89	0.04
69	7659	253.1	-12.06	-12.04	0.02
70	7845	258.5	-12.24	-12.18	0.06
71	8037	263.2	-12.31	-12.34	-0.03
72	8228	257.8	-12.61	-12.53	0.08
73	8419	271.2	-12.72	-12.69	0.03
74	8611	275.3	-12.87	-12.87	0.00
75	8802	277.1	-13.12	-13.06	0.06
76	8994	279.5	-13.27	-13.25	0.02
77	9185	281.5	-13.41	-13.43	-0.02
78	9377	283.3	-13.61	-13.60	0.01
79	9568	284.1	-13.81	-13.76	0.05
80	9759	287.2	-13.99	-13.89	0.10
81	9951	289.1	-14.12	-14.01	0.11
82	10142	291.0	-14.22	-14.10	0.12
83	10334	291.2	-14.23	-14.14	0.09
84	10525	294.3	-14.27	-14.15	0.12
85	10717	296.0	-14.29	-14.15	0.14
86	10908	293.3	-14.35	-14.15	0.20
87	11099	300.3	-14.35	-14.12	0.23
88	11224	297.8	-14.35	-14.12	0.23
89	11349	311.7	-14.19	-14.06	0.13
90	11516	314.0	-14.11	-14.03	0.08
91	11683	315.8	-14.07	-14.00	0.07
92	11849	317.1	-14.03	-13.97	0.06
93	12016	318.6	-14.02	-13.94	0.08
94	12183	319.6	-13.99	-13.92	0.07
95	12349	320.7	-13.91	-13.89	0.02
96	12516	322.0	-13.86	-13.86	0.00
97	12683	324.0	-13.91	-13.83	0.08
98	12849	325.7	-13.86	-13.80	0.06
99	13016	326.2	-13.82	-13.77	0.05
100	13183	327.5	-13.82	-13.72	0.10
101	13349	329.7	-13.42	-13.62	-0.20
102	13483	324.3	-13.72	-13.55	0.17
103	13616	308.7	-13.89	-13.51	0.38
104	13749	309.8	-13.72	-13.40	0.32
105	13816	315.0	-13.59	-13.34	0.25

Gravity models      **KK1 (Continued)**

Station No	Distance (m)	Elevation (m)	Data	Gravity (mgal) Synthetic	Difference
106	13924	318.1	-13.46	-13.27	0.19
107	14104	327.1	-13.35	-13.13	0.22
108	14314	330.6	-13.01	-12.95	0.06
109	14524	334.7	-12.83	-12.71	0.12
110	14734	337.7	-12.52	-12.41	0.11
111	14944	341.2	-12.06	-12.04	0.02
112	15154	345.2	-11.47	-11.57	-0.10
113	15364	350.5	-11.02	-10.97	0.05
114	15574	357.6	-10.30	-10.23	0.07
115	15784	356.7	-9.61	-9.38	0.23
116	15994	374.7	-8.93	-8.44	0.49
117	16141	386.6	-8.30	-7.83	0.47
118	16224	396.7	-7.78	-7.52	0.26
119	16308	408.3	-7.38	-7.25	0.13
120	16433	415.8	-6.87	-6.90	-0.03
121	16599	417.2	-6.26	-6.37	-0.11
122	16766	408.6	-5.88	-5.85	0.03
123	16933	401.2	-5.53	-5.40	0.13
124	17099	393.5	-5.23	-5.00	0.23
125	17316	389.6	-4.76	-4.60	0.16
126	17533	384.1	-4.17	-4.12	0.05
127	17749	380.0	-3.69	-3.48	0.21
128	17899	390.0	-2.91	-2.88	0.03
129	18049	402.5	-1.99	-2.18	-0.19
130	18237	409.5	-1.02	-1.39	-0.37
131	18424	411.7	-0.52	-0.62	-0.10
132	18612	411.0	-0.17	0.20	0.37
133	18799	405.5	0.52	0.31	-0.22
134	18999	402.3	-0.31	0.12	0.43
135	19199	403.2	-0.43	-0.05	0.38
136	19399	406.7	-0.16	-0.16	0.01
137	19599	410.1	-0.10	-0.21	-0.11



KK1 END

Gravity models      **Model KK2**

Densities:      TMS: 2.61 g/cc  
                    Cretaceous 2.34 g/cc  
                    Sulphides on Swartberg Fault 4.5 g/cc

Grav Model Data  
KK2 Model Date 31/10/2005  
Sulphides on Swartberg Fault

Data Set :      KK2.MGX

Location:      Calitzdorp      Profile: Profile 1  
County:      Klein Karoo      X-units      m  
Project Grav      Z-units m

Start point of profile  
X (grid easting)      0.00 m  
Y Grid northing)      0.00m  
Distance value at start      0.00m

Profile is oriented      0.000 deg east of true north  
Strike direction is      90.00 deg east of true north  
Grid north is      0.000 deg east of true north

Base line intersects profile at      0.000 m

All angles are measured clockwise from true north

Gravity Field      milligals  
Density units      g/cc  
Fitting error      0.148 units

There are no regional values

Body: Background      Layer: Yes  
Density: 0      Free parameter      No  
Background is 2-dimensional

Gravity models      **KK2 (Continued)**

Body: 1      38 Vertices      0 free parameters      Layer: No  
 Density:      -0.27      Free Parameter: No      (-.27)  
 Symmetric Body; Strike length:      10000.000 m  
 Sulph 4.5      (+1.88)  
 Body Direction:      CW

Internal Coordinate Positions:

Vertex No	X-Loc	Z-Loc	Vertex No	X-Loc	Z-Loc
1	264.36	-306.14	20	15455.12	1004.20
2	3281.41	-208.86	21	14188.63	1215.89
3	5387.04	-221.54	22	12462.26	1037.65
4	7921.78	-242.58	23	11190.51	1108.17
5	10190.10	-288.42	24	10487.89	1380.66
6	10814.36	-288.94	25	9267.86	1221.17
7	13190.24	-314.81	26	8914.25	938.00
8	13821.04	-300.37	27	8117.18	897.23
9	15705.95	-336.40	28	7718.90	952.14
10	16505.99	-409.45	29	6376.76	903.05
11	17153.31	-359.06	30	5725.63	563.68
12	18558.22	-400.26	31	3821.87	440.47
13	18391.64	-318.24	32	3648.01	293.52
14	18082.48	-279.49	33	2840.88	352.62
15	17889.24	-113.88	34	2400.30	248.79
16	17366.55	28.84	35	2020.41	128.27
17	16653.13	-93.47	36	1570.93	-34.35
18	16084.23	-77.73	37	987.51	-121.10
19	16017.81	447.52	38	702.53	-241.00

Body: 2      4 Vertices      0 free parameters      Layer: No  
 Density:      1.88      Free Parameter: No  
 Symmetric Body; Strike length:      10000.000 m  
 Body Direction:      CW

Internal Coordinate Positions:

Vertex No	X-Loc	Z-Loc	Vertex No	X-Loc	Z-Loc
1	18676.0	-114.0	3	18167.0	1750.0
2	18726.0	-142.0	4	18171.0	1730.0

Gravity models      **KK2 (Continued)**

Station No	Distance (m)	Elevation (m)	Data	Gravity (mgal) Synthetic	Difference
1	0	325.7	0.00	-0.45	-0.46
2	94	321.1	-0.17	-0.48	-0.31
3	187	318.3	-0.25	-0.52	-0.27
4	280	316.7	-0.35	-0.59	-0.24
5	373	314.1	-0.64	-0.75	-0.11
6	466	310.8	-0.97	-0.92	0.05
7	559	308.1	-1.30	-1.09	0.21
8	653	305.3	-1.54	-1.30	0.24
9	747	302.3	-1.74	-1.58	0.16
10	840	299.6	-1.94	-1.88	0.06
11	933	296.7	-2.14	-2.16	-0.02
12	1027	294.8	-2.36	-2.39	-0.03
13	1119	293.0	-2.55	-2.58	-0.03
14	1213	290.7	-2.76	-2.76	0.00
15	1306	289.3	-2.98	-2.93	0.05
16	1401	287.3	-3.21	-3.11	0.10
17	1494	284.7	-3.40	-3.30	0.10
18	1588	282.2	-3.62	-3.51	0.11
19	1682	280.7	-3.65	-3.73	-0.08
20	1776	273.1	-3.85	-3.96	-0.11
21	1868	269.2	-4.07	-4.18	-0.11
22	1962	266.7	-4.41	-4.40	0.01
23	2055	264.2	-4.59	-4.61	-0.02
24	2148	261.2	-4.78	-4.81	-0.03
25	2242	258.3	-4.95	-5.00	-0.05
26	2335	255.7	-5.20	-5.17	0.03
27	2429	253.2	-5.29	-5.33	-0.04
28	2522	250.5	-5.43	-5.47	-0.04
29	2615	248.2	-5.56	-5.60	-0.04
30	2708	245.6	-5.64	-5.72	-0.08
31	2802	243.2	-5.75	-5.82	-0.07
32	2895	240.8	-5.85	-5.91	-0.06
33	2989	239.0	-5.97	-5.99	-0.02
34	3082	236.7	-6.06	-6.06	0.00
35	3175	232.7	-6.26	-6.13	0.13
36	3268	230.0	-6.42	-6.19	0.23
37	3362	227.8	-6.49	-6.29	0.20
38	3460	226.3	-6.50	-6.40	0.10
39	3561	222.6	-6.66	-6.53	0.13
40	3661	221.3	-6.76	-6.67	0.09
41	3762	218.7	-6.80	-6.81	-0.01

Gravity models      **KK2 (Continued)**

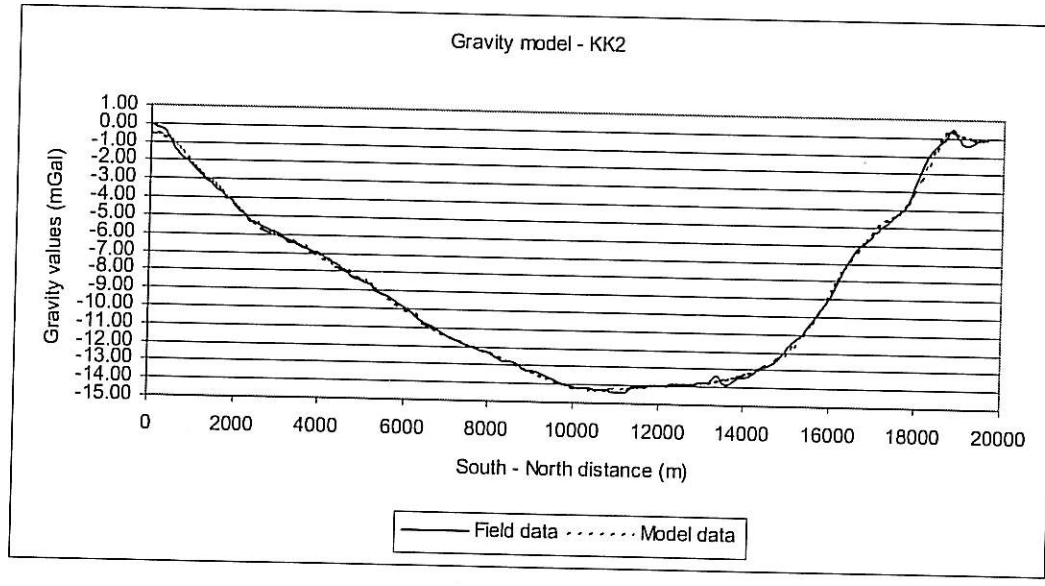
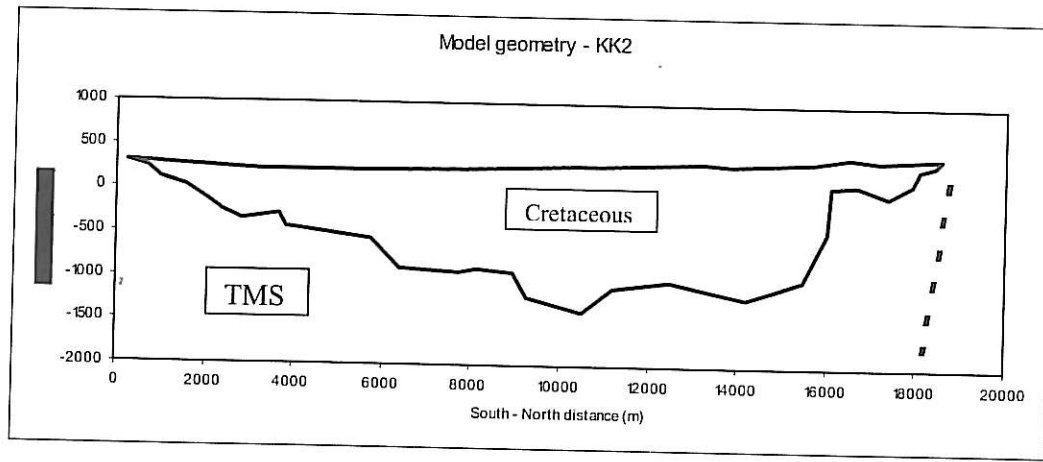
Station No	Distance (m)	Elevation (m)	Data	Gravity (mgal) Synthetic	Difference
42	3862	217.3	-6.91	-6.96	-0.05
43	3962	218.3	-6.96	-7.10	-0.14
44	4063	220.5	-7.16	-7.24	-0.08
45	4164	223.2	-7.27	-7.38	-0.11
46	4265	223.5	-7.39	-7.51	-0.12
47	4366	223.7	-7.56	-7.64	-0.08
48	4467	223.8	-7.68	-7.76	-0.08
49	4567	224.3	-7.89	-7.89	0.00
50	4669	224.7	-8.09	-8.01	0.08
51	4769	225.3	-8.26	-8.14	0.12
52	4870	226.0	-8.37	-8.26	0.11
53	4971	227.0	-8.47	-8.39	0.08
54	5073	228.0	-8.57	-8.52	0.05
55	5173	229.3	-8.73	-8.66	0.07
56	5274	229.8	-8.88	-8.80	0.08
57	5299	233.1	-8.97	-8.83	0.14
58	5479	238.2	-9.17	-9.10	0.07
59	5659	243.2	-9.38	-9.38	0.00
60	5849	248.0	-9.69	-9.69	0.00
61	6049	246.5	-9.99	-10.04	-0.05
62	6249	250.2	-10.37	-10.36	0.01
63	6449	248.6	-10.73	-10.67	0.06
64	6649	249.3	-10.97	-10.95	0.02
65	6859	252.0	-11.27	-11.20	0.07
66	7079	250.8	-11.57	-11.44	0.13
67	7299	250.6	-11.72	-11.65	0.07
68	7479	250.7	-11.93	-11.81	0.12
69	7659	253.1	-12.06	-11.96	0.10
70	7845	258.5	-12.24	-12.10	0.14
71	8037	263.2	-12.31	-12.27	0.04
72	8228	257.8	-12.61	-12.46	0.15
73	8419	271.2	-12.72	-12.63	0.09
74	8611	275.3	-12.87	-12.83	0.04
75	8802	277.1	-13.12	-13.03	0.09
76	8994	279.5	-13.27	-13.24	0.03
77	9185	281.5	-13.41	-13.44	-0.03
78	9377	283.3	-13.61	-13.64	-0.03
79	9568	284.1	-13.81	-13.82	-0.01
80	9759	287.2	-13.99	-13.97	0.02
81	9951	289.1	-14.12	-14.10	0.02
82	10142	291.0	-14.22	-14.20	0.02

Gravity models **KK2 (Continued)**

Station No	Distance (m)	Elevation (m)	Data	Gravity (mgal) Synthetic	Difference
83	10334	291.2	-14.23	-14.25	-0.02
84	10525	294.3	-14.27	-14.25	0.02
85	10717	296.0	-14.29	-14.24	0.05
86	10908	293.3	-14.35	-14.23	0.12
87	11099	300.3	-14.35	-14.19	0.16
88	11224	297.8	-14.35	-14.17	0.18
89	11349	311.7	-14.19	-14.11	0.08
90	11516	314.0	-14.11	-14.07	0.04
91	11683	315.8	-14.07	-14.04	0.03
92	11849	317.1	-14.03	-14.00	0.03
93	12016	318.6	-14.02	-13.97	0.05
94	12183	319.6	-13.99	-13.94	0.05
95	12349	320.7	-13.91	-13.91	0.00
96	12516	322.0	-13.86	-13.89	-0.03
97	12683	324.0	-13.91	-13.86	0.05
98	12849	325.7	-13.86	-13.84	0.02
99	13016	326.2	-13.82	-13.81	0.01
100	13183	327.5	-13.82	-13.78	0.04
101	13349	329.7	-13.42	-13.68	-0.26
102	13483	324.3	-13.72	-13.61	0.11
103	13616	308.7	-13.89	-13.56	0.33
104	13749	309.8	-13.72	-13.45	0.27
105	13816	315.0	-13.59	-13.39	0.20
106	13924	318.1	-13.46	-13.32	0.14
107	14104	327.1	-13.35	-13.18	0.17
108	14314	330.6	-13.01	-13.00	0.01
109	14524	334.7	-12.83	-12.77	0.06
110	14734	337.7	-12.52	-12.48	0.04
111	14944	341.2	-12.06	-12.11	-0.05
112	15154	345.2	-11.47	-11.65	-0.18
113	15364	350.5	-11.02	-11.07	-0.05
114	15574	357.6	-10.30	-10.35	-0.05
115	15784	356.7	-9.61	-9.53	0.08
116	15994	374.7	-8.93	-8.57	0.36
117	16141	386.6	-8.30	-7.89	0.41
118	16224	396.7	-7.78	-7.54	0.24
119	16308	408.3	-7.38	-7.22	0.16
120	16433	415.8	-6.87	-6.84	0.03
121	16599	417.2	-6.26	-6.30	-0.04
122	16766	408.6	-5.88	-5.77	0.11

Gravity models      **KK2 (Continued)**

Station No	Distance (m)	Elevation (m)	Data	Gravity (mgal) Synthetic	Difference
123	16933	401.2	-5.53	-5.33	0.20
124	17099	393.5	-5.23	-4.95	0.28
125	17316	389.6	-4.76	-4.59	0.17
126	17533	384.1	-4.17	-4.18	-0.01
127	17749	380.0	-3.69	-3.58	0.11
128	17899	390.0	-2.91	-2.99	-0.08
129	18049	402.5	-1.99	-2.27	-0.28
130	18237	409.5	-1.02	-1.42	-0.40
131	18424	411.7	-0.52	-0.64	-0.12
132	18612	411.0	-0.17	0.29	0.46
133	18799	405.5	0.52	0.41	-0.11
134	18999	402.3	-0.31	0.22	0.53
135	19199	403.2	-0.43	0.04	0.47
136	19399	406.7	-0.16	-0.07	0.09
137	19599	410.1	-0.10	-0.14	-0.04



**KK2 END**

Gravity models **KK3**

Model Date 31/08/2009

Data Set : **KK3.MGX**

Location: Calitzdorp Profile:Lyn 2  
County: Klein Karoo X-units m  
Project Grav Z-units m

Start point of profile

X (grid easting) 0.00 m  
Y Grid northing) 0.00m  
Distance value at start 0.00m

Profile is oriented 90 deg east of true north  
Strike direction is 0.00 deg east of true north  
Grid north is 0.000 deg east of true north

All angles are measured clockwise from true north

Gravity Field milligals  
Density units g/cc  
Fitting error 0.125 units

There are no regional values

Body: Background Layer: Yes  
Density: 0 Free parameter No  
Background is 2-dimensional

Body: 1 6 Vertices 8 free parameters Layer: No  
Density: -0.24 Free Parameter: No  
Symmetric Body; Strike length: 10000.000 m  
Body Direction: ACW

Internal Coordinate Positions:

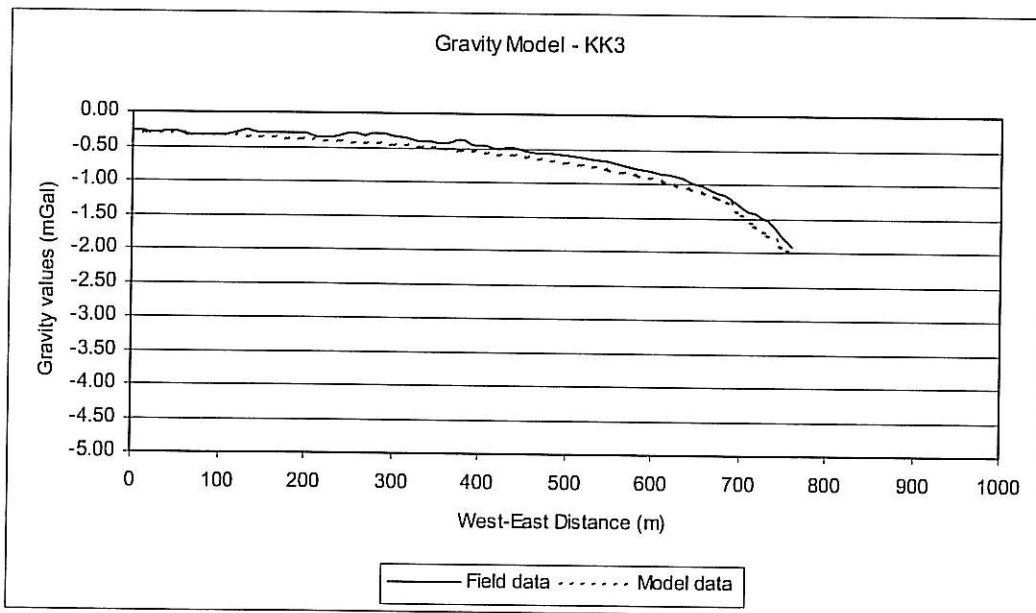
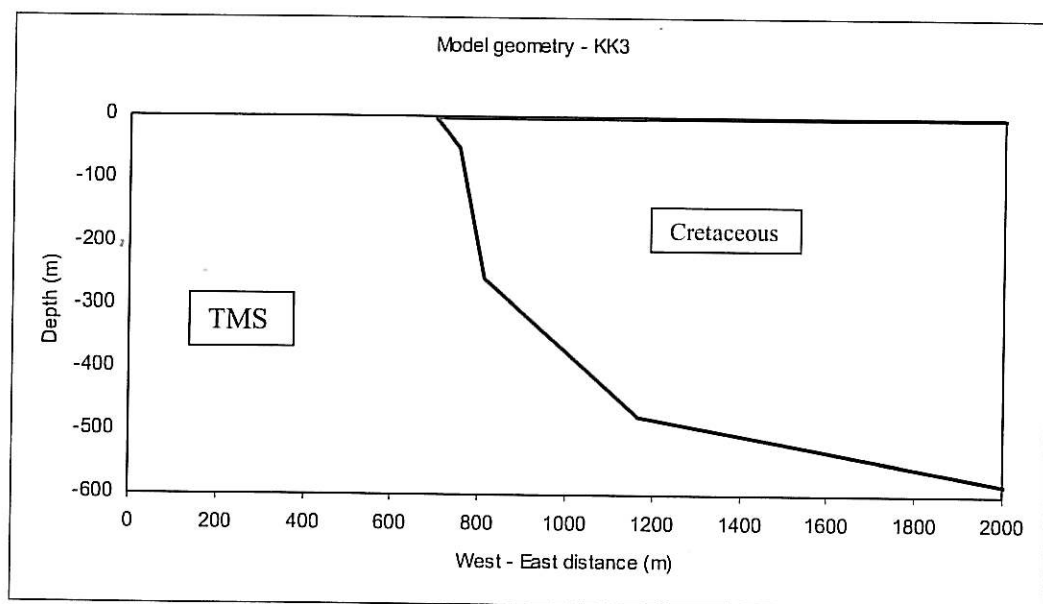
Vertex No	X-Loc	Z-Loc	Vertex No	X-Loc	Z-Loc
1	700.20	0.77	4	1166.78	475.89
2	753.08	50.00	5	2684.81	670.75
3	812.57	256.78	6	2700.00	0.00

Gravity models      **KK3 (Continued)**

Station No	Distance (m)	Elevation (m)	Data	Gravity (mgal)	Difference
				Data	Synthetic
1	0	0.0	-0.28	-0.283	0.00
2	9.6	0.0	-0.28	-0.287	-0.01
3	19.7	0.0	-0.29	-0.291	0.00
4	31.8	0.0	-0.29	-0.296	0.00
5	44.1	0.0	-0.28	-0.302	-0.03
6	55.8	0.0	-0.29	-0.307	-0.01
7	68.1	0.0	-0.32	-0.312	0.01
8	80.2	0.0	-0.34	-0.318	0.02
9	93	0.0	-0.33	-0.324	0.01
10	105.6	0.0	-0.34	-0.330	0.01
11	118.5	0.0	-0.31	-0.337	-0.03
12	132.1	0.0	-0.25	-0.344	-0.09
13	147	0.0	-0.30	-0.352	-0.05
14	162.7	0.0	-0.30	-0.361	-0.06
15	177.6	0.0	-0.29	-0.370	-0.08
16	192.7	0.0	-0.30	-0.379	-0.08
17	207.1	0.0	-0.33	-0.388	-0.06
18	222.1	0.0	-0.34	-0.398	-0.06
19	237.3	0.0	-0.32	-0.408	-0.08
20	252.2	0.0	-0.30	-0.419	-0.12
21	267.4	0.0	-0.31	-0.430	-0.12
22	282.9	0.0	-0.30	-0.443	-0.14
23	298.2	0.0	-0.33	-0.455	-0.12
24	314	0.0	-0.34	-0.469	-0.13
25	329.5	0.0	-0.39	-0.483	-0.09
26	344.5	0.0	-0.40	-0.497	-0.09
27	359.8	0.0	-0.42	-0.512	-0.09
28	375.9	0.0	-0.38	-0.529	-0.15
29	391.8	0.0	-0.45	-0.547	-0.09
30	406.6	0.0	-0.45	-0.564	-0.12
31	421.7	0.0	-0.50	-0.583	-0.08
32	437.3	0.0	-0.49	-0.603	-0.11
33	452.9	0.0	-0.53	-0.625	-0.09
34	467.4	0.0	-0.56	-0.646	-0.09
35	482.7	0.0	-0.57	-0.670	-0.10
36	498.8	0.0	-0.59	-0.697	-0.11
37	514.8	0.0	-0.61	-0.726	-0.11
38	530.5	0.0	-0.66	-0.757	-0.10
39	547.8	0.0	-0.67	-0.793	-0.12
40	564.7	0.0	-0.73	-0.831	-0.10
41	580	0.0	-0.79	-0.869	-0.08

Gravity models      **KK3 (Continued)**

Station No	Distance (m)	Elevation (m)	Data	Gravity (mgal) Synthetic	Difference
42	595.3	0.0	-0.81	-0.911	-0.10
43	610	0.0	-0.86	-0.956	-0.10
44	626.2	0.0	-0.88	-1.000	-0.12
45	641.6	0.0	-0.97	-1.060	-0.09
46	656.4	0.0	-1.03	-1.120	-0.09
47	672.7	0.0	-1.13	-1.200	-0.07
48	687.8	0.0	-1.21	-1.280	-0.07
49	703.5	0.0	-1.34	-1.430	-0.09
50	717.4	0.0	-1.42	-1.590	-0.17
51	731.8	0.0	-1.53	-1.740	-0.21
52	746.8	0.0	-1.75	-1.890	-0.14
53	760.5	0.0	-1.91	-2.010	-0.10
54	1100	0.0	-4.00	-3.570	0.43
55	2000	0.0	-5.00	-4.570	0.43



END KK3

Gravity models **KK4**

Model Date 2/9/2009

Data Set : **KK4.MGX**

Location: Calitzdorp Profile:Lyn 3  
County: Klein Karoo X-units m  
Project Grav Z-units m

Start point of profile

X (grid easting) 0.00 m  
Y Grid northing) 0.00m  
Distance value at start 0.00m

Profile is oriented 90 deg east of true north  
Strike direction is 0.00 deg east of true north  
Grid north is 0.000 deg east of true north

All angles are measured clockwise from true north

Gravity Field milligals  
Density units g/cc  
Fitting error 0.213 units

There are no regional values

Body: Background Layer: Yes  
Density: 0 Free parameter No  
Background is 2-dimensional  
Body: 1 7 Vertices 0 free parameters Layer: No  
Density: -0.24 Free Parameter: No  
Symmetric Body; Strike length: 10000.000 m  
Body Direction: ACW

Internal Coordinate Positions:

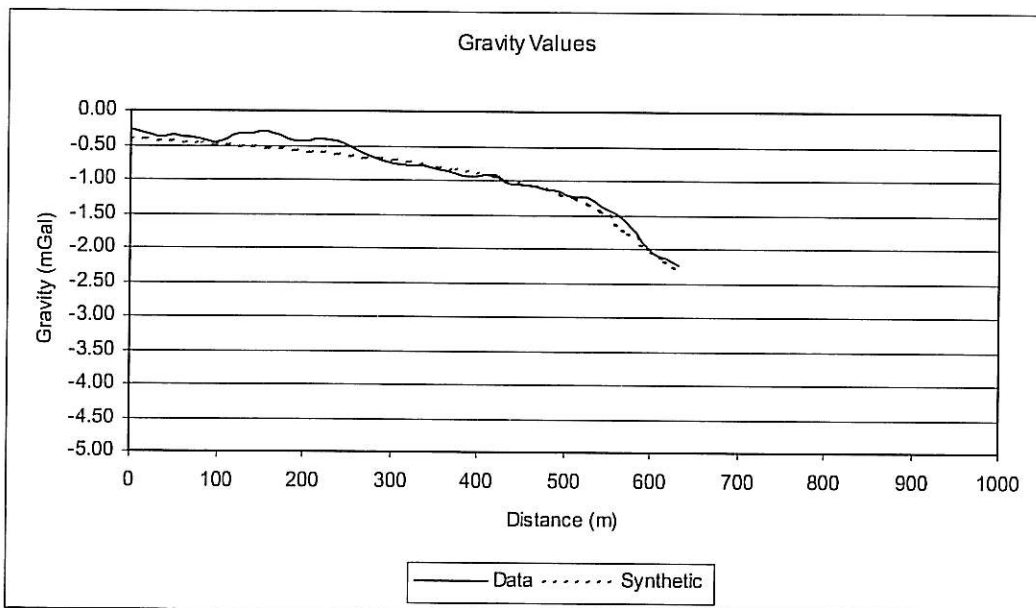
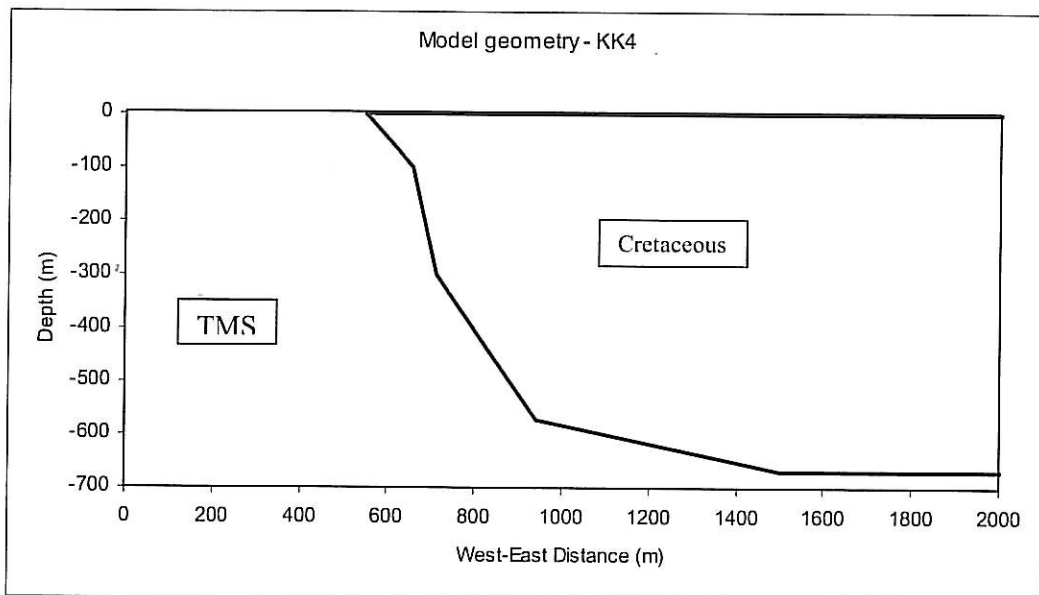
Vertex No	X-Loc	Z-Loc	Vertex No	X-Loc	Z-Loc
1	548.02	0.00	5	1500.00	667.31
2	655.66	100.00	6	2003.38	667.44
3	711.83	100.00	7	2000.00	0.00
4	942.63	571.20			

Gravity models      **KK4 (Continued)**

Station No	Distance (m)	Elevation (m)	Data	Gravity (mgal) Synthetic	Difference
1	0	0	-0.27	-0.404	-0.13
2	16	0	-0.32	-0.415	-0.10
3	31.2	0	-0.37	-0.426	-0.06
4	47	0	-0.35	-0.437	-0.09
5	62.1	0	-0.39	-0.448	-0.06
6	79.9	0	-0.41	-0.462	-0.05
7	96.2	0	-0.46	-0.475	-0.02
8	111.7	0	-0.41	-0.489	-0.08
9	126.3	0	-0.32	-0.502	-0.18
10	141	0	-0.32	-0.515	-0.20
11	157.2	0	-0.30	-0.531	-0.23
12	173.5	0	-0.35	-0.547	-0.20
13	190.2	0	-0.42	-0.565	-0.15
14	206.4	0	-0.43	-0.583	-0.15
15	222.1	0	-0.41	-0.602	-0.19
16	237.4	0	-0.44	-0.621	-0.18
17	252.5	0	-0.50	-0.640	-0.14
18	269	0	-0.61	-0.663	-0.05
19	287	0	-0.71	-0.689	0.02
20	303.2	0	-0.74	-0.714	0.03
21	320.3	0	-0.79	-0.742	0.05
22	336.1	0	-0.79	-0.769	0.02
23	354.7	0	-0.84	-0.803	0.03
24	371.6	0	-0.89	-0.837	0.05
25	385.9	0	-0.94	-0.867	0.07
26	397.4	0	-0.96	-0.893	0.06
27	412.2	0	-0.92	-0.928	-0.01
28	421.2	0	-0.92	-0.950	-0.03
29	432.1	0	-1.01	-0.979	0.03
30	449.3	0	-1.07	-1.020	0.05
31	464.8	0	-1.09	-1.070	0.02
32	479.7	0	-1.13	-1.120	0.01
33	495	0	-1.17	-1.180	-0.01
34	510.7	0	-1.24	-1.240	0.00
35	526.4	0	-1.25	-1.320	-0.07
36	543.4	0	-1.38	-1.420	-0.04
37	559.1	0	-1.50	-1.610	-0.11
38	574.3	0	-1.66	-1.770	-0.11
39	589.8	0	-1.89	-1.920	-0.03
40	602.4	0	-2.04	-2.030	0.01

Gravity models      **KK4 (Continued)**

Station No	Distance (m)	Elevation (m)	Gravity (mgal)		Difference
			Data	Synthetic	
41	617.1	0	-2.13	-2.160	-0.03
42	632.6	0	-2.25	-2.290	-0.04
43	650	0	-2.50	-2.430	0.07
44	1000	0	-4.00	-4.030	-0.03
45	2000	0	-4.00	-2.720	1.28



END KK4

## II Gravity method sensitivity tests

Testing the sensitivity of the gravity method in this application was carried out by comparing the modeled response of various fault geometries: The fault position was moved horizontally from the base model position, and the fault plane dip was altered from the base model geometry. The amount of overburden covering the fault was also varied.

### Test Series 1

Overburden 300 m.

#### TST1 – Base model 1

Data Set : TST1.MGX

Location: Calitzdorp Profile: TST1  
County: Klein Karoo X-units m  
Project Grav Z-units m

Start point of profile

X (grid easting) 0.00 m  
Y Grid northing) 0.00m  
Distance value at start 0.00m

Profile is oriented 90.000 deg east of true north  
Strike direction is 0.00 deg east of true north  
Grid north is 0.000 deg east of true north

All angles are measured clockwise from true north

Gravity Field milligals  
Density units g/cc  
Fitting error 0.0 units

There are no regional values

Body: Background Layer: Yes  
Density: 0 Free parameter No  
Background is 2-dimensional

Gravity method sensitivity tests      **TST1 (Continued)**

Body: 1      7 Vertices      0 free parameters      Layer: No  
 Density:      -0.24      Free Parameter: No  
 Symmetric Body; Strike length:      20000.00 m  
 Body Direction:      CW

Internal Coordinate Positions:

Vertex No	X-Loc	Z-Loc	Vertex No	X-Loc	Z-Loc
1	-6000.00	0.00	5	9000.00	1500.00
2	17000.00	0.00	6	4300.00	1500.00
3	16200.00	200.00	7	-500.00	1000.00
4	9500.00	300.00			

Station No	Distance (m)	Elevation (m)	Gravity (mgal)
1	-5000	0.0	-2.44
2	0	0.0	-9.95
3	200	0.0	-10.14
4	400	0.0	-10.34
5	600	0.0	-10.52
6	800	0.0	-10.70
7	1000	0.0	-10.87
8	1200	0.0	-11.04
9	1400	0.0	-11.21
10	1600	0.0	-11.37
11	1800	0.0	-11.53
12	2000	0.0	-11.68
13	2200	0.0	-11.83
14	2400	0.0	-11.97
15	2600	0.0	-12.11
16	2800	0.0	-12.25
17	3000	0.0	-12.37
18	3200	0.0	-12.49
19	3400	0.0	-12.60
20	3600	0.0	-12.71
21	3800	0.0	-12.80
22	4000	0.0	-12.88
23	4200	0.0	-12.96
24	4400	0.0	-13.02
25	4600	0.0	-13.07
26	4800	0.0	-13.11

Gravity method sensitivity tests **TST1 (Continued)**

Station No	Distance (m)	Elevation (m)	Gravity (mgal)
27	5000	0.0	-13.14
28	5200	0.0	-13.16
29	5400	0.0	-13.16
30	5600	0.0	-13.16
31	5800	0.0	-13.15
32	6000	0.0	-13.13
33	6200	0.0	-13.10
34	6400	0.0	-13.06
35	6600	0.0	-13.01
36	6800	0.0	-12.94
37	7000	0.0	-12.85
38	7200	0.0	-12.75
39	7400	0.0	-12.62
40	7600	0.0	-12.47
41	7800	0.0	-12.28
42	8000	0.0	-12.06
43	8200	0.0	-11.77
44	8400	0.0	-11.43
45	8600	0.0	-10.99
46	8800	0.0	-10.45
47	9000	0.0	-9.78
48	9200	0.0	-8.96
49	9400	0.0	-8.00
50	9600	0.0	-7.03
51	9800	0.0	-6.22
52	10000	0.0	-5.61
53	10200	0.0	-5.15
54	10400	0.0	-4.78
55	10600	0.0	-4.49
56	10800	0.0	-4.25
57	11000	0.0	-4.05
58	11200	0.0	-3.87
59	11400	0.0	-3.72
60	11600	0.0	-3.59
61	11800	0.0	-3.48
62	12000	0.0	-3.37
63	12200	0.0	-3.27
64	12400	0.0	-3.19
65	12600	0.0	-3.11
66	12800	0.0	-3.03
67	13000	0.0	-2.96

Gravity method sensitivity tests      **TST1 (Continued)**

Station No	Distance (m)	Elevation (m)	Gravity (mgal)
68	13200	0.0	-2.90
69	13400	0.0	-2.83
70	13600	0.0	-2.77
71	13800	0.0	-2.72
72	14000	0.0	-2.66
73	14200	0.0	-2.61
74	14400	0.0	-2.56
75	14600	0.0	-2.51
76	14800	0.0	-2.46
77	15000	0.0	-2.41
78	15200	0.0	-2.36
79	15400	0.0	-2.31
80	15600	0.0	-2.25
81	15800	0.0	-2.19
82	16000	0.0	-2.11

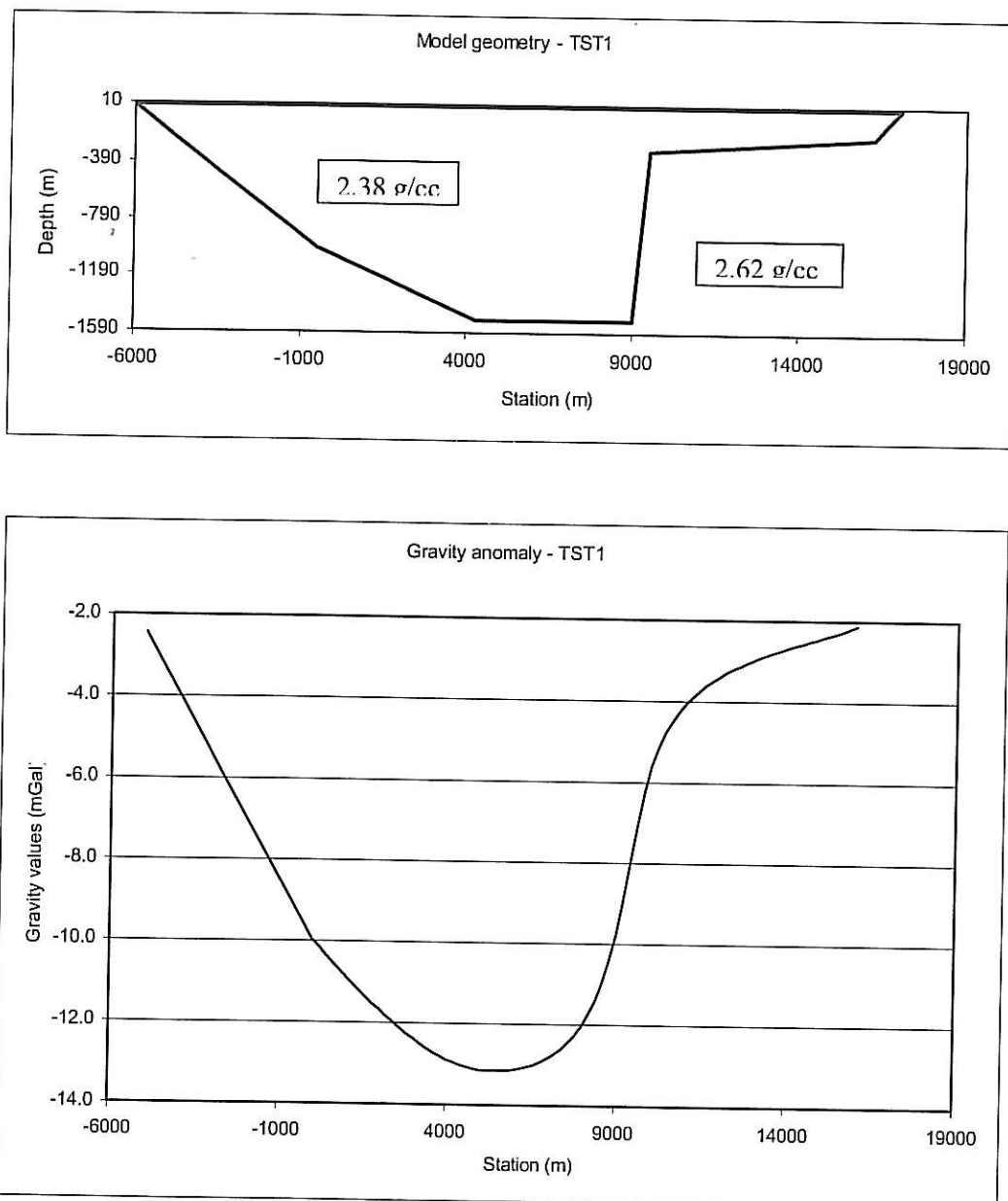


**Figure C1** Base Model 1

**END TST1**

## Gravity method sensitivity tests **TST2**

Shift fault position by 100 meters.

Data Set : TST2.MGX

Location: Calitzdorp Profile:TST2  
County: Klein Karoo X-units m  
Project Grav Z-units m

### Start point of profile

Start point of profile

X (grid easting)	0.00 m
Y Grid northing)	0.00m
Distance value at start	0.00m

Profile is oriented 90.000 deg east of true north  
Strike direction is 0.00 deg east of true north  
Grid north is 0.000 deg east of true north

All angles are measured clockwise from true north

Gravity Field milligals  
 Density units g/cc  
 Fitting error 0.0 units

There are no regional values

Body: Background Layer: Yes  
Density: 0 Free parameter No  
Background is 2-dimensional

Body: 1 7 Vertices 0 free parameters Layer: No  
Density: -0.24 Free Parameter: No  
Symmetric Body; Strike length: 20000.00 m  
Body Direction: CW

### Internal Coordinate Positions:

Vertex No	X-Loc	Z-Loc	Vertex No	X-Loc	Z-Loc
1	-6000.00	0.00	5	9100.00	1500.00
2	17000.00	0.00	6	4300.00	1500.00
3	16200.00	200.00	7	-500.00	1000.00
4	9600.00	300.00			

Gravity method sensitivity tests **TST2 (Continued)**

Station No	Distance (m)	Elevation (m)	Data	Gravity (mgal)	Difference
				Data	Synthetic
1	-5000	0.0	-2.44	-2.44	0.00
2	0	0.0	-9.95	-9.95	0.00
3	200	0.0	-10.14	-10.15	-0.01
4	400	0.0	-10.34	-10.34	0.00
5	600	0.0	-10.52	-10.52	0.00
6	800	0.0	-10.70	-10.70	0.00
7	1000	0.0	-10.87	-10.88	-0.01
8	1200	0.0	-11.04	-11.05	-0.01
9	1400	0.0	-11.21	-11.22	-0.01
10	1600	0.0	-11.37	-11.38	-0.01
11	1800	0.0	-11.53	-11.53	0.00
12	2000	0.0	-11.68	-11.69	-0.01
13	2200	0.0	-11.83	-11.84	-0.01
14	2400	0.0	-11.97	-11.98	-0.01
15	2600	0.0	-12.11	-12.12	-0.01
16	2800	0.0	-12.25	-12.25	0.00
17	3000	0.0	-12.37	-12.38	-0.01
18	3200	0.0	-12.49	-12.50	-0.01
19	3400	0.0	-12.60	-12.61	-0.01
20	3600	0.0	-12.71	-12.71	0.00
21	3800	0.0	-12.80	-12.81	-0.01
22	4000	0.0	-12.88	-12.89	-0.01
23	4200	0.0	-12.96	-12.97	-0.01
24	4400	0.0	-13.02	-13.03	-0.01
25	4600	0.0	-13.07	-13.08	-0.01
26	4800	0.0	-13.11	-13.12	-0.01
27	5000	0.0	-13.14	-13.15	-0.01
28	5200	0.0	-13.16	-13.17	-0.01
29	5400	0.0	-13.16	-13.19	-0.03
30	5600	0.0	-13.16	-13.19	-0.03
31	5800	0.0	-13.15	-13.18	-0.03
32	6000	0.0	-13.13	-13.16	-0.03
33	6200	0.0	-13.10	-13.13	-0.03
34	6400	0.0	-13.06	-13.10	-0.04
35	6600	0.0	-13.01	-13.05	-0.04
36	6800	0.0	-12.94	-12.98	-0.04
37	7000	0.0	-12.85	-12.91	-0.06
38	7200	0.0	-12.75	-12.81	-0.06
39	7400	0.0	-12.62	-12.70	-0.08
40	7600	0.0	-12.47	-12.56	-0.09
41	7800	0.0	-12.28	-12.39	-0.11

Gravity method sensitivity tests **TST2 (Continued)**

Station No	Distance (m)	Elevation (m)	Data	Gravity (mgal)	Difference
				Data	Synthetic
42	8000	0.0	-12.06	-12.18	-0.12
43	8200	0.0	-11.77	-11.93	-0.16
44	8400	0.0	-11.43	-11.61	-0.18
45	8600	0.0	-10.99	-11.23	-0.24
46	8800	0.0	-10.45	-10.74	-0.29
47	9000	0.0	-9.78	-10.14	-0.36
48	9200	0.0	-8.96	-9.40	-0.44
49	9400	0.0	-8.00	-8.50	-0.50
50	9600	0.0	-7.03	-7.51	-0.48
51	9800	0.0	-6.22	-6.60	-0.38
52	10000	0.0	-5.61	-5.90	-0.29
53	10200	0.0	-5.15	-5.37	-0.22
54	10400	0.0	-4.78	-4.96	-0.18
55	10600	0.0	-4.49	-4.63	-0.14
56	10800	0.0	-4.25	-4.36	-0.11
57	11000	0.0	-4.05	-4.14	-0.09
58	11200	0.0	-3.87	-3.96	-0.09
59	11400	0.0	-3.72	-3.79	-0.07
60	11600	0.0	-3.59	-3.65	-0.06
61	11800	0.0	-3.48	-3.53	-0.05
62	12000	0.0	-3.37	-3.42	-0.05
63	12200	0.0	-3.27	-3.32	-0.05
64	12400	0.0	-3.19	-3.23	-0.04
65	12600	0.0	-3.11	-3.14	-0.03
66	12800	0.0	-3.03	-3.06	-0.03
67	13000	0.0	-2.96	-2.99	-0.03
68	13200	0.0	-2.90	-2.92	-0.02
69	13400	0.0	-2.83	-2.86	-0.03
70	13600	0.0	-2.77	-2.80	-0.03
71	13800	0.0	-2.72	-2.74	-0.02
72	14000	0.0	-2.66	-2.68	-0.02
73	14200	0.0	-2.61	-2.63	-0.02
74	14400	0.0	-2.56	-2.57	-0.01
75	14600	0.0	-2.51	-2.52	-0.01
76	14800	0.0	-2.46	-2.47	-0.01
77	15000	0.0	-2.41	-2.42	-0.01
78	15200	0.0	-2.36	-2.37	-0.01
79	15400	0.0	-2.31	-2.32	-0.01
80	15600	0.0	-2.25	-2.26	-0.01
81	15800	0.0	-2.19	-2.20	-0.01
82	16000	0.0	-2.11	-2.11	0.00

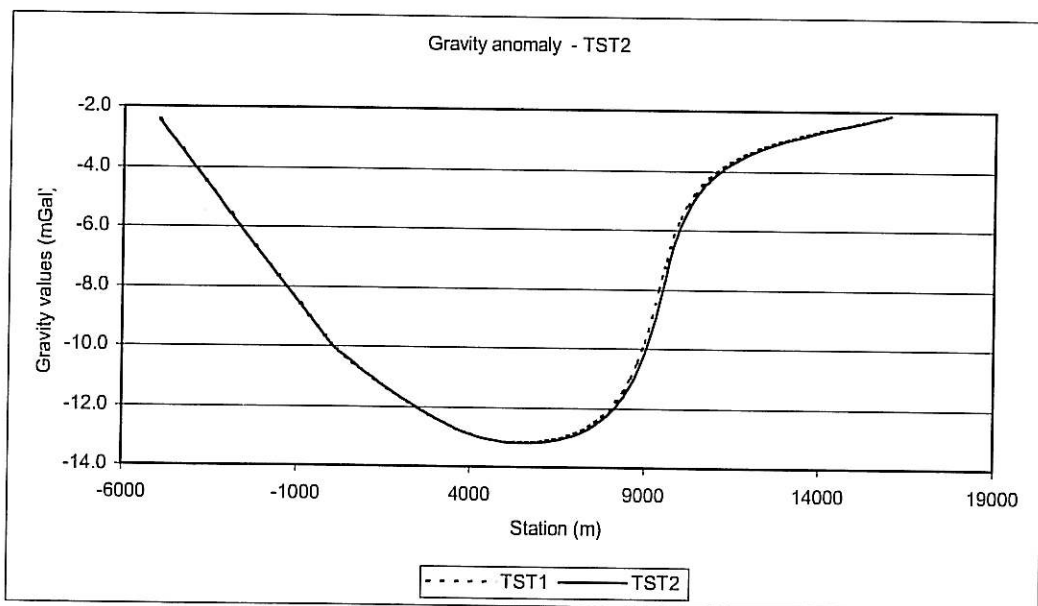
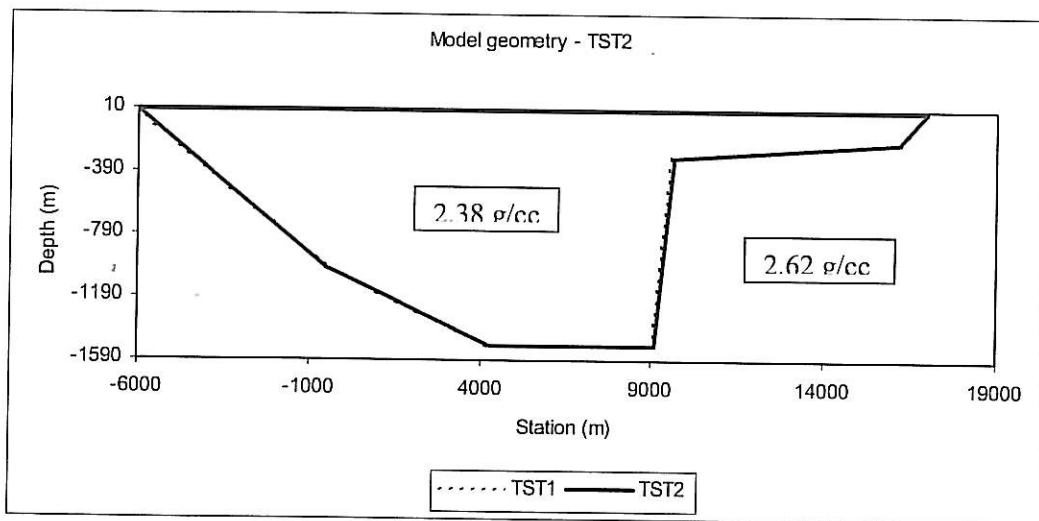


**Figure C2**

**END TST2**

Gravity method sensitivity tests **TST3**

Increase fault plane dip

Data Set : **TST3.MGX**

Location: Calitzdorp Profile:TST3  
County: Klein Karoo X-units m  
Project Grav Z-units m

Start point of profile

X (grid easting) 0.00 m  
Y Grid northing) 0.00m  
Distance value at start 0.00m

Profile is oriented 90.000 deg east of true north  
Strike direction is 0.00 deg east of true north  
Grid north is 0.000 deg east of true north

All angles are measured clockwise from true north

Gravity Field milligals  
Density units g/cc  
Fitting error 0.0 units

There are no regional values

Body: Background Layer: Yes  
Density: 0 Free parameter No  
Background is 2-dimensional

Body: 1 7 Vertices 0 free parameters Layer: No  
Density: -0.24 Free Parameter: No  
Symmetric Body; Strike length: 20000.00 m  
Body Direction: CW

Internal Coordinate Positions:

Vertex No	X-Loc	Z-Loc	Vertex No	X-Loc	Z-Loc
1	-6000.00	0.00	5	9289.00	1500.00
2	17000.00	0.00	6	4300.00	1500.00
3	16200.00	200.00	7	-500.00	1000.00
4	9500.00	300.00			

Gravity method sensitivity tests **TST3 (Continued)**

Station No	Distance (m)	Elevation (m)	Data	Gravity (mgal) Synthetic	Difference
1	-5000	0.0	-2.44	-2.44	0.00
2	0	0.0	-9.95	-9.95	0.00
3	200	0.0	-10.14	-10.15	-0.01
4	400	0.0	-10.34	-10.34	0.00
5	600	0.0	-10.52	-10.53	-0.01
6	800	0.0	-10.70	-10.71	-0.01
7	1000	0.0	-10.87	-10.88	-0.01
8	1200	0.0	-11.04	-11.05	-0.01
9	1400	0.0	-11.21	-11.22	-0.01
10	1600	0.0	-11.37	-11.38	-0.01
11	1800	0.0	-11.53	-11.54	-0.01
12	2000	0.0	-11.68	-11.69	-0.01
13	2200	0.0	-11.83	-11.84	-0.01
14	2400	0.0	-11.97	-11.99	-0.02
15	2600	0.0	-12.11	-12.12	-0.01
16	2800	0.0	-12.25	-12.26	-0.01
17	3000	0.0	-12.37	-12.38	-0.01
18	3200	0.0	-12.49	-12.50	-0.01
19	3400	0.0	-12.60	-12.62	-0.02
20	3600	0.0	-12.71	-12.72	-0.01
21	3800	0.0	-12.80	-12.82	-0.02
22	4000	0.0	-12.88	-12.90	-0.02
23	4200	0.0	-12.96	-12.98	-0.02
24	4400	0.0	-13.02	-13.04	-0.02
25	4600	0.0	-13.07	-13.09	-0.02
26	4800	0.0	-13.11	-13.13	-0.02
27	5000	0.0	-13.14	-13.17	-0.03
28	5200	0.0	-13.16	-13.19	-0.03
29	5400	0.0	-13.16	-13.20	-0.04
30	5600	0.0	-13.16	-13.20	-0.04
31	5800	0.0	-13.15	-13.20	-0.05
32	6000	0.0	-13.13	-13.18	-0.05
33	6200	0.0	-13.10	-13.16	-0.06
34	6400	0.0	-13.06	-13.12	-0.06
35	6600	0.0	-13.01	-13.07	-0.06
36	6800	0.0	-12.94	-13.02	-0.08
37	7000	0.0	-12.85	-12.94	-0.09
38	7200	0.0	-12.75	-12.86	-0.11
39	7400	0.0	-12.62	-12.75	-0.13
40	7600	0.0	-12.47	-12.62	-0.15

Gravity method sensitivity tests **TST3 (Continued)**

Station No	Distance (m)	Elevation (m)	Data	Gravity (mgal) Synthetic	Difference
41	7800	0.0	-12.28	-12.46	-0.18
42	8000	0.0	-12.06	-12.26	-0.20
43	8200	0.0	-11.77	-12.02	-0.25
44	8400	0.0	-11.43	-11.72	-0.29
45	8600	0.0	-10.99	-11.34	-0.35
46	8800	0.0	-10.45	-10.86	-0.41
47	9000	0.0	-9.78	-10.26	-0.48
48	9200	0.0	-8.96	-9.49	-0.53
49	9400	0.0	-8.00	-8.55	-0.55
50	9600	0.0	-7.03	-7.53	-0.50
51	9800	0.0	-6.22	-6.65	-0.43
52	10000	0.0	-5.61	-5.96	-0.35
53	10200	0.0	-5.15	-5.43	-0.28
54	10400	0.0	-4.78	-5.02	-0.24
55	10600	0.0	-4.49	-4.68	-0.19
56	10800	0.0	-4.25	-4.41	-0.16
57	11000	0.0	-4.05	-4.18	-0.13
58	11200	0.0	-3.87	-3.99	-0.12
59	11400	0.0	-3.72	-3.82	-0.10
60	11600	0.0	-3.59	-3.68	-0.09
61	11800	0.0	-3.48	-3.55	-0.07
62	12000	0.0	-3.37	-3.44	-0.07
63	12200	0.0	-3.27	-3.33	-0.06
64	12400	0.0	-3.19	-3.24	-0.05
65	12600	0.0	-3.11	-3.15	-0.04
66	12800	0.0	-3.03	-3.07	-0.04
67	13000	0.0	-2.96	-3.00	-0.04
68	13200	0.0	-2.90	-2.92	-0.02
69	13400	0.0	-2.83	-2.86	-0.03
70	13600	0.0	-2.77	-2.80	-0.03
71	13800	0.0	-2.72	-2.74	-0.02
72	14000	0.0	-2.66	-2.68	-0.02
73	14200	0.0	-2.61	-2.63	-0.02
74	14400	0.0	-2.56	-2.58	-0.02
75	14600	0.0	-2.51	-2.52	-0.01
76	14800	0.0	-2.46	-2.47	-0.01
77	15000	0.0	-2.41	-2.42	-0.01
78	15200	0.0	-2.36	-2.37	-0.01
79	15400	0.0	-2.31	-2.32	-0.01
80	15600	0.0	-2.25	-2.27	-0.02

81	15800	0.0	-2.19	-2.20	-0.01
82	16000	0.0	-2.11	-2.12	-0.01

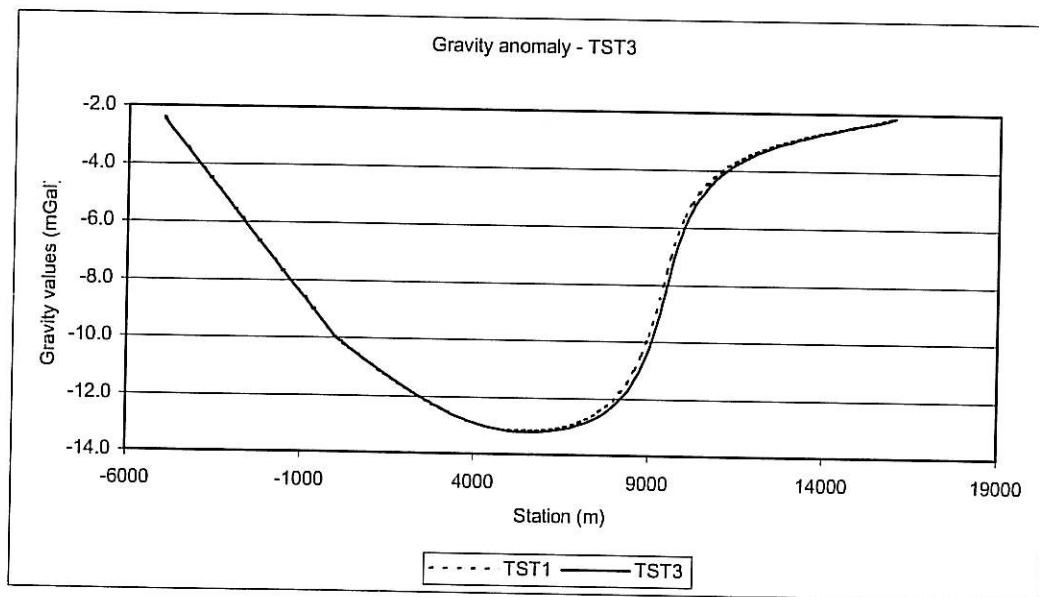
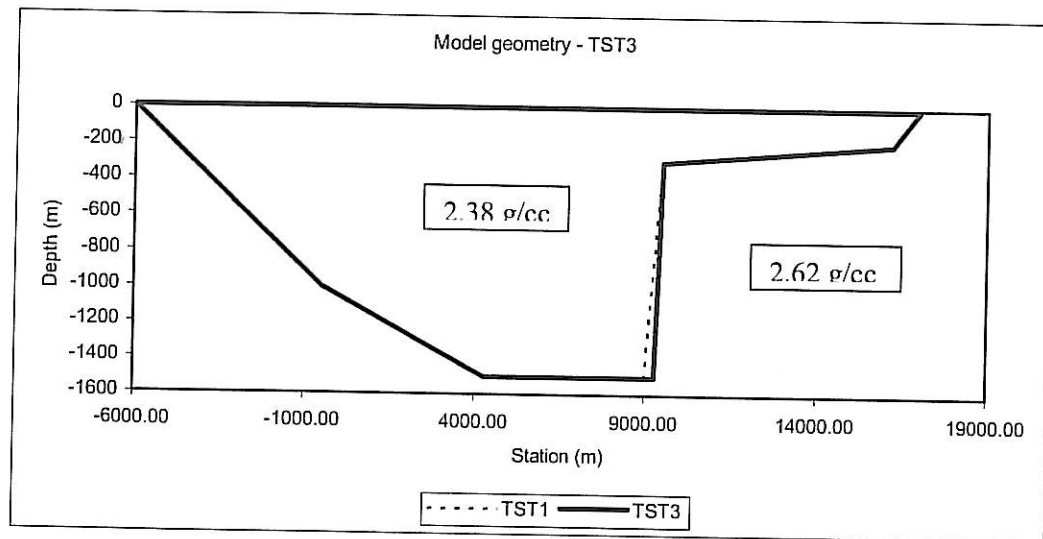


Figure C3

END TST3

## Gravity method sensitivity tests TST4

Decrease fault plane dip.

Data Set : TST4.MGX

Location: Calitzdorp Profile:TST4  
County: Klein Karoo X-units m  
Project Grav Z-units m

Start point of profile

X (grid easting) 0.00 m  
Y Grid northing) 0.00m  
Distance value at start 0.00m

Profile is oriented 90.000 deg east of true north  
Strike direction is 0.00 deg east of true north  
Grid north is 0.000 deg east of true north

All angles are measured clockwise from true north

Gravity Field milligals  
Density units g/cc  
Fitting error 0.0 units

There are no regional values

Body: Background Layer: Yes  
Density: 0 Free parameter No  
Background is 2-dimensional

Body: 1 7 Vertices 0 free parameters Layer: No  
Density: -0.24 Free Parameter: No  
Symmetric Body; Strike length: 20000.00 m  
Body Direction: CW

Internal Coordinate Positions:

Vertex No	X-Loc	Z-Loc	Vertex No	X-Loc	Z-Loc
1	-6000.00	0.00	5	8808.00	1500.00
2	17000.00	0.00	6	4300.00	1500.00
3	16200.00	200.00	7	-500.00	1000.00
4	9500.00	300.00			

Gravity method sensitivity tests **TST4 (Continued)**

Station No	Distance (m)	Elevation (m)	Gravity (mgal) Data	Gravity (mgal) Synthetic	Difference
1	-5000	0.0	-2.44	-2.44	0.00
2	0	0.0	-9.95	-9.94	0.01
3	200	0.0	-10.14	-10.14	0.00
4	400	0.0	-10.34	-10.33	0.01
5	600	0.0	-10.52	-10.52	0.00
6	800	0.0	-10.70	-10.71	-0.01
7	1000	0.0	-10.87	-10.87	0.00
8	1200	0.0	-11.04	-11.04	0.00
9	1400	0.0	-11.21	-11.21	0.00
10	1600	0.0	-11.37	-11.37	0.00
11	1800	0.0	-11.53	-11.52	0.01
12	2000	0.0	-11.68	-11.68	0.00
13	2200	0.0	-11.83	-11.82	0.01
14	2400	0.0	-11.97	-11.97	0.00
15	2600	0.0	-12.11	-12.11	0.00
16	2800	0.0	-12.25	-12.24	0.01
17	3000	0.0	-12.37	-12.36	0.01
18	3200	0.0	-12.49	-12.48	0.01
19	3400	0.0	-12.60	-12.59	0.01
20	3600	0.0	-12.71	-12.69	0.02
21	3800	0.0	-12.80	-12.79	0.01
22	4000	0.0	-12.88	-12.87	0.01
23	4200	0.0	-12.96	-12.94	0.02
24	4400	0.0	-13.02	-13.00	0.02
25	4600	0.0	-13.07	-13.05	0.02
26	4800	0.0	-13.11	-13.09	0.02
27	5000	0.0	-13.14	-13.12	0.02
28	5200	0.0	-13.16	-13.13	0.03
29	5400	0.0	-13.16	-13.14	0.02
30	5600	0.0	-13.16	-13.14	0.02
31	5800	0.0	-13.15	-13.12	0.03
32	6000	0.0	-13.13	-13.10	0.03
33	6200	0.0	-13.10	-13.06	0.04
34	6400	0.0	-13.06	-13.01	0.05
35	6600	0.0	-13.01	-12.95	0.06
36	6800	0.0	-12.94	-12.88	0.06
37	7000	0.0	-12.85	-12.78	0.07
38	7200	0.0	-12.75	-12.67	0.08
39	7400	0.0	-12.62	-12.53	0.09
40	7600	0.0	-12.47	-12.36	0.11
41	7800	0.0	-12.28	-12.15	0.13

Gravity method sensitivity tests **TST4 (Continued)**

Station No	Distance (m)	Elevation (m)	Data	Gravity (mgal)	Difference
				Data	Synthetic
42	8000	0.0	-12.06	-11.90	0.16
43	8200	0.0	-11.77	-11.59	0.18
44	8400	0.0	-11.43	-11.20	0.23
45	8600	0.0	-10.99	-10.73	0.26
46	8800	0.0	-10.45	-10.15	0.30
47	9000	0.0	-9.78	-9.45	0.33
48	9200	0.0	-8.96	-8.61	0.35
49	9400	0.0	-8.00	-7.66	0.34
50	9600	0.0	-7.03	-6.73	0.30
51	9800	0.0	-6.22	-5.97	0.25
52	10000	0.0	-5.61	-5.41	0.20
53	10200	0.0	-5.15	-4.98	0.17
54	10400	0.0	-4.78	-4.65	0.13
55	10600	0.0	-4.49	-4.38	0.11
56	10800	0.0	-4.25	-4.15	0.10
57	11000	0.0	-4.05	-3.97	0.08
58	11200	0.0	-3.87	-3.81	0.06
59	11400	0.0	-3.72	-3.67	0.05
60	11600	0.0	-3.59	-3.54	0.05
61	11800	0.0	-3.48	-3.43	0.05
62	12000	0.0	-3.37	-3.33	0.04
63	12200	0.0	-3.27	-3.24	0.03
64	12400	0.0	-3.19	-3.16	0.03
65	12600	0.0	-3.11	-3.08	0.03
66	12800	0.0	-3.03	-3.01	0.02
67	13000	0.0	-2.96	-2.94	0.02
68	13200	0.0	-2.90	-2.88	0.02
69	13400	0.0	-2.83	-2.81	0.02
70	13600	0.0	-2.77	-2.76	0.01
71	13800	0.0	-2.72	-2.70	0.02
72	14000	0.0	-2.66	-2.65	0.01
73	14200	0.0	-2.61	-2.60	0.01
74	14400	0.0	-2.56	-2.55	0.01
75	14600	0.0	-2.51	-2.50	0.01
76	14800	0.0	-2.46	-2.45	0.01
77	15000	0.0	-2.41	-2.40	0.01
78	15200	0.0	-2.36	-2.35	0.01
79	15400	0.0	-2.31	-2.30	0.01
80	15600	0.0	-2.25	-2.25	0.00
81	15800	0.0	-2.19	-2.18	0.01
82	16000	0.0	-2.11	-2.10	0.01

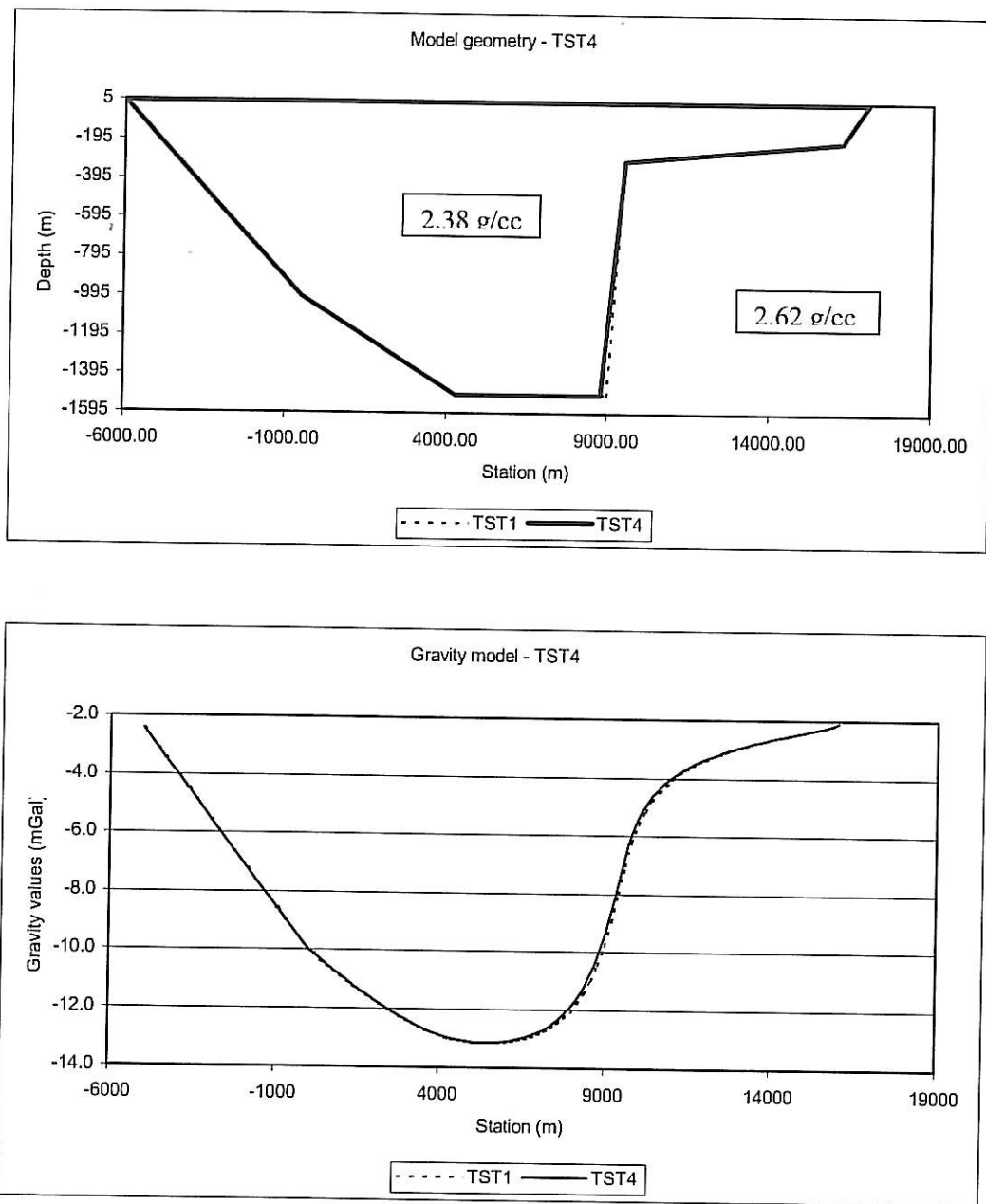
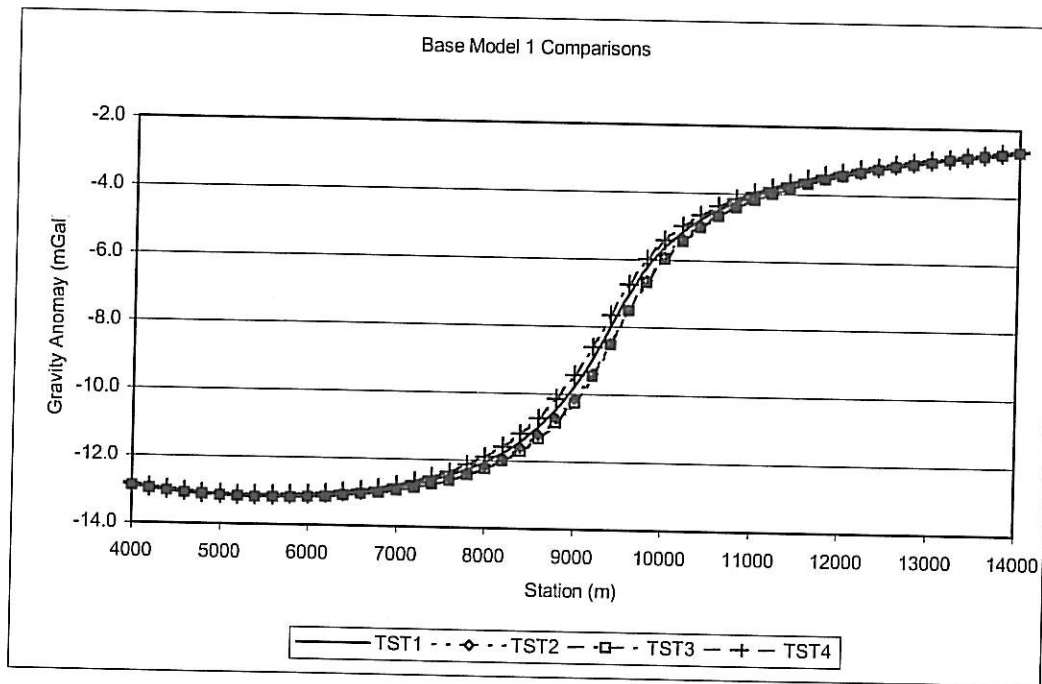
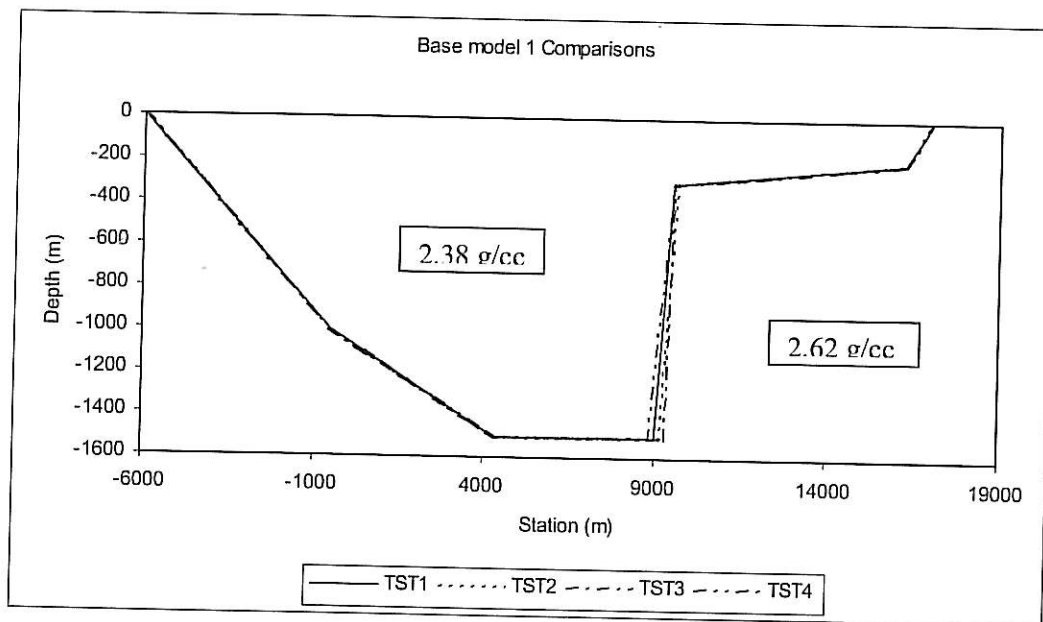


Figure C4

END TST4



**Figure C5** Base Model 1 comparisons

## Gravity method sensitivity tests Test Series 2

Overburden 1000 m.

## TST10 – Base model 2

Data Set : TST10.MGX

Location: Calitzdorp Profile: TST10  
County: Klein Karoo X-units m  
Project Gray Z-units m

Start point of profile  
 X (grid easting) 0.00 m  
 Y Grid northing) 0.00m  
 Distance value at start 0.00m

Profile is oriented 90.000 deg east of true north  
Strike direction is 0.00 deg east of true north  
Grid north is 0.000 deg east of true north

All angles are measured clockwise from true north.

Gravity Field      milligals  
 Density units      g/cc  
 Fitting error      0.0      units

There are no regional values

Body: Background Layer: Yes  
Density: 0 Free parameter No  
Background is 2-dimensional

Body: 1 7 Vertices 0 free parameters Layer: No  
Density: -0.24 Free Parameter: No  
Symmetric Body; Strike length: 20000.00 m  
Body Direction: CW

### Internal Coordinate Positions:

Vertex No	X-Loc	Z-Loc	Vertex No	X-Loc	Z-Loc
1	-6000.00	0.00	5	9000.00	2000.00
2	17000.00	0.00	6	4300.00	2000.00
3	16200.00	1000.00	7	-500.00	1000.00

Gravity method sensitivity tests **TST10 (Continued)**

Vertex No	X-Loc	Z-Loc	Vertex No	X-Loc	Z-Loc
4	9500.00	1000.00			
Station No	Distance (m)	Elevation (m)	Gravity (mgal)		
1	-5000	0.0	-2.60		
2	0	0.0	-11.08		
3	200	0.0	-11.40		
4	400	0.0	-11.71		
5	600	0.0	-12.02		
6	800	0.0	-12.33		
7	1000	0.0	-12.63		
8	1200	0.0	-12.92		
9	1400	0.0	-13.21		
10	1600	0.0	-13.50		
11	1800	0.0	-13.77		
12	2000	0.0	-14.04		
13	2200	0.0	-14.30		
14	2400	0.0	-14.55		
15	2600	0.0	-14.79		
16	2800	0.0	-15.03		
17	3000	0.0	-15.25		
18	3200	0.0	-15.45		
19	3400	0.0	-15.65		
20	3600	0.0	-15.83		
21	3800	0.0	-16.00		
22	4000	0.0	-16.15		
23	4200	0.0	-16.28		
24	4400	0.0	-16.40		
25	4600	0.0	-16.51		
26	4800	0.0	-16.59		
27	5000	0.0	-16.67		
28	5200	0.0	-16.72		
29	5400	0.0	-16.77		
30	5600	0.0	-16.80		
31	5800	0.0	-16.81		
32	6000	0.0	-16.81		
33	6200	0.0	-16.80		
34	6400	0.0	-16.77		
35	6600	0.0	-16.73		
36	6800	0.0	-16.67		
37	7000	0.0	-16.60		
38	7200	0.0	-16.50		

Gravity method sensitivity tests **TST10 (Continued)**

Station No	Distance (m)	Elevation (m)	Gravity (mgal)
39	7400	0.0	-16.38
40	7600	0.0	-16.24
41	7800	0.0	-16.08
42	8000	0.0	-15.88
43	8200	0.0	-15.65
44	8400	0.0	-15.38
45	8600	0.0	-15.07
46	8800	0.0	-14.72
47	9000	0.0	-14.34
48	9200	0.0	-13.93
49	9400	0.0	-13.51
50	9600	0.0	-13.10
51	9800	0.0	-12.70
52	10000	0.0	-12.34
53	10200	0.0	-12.02
54	10400	0.0	-11.73
55	10600	0.0	-11.49
56	10800	0.0	-11.27
57	11000	0.0	-11.09
58	11200	0.0	-10.92
59	11400	0.0	-10.78
60	11600	0.0	-10.65
61	11800	0.0	-10.54
62	12000	0.0	-10.43
63	12200	0.0	-10.34
64	12400	0.0	-10.25
65	12600	0.0	-10.17
66	12800	0.0	-10.10
67	13000	0.0	-10.02
68	13200	0.0	-9.95
69	13400	0.0	-9.88
70	13600	0.0	-9.81
71	13800	0.0	-9.74
72	14000	0.0	-9.67
73	14200	0.0	-9.59
74	14400	0.0	-9.50
75	14600	0.0	-9.41
76	14800	0.0	-9.30
77	15000	0.0	-9.17
78	15200	0.0	-9.02
79	15400	0.0	-8.84

Gravity method sensitivity tests      **TST10 (Continued)**

Station No	Distance (m)	Elevation (m)	Gravity (mgal)
80	15600	0.0	-8.60
81	15800	0.0	-8.30
82	16000	0.0	-7.91
83	17000	0.0	-2.89
84	18000	0.0	-0.99

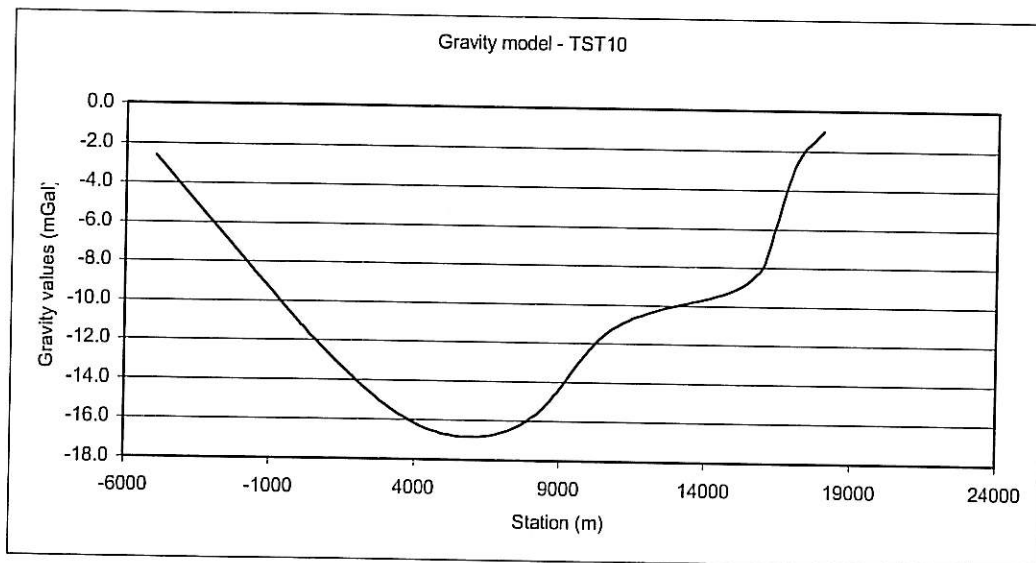
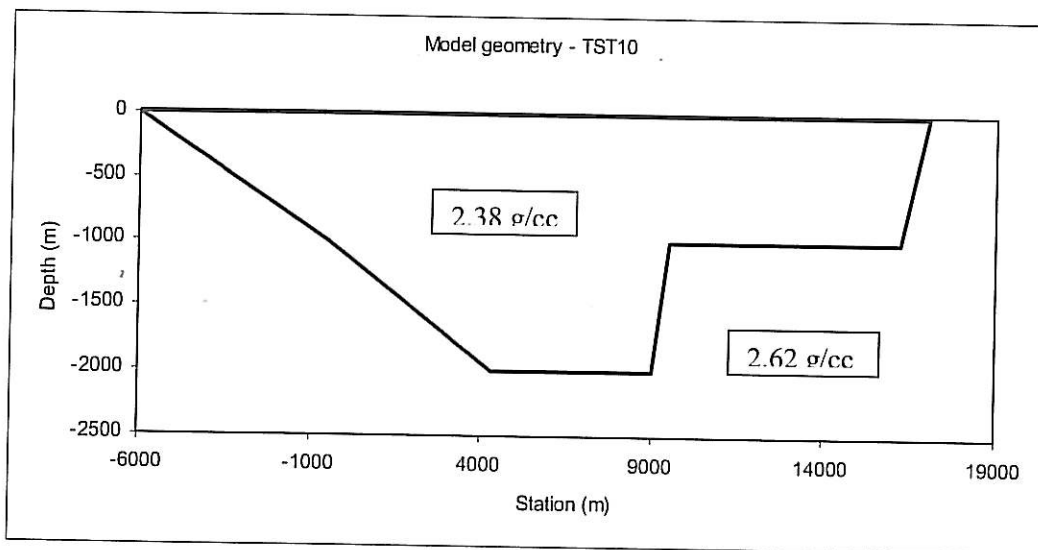


**Figure C6** Base model 2

**END TST10**

Gravity method sensitivity tests **TST11**

Shift fault 100 m.

Data Set : TST11.MGX

Location: Calitzdorp Profile:TST11  
 County: Klein Karoo X-units m  
 Project Grav Z-units m

### Start point of profile

Start point of profile

X (grid easting)	0.00 m
Y Grid northing)	0.00m
Distance value at start	0.00m

Profile is oriented 90.000 deg east of true north  
 Strike direction is 0.00 deg east of true north  
 Grid north is 0.000 deg east of true north

All angles are measured clockwise from true north

Gravity Field milligals  
 Density units g/cc  
 Fitting error 0.0 units

There are no regional values

Body: Background Layer: Yes  
Density: 0 Free parameter No  
Background is 2-dimensional

Body: 1      7 Vertices      0 free parameters      Layer: No  
 Density:      -0.24      Free Parameter: No  
 Symmetric Body; Strike length:      20000.00 m  
 Body Direction:      CW

### Internal Coordinate Positions:

Vertex No	X-Loc	Z-Loc	Vertex No	X-Loc	Z-Loc
1	-6000.00	0.00	5	9100.00	2000.00
2	17000.00	0.00	6	4300.00	2000.00
3	16200.00	1000.00	7	-500.00	1000.00
4	9600.00	1000.00			

Gravity method sensitivity tests **TST11 (Continued)**

Station No	Distance (m)	Elevation (m)	Gravity (mgal) Data	Gravity (mgal) Synthetic	Difference
1	-5000	0.0	-2.60	-2.60	0.00
2	0	0.0	-11.08	-11.08	0.00
3	200	0.0	-11.40	-11.40	0.00
4	400	0.0	-11.71	-11.72	-0.01
5	600	0.0	-12.02	-12.03	-0.01
6	800	0.0	-12.33	-12.33	0.00
7	1000	0.0	-12.63	-12.63	0.00
8	1200	0.0	-12.92	-12.93	-0.01
9	1400	0.0	-13.21	-13.22	-0.01
10	1600	0.0	-13.50	-13.50	0.00
11	1800	0.0	-13.77	-13.78	-0.01
12	2000	0.0	-14.04	-14.05	-0.01
13	2200	0.0	-14.30	-14.31	-0.01
14	2400	0.0	-14.55	-14.55	0.00
15	2600	0.0	-14.79	-14.80	-0.01
16	2800	0.0	-15.03	-15.03	0.00
17	3000	0.0	-15.25	-15.26	-0.01
18	3200	0.0	-15.45	-15.46	-0.01
19	3400	0.0	-15.65	-15.66	-0.01
20	3600	0.0	-15.83	-15.84	-0.01
21	3800	0.0	-16.00	-16.01	-0.01
22	4000	0.0	-16.15	-16.16	-0.01
23	4200	0.0	-16.28	-16.30	-0.02
24	4400	0.0	-16.40	-16.42	-0.02
25	4600	0.0	-16.51	-16.52	-0.01
26	4800	0.0	-16.59	-16.61	-0.02
27	5000	0.0	-16.67	-16.69	-0.02
28	5200	0.0	-16.72	-16.75	-0.03
29	5400	0.0	-16.77	-16.79	-0.02
30	5600	0.0	-16.80	-16.82	-0.02
31	5800	0.0	-16.81	-16.84	-0.03
32	6000	0.0	-16.81	-16.85	-0.04
33	6200	0.0	-16.80	-16.84	-0.04
34	6400	0.0	-16.77	-16.82	-0.05
35	6600	0.0	-16.73	-16.78	-0.05
36	6800	0.0	-16.67	-16.73	-0.06
37	7000	0.0	-16.60	-16.66	-0.06
38	7200	0.0	-16.50	-16.57	-0.07
39	7400	0.0	-16.38	-16.46	-0.08
40	7600	0.0	-16.24	-16.33	-0.09
41	7800	0.0	-16.08	-16.18	-0.10

Gravity method sensitivity tests **TST11 (Continued)**

Station No	Distance (m)	Elevation (m)	Data	Gravity (mgal) Synthetic	Difference
42	8000	0.0	-15.88	-15.99	-0.11
43	8200	0.0	-15.65	-15.78	-0.13
44	8400	0.0	-15.38	-15.53	-0.15
45	8600	0.0	-15.07	-15.24	-0.17
46	8800	0.0	-14.72	-14.91	-0.19
47	9000	0.0	-14.34	-14.54	-0.20
48	9200	0.0	-13.93	-14.15	-0.22
49	9400	0.0	-13.51	-13.73	-0.22
50	9600	0.0	-13.10	-13.31	-0.21
51	9800	0.0	-12.70	-12.90	-0.20
52	10000	0.0	-12.34	-12.52	-0.18
53	10200	0.0	-12.02	-12.18	-0.16
54	10400	0.0	-11.73	-11.87	-0.14
55	10600	0.0	-11.49	-11.61	-0.12
56	10800	0.0	-11.27	-11.38	-0.11
57	11000	0.0	-11.09	-11.18	-0.09
58	11200	0.0	-10.92	-11.00	-0.08
59	11400	0.0	-10.78	-10.85	-0.07
60	11600	0.0	-10.65	-10.71	-0.06
61	11800	0.0	-10.54	-10.59	-0.05
62	12000	0.0	-10.43	-10.48	-0.05
63	12200	0.0	-10.34	-10.38	-0.04
64	12400	0.0	-10.25	-10.29	-0.04
65	12600	0.0	-10.17	-10.21	-0.04
66	12800	0.0	-10.10	-10.13	-0.03
67	13000	0.0	-10.02	-10.05	-0.03
68	13200	0.0	-9.95	-9.98	-0.03
69	13400	0.0	-9.88	-9.91	-0.03
70	13600	0.0	-9.81	-9.84	-0.03
71	13800	0.0	-9.74	-9.76	-0.02
72	14000	0.0	-9.67	-9.69	-0.02
73	14200	0.0	-9.59	-9.61	-0.02
74	14400	0.0	-9.50	-9.52	-0.02
75	14600	0.0	-9.41	-9.42	-0.01
76	14800	0.0	-9.30	-9.31	-0.01
77	15000	0.0	-9.17	-9.19	-0.02
78	15200	0.0	-9.02	-9.03	-0.01
79	15400	0.0	-8.84	-8.85	-0.01
80	15600	0.0	-8.60	-8.61	-0.01
81	15800	0.0	-8.30	-8.31	-0.01
82	16000	0.0	-7.91	-7.92	-0.01

Gravity method sensitivity tests **TST11 (Continued)**

Station No	Distance (m)	Elevation (m)	Data	Gravity (mgal) Synthetic	Difference
83	17000	0.0		-2.89	-2.89
84	18000	0.0		-0.99	-1.00

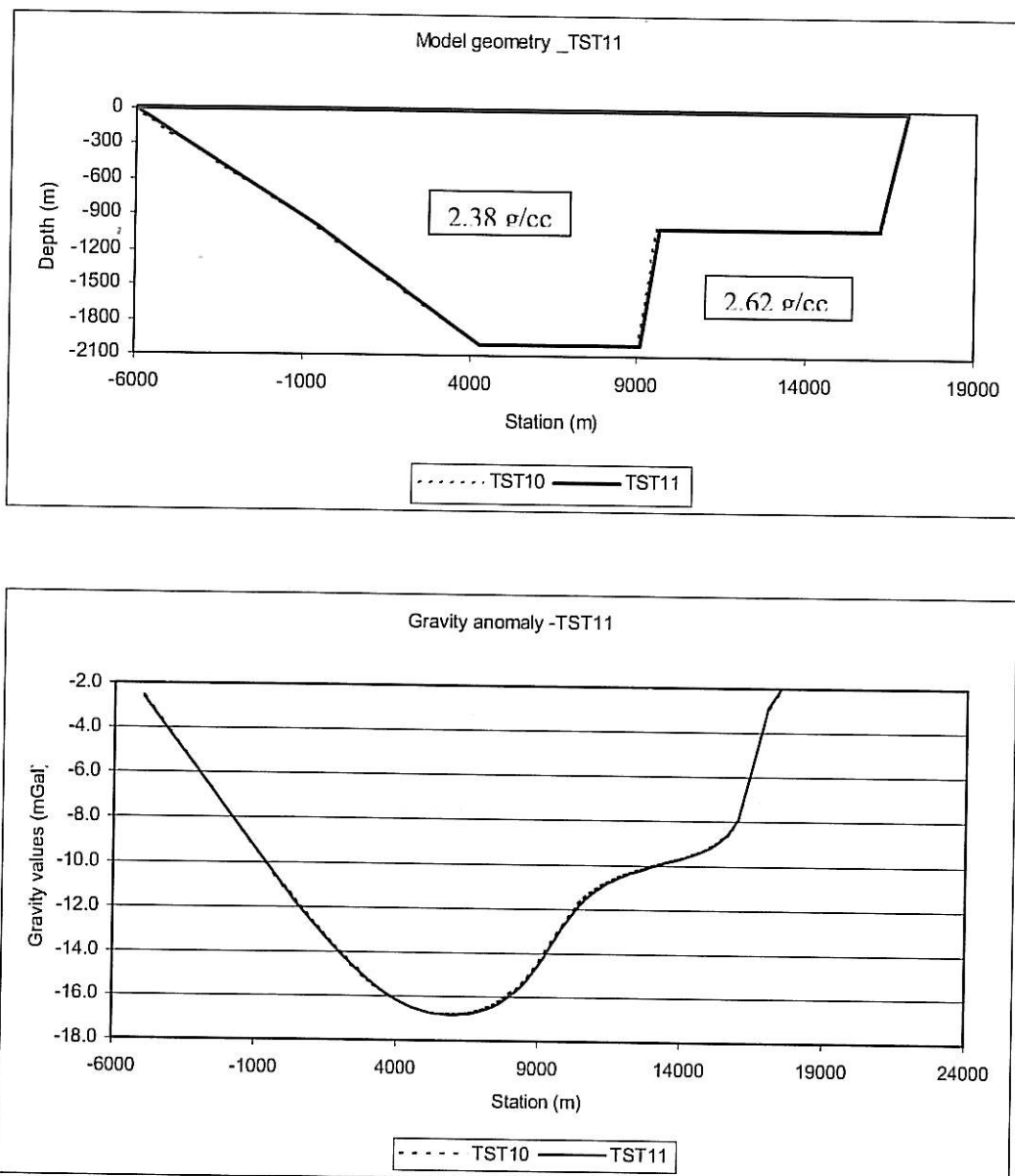


**Figure C7**

**END TST11**

Gravity method sensitivity tests TST13

Shift fault 200 m.

Data Set : TST13.MGX

Location: Calitzdorp Profile: TST13  
 County: Klein Karoo X-units m  
 Project Grav Z-units m

### Start point of profile

Start point of profile

X (grid easting)	0.00 m
Y Grid northing)	0.00m
Distance value at start	0.00m

Profile is oriented 90.000 deg east of true north  
Strike direction is 0.00 deg east of true north  
Grid north is 0.000 deg east of true north

All angles are measured clockwise from true north

Gravity Field milligals  
 Density units g/cc  
 Fitting error 0.0 units

There are no regional values

Body: Background Layer: Yes  
Density: 0 Free parameter No  
Background is 2-dimensional

Body: 1      7 Vertices      0 free parameters      Layer: No  
Density:      -0.24      Free Parameter: No  
Symmetric Body; Strike length:      20000.00 m  
Body Direction:      CW

### Internal Coordinate Positions:

Vertex No	X-Loc	Z-Loc	Vertex No	X-Loc	Z-Loc
1	-6000.00	0.00	5	9200.00	2000.00
2	17000.00	0.00	6	4300.00	2000.00
3	16200.00	1000.00	7	-500.00	1000.00
4	9700.00	1000.00			

Gravity method sensitivity tests **TST13 (Continued)**

Station No	Distance (m)	Elevation (m)	Data	Gravity (mgal)	Difference
				Data	Synthetic
1	-5000	0.0	-2.60	-2.60	0.00
2	0	0.0	-11.08	-11.09	-0.01
3	200	0.0	-11.40	-11.41	-0.01
4	400	0.0	-11.71	-11.72	-0.01
5	600	0.0	-12.02	-12.03	-0.01
6	800	0.0	-12.33	-12.34	-0.01
7	1000	0.0	-12.63	-12.64	-0.01
8	1200	0.0	-12.92	-12.93	-0.01
9	1400	0.0	-13.21	-13.23	-0.02
10	1600	0.0	-13.50	-13.51	-0.01
11	1800	0.0	-13.77	-13.79	-0.02
12	2000	0.0	-14.04	-14.05	-0.01
13	2200	0.0	-14.30	-14.32	-0.02
14	2400	0.0	-14.55	-14.57	-0.02
15	2600	0.0	-14.79	-14.81	-0.02
16	2800	0.0	-15.03	-15.04	-0.01
17	3000	0.0	-15.25	-15.26	-0.01
18	3200	0.0	-15.45	-15.47	-0.02
19	3400	0.0	-15.65	-15.67	-0.02
20	3600	0.0	-15.83	-15.85	-0.02
21	3800	0.0	-16.00	-16.02	-0.02
22	4000	0.0	-16.15	-16.17	-0.02
23	4200	0.0	-16.28	-16.31	-0.03
24	4400	0.0	-16.40	-16.43	-0.03
25	4600	0.0	-16.51	-16.54	-0.03
26	4800	0.0	-16.59	-16.63	-0.04
27	5000	0.0	-16.67	-16.71	-0.04
28	5200	0.0	-16.72	-16.77	-0.05
29	5400	0.0	-16.77	-16.82	-0.05
30	5600	0.0	-16.80	-16.85	-0.05
31	5800	0.0	-16.81	-16.87	-0.06
32	6000	0.0	-16.81	-16.88	-0.07
33	6200	0.0	-16.80	-16.87	-0.07
34	6400	0.0	-16.77	-16.86	-0.09
35	6600	0.0	-16.73	-16.82	-0.09
36	6800	0.0	-16.67	-16.78	-0.11
37	7000	0.0	-16.60	-16.71	-0.11
38	7200	0.0	-16.50	-16.63	-0.13
39	7400	0.0	-16.38	-16.54	-0.16
40	7600	0.0	-16.24	-16.42	-0.18
41	7800	0.0	-16.08	-16.27	-0.19

Gravity method sensitivity tests **TST13 (Continued)**

Station No	Distance (m)	Elevation (m)	Data	Gravity (mgal) Synthetic	Difference
42	8000	0.0	-15.88	-16.10	-0.22
43	8200	0.0	-15.65	-15.90	-0.25
44	8400	0.0	-15.38	-15.67	-0.29
45	8600	0.0	-15.07	-15.40	-0.33
46	8800	0.0	-14.72	-15.09	-0.37
47	9000	0.0	-14.34	-14.74	-0.40
48	9200	0.0	-13.93	-14.36	-0.43
49	9400	0.0	-13.51	-13.95	-0.44
50	9600	0.0	-13.10	-13.52	-0.42
51	9800	0.0	-12.70	-13.11	-0.41
52	10000	0.0	-12.34	-12.71	-0.37
53	10200	0.0	-12.02	-12.35	-0.33
54	10400	0.0	-11.73	-12.02	-0.29
55	10600	0.0	-11.49	-11.74	-0.25
56	10800	0.0	-11.27	-11.49	-0.22
57	11000	0.0	-11.09	-11.27	-0.18
58	11200	0.0	-10.92	-11.09	-0.17
59	11400	0.0	-10.78	-10.92	-0.14
60	11600	0.0	-10.65	-10.78	-0.13
61	11800	0.0	-10.54	-10.65	-0.11
62	12000	0.0	-10.43	-10.53	-0.10
63	12200	0.0	-10.34	-10.43	-0.09
64	12400	0.0	-10.25	-10.33	-0.08
65	12600	0.0	-10.17	-10.24	-0.07
66	12800	0.0	-10.10	-10.16	-0.06
67	13000	0.0	-10.02	-10.08	-0.06
68	13200	0.0	-9.95	-10.01	-0.06
69	13400	0.0	-9.88	-9.93	-0.05
70	13600	0.0	-9.81	-9.86	-0.05
71	13800	0.0	-9.74	-9.78	-0.04
72	14000	0.0	-9.67	-9.70	-0.03
73	14200	0.0	-9.59	-9.62	-0.03
74	14400	0.0	-9.50	-9.53	-0.03
75	14600	0.0	-9.41	-9.44	-0.03
76	14800	0.0	-9.30	-9.33	-0.03
77	15000	0.0	-9.17	-9.20	-0.03
78	15200	0.0	-9.02	-9.04	-0.02
79	15400	0.0	-8.84	-8.86	-0.02
80	15600	0.0	-8.60	-8.62	-0.02
81	15800	0.0	-8.30	-8.32	-0.02
82	16000	0.0	-7.91	-7.92	-0.01

Gravity method sensitivity tests **TST13 (Continued)**

Station No	Distance (m)	Elevation (m)	Data	Gravity (mgal) Synthetic	Difference
83	17000	0.0	-2.89	-2.90	-0.01
84	18000	0.0	-0.99	-1.00	-0.01

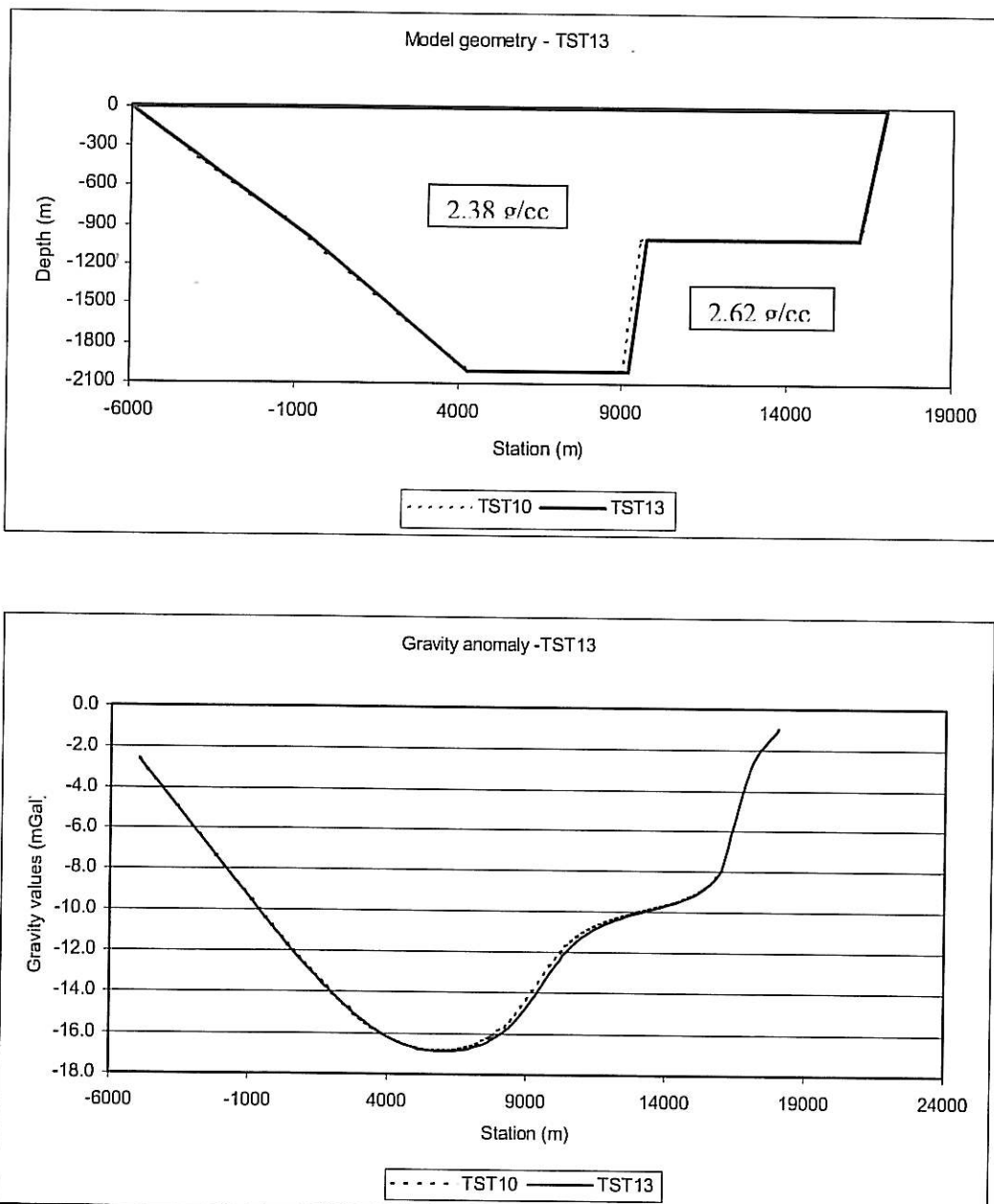
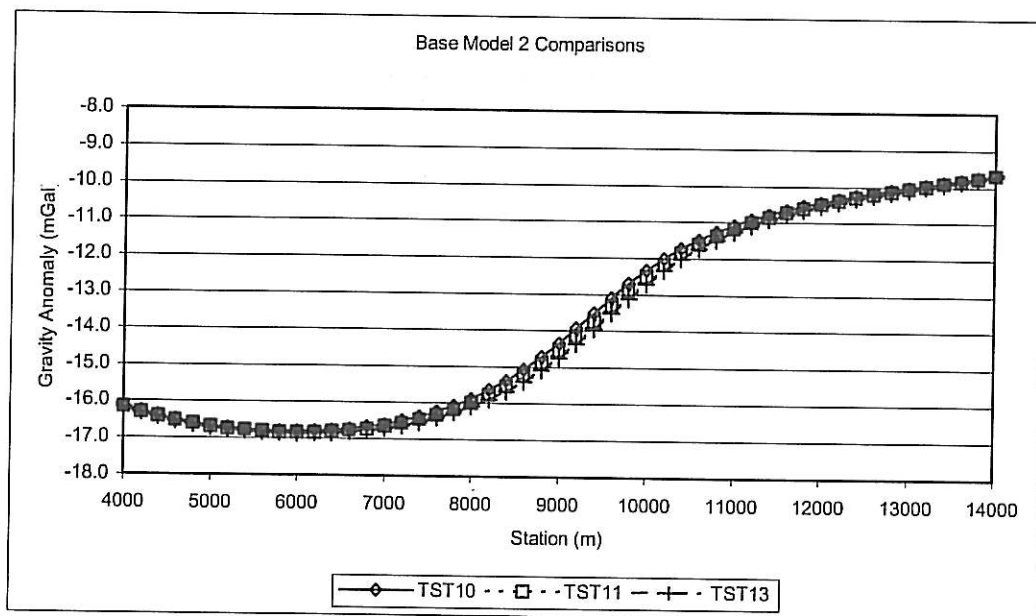
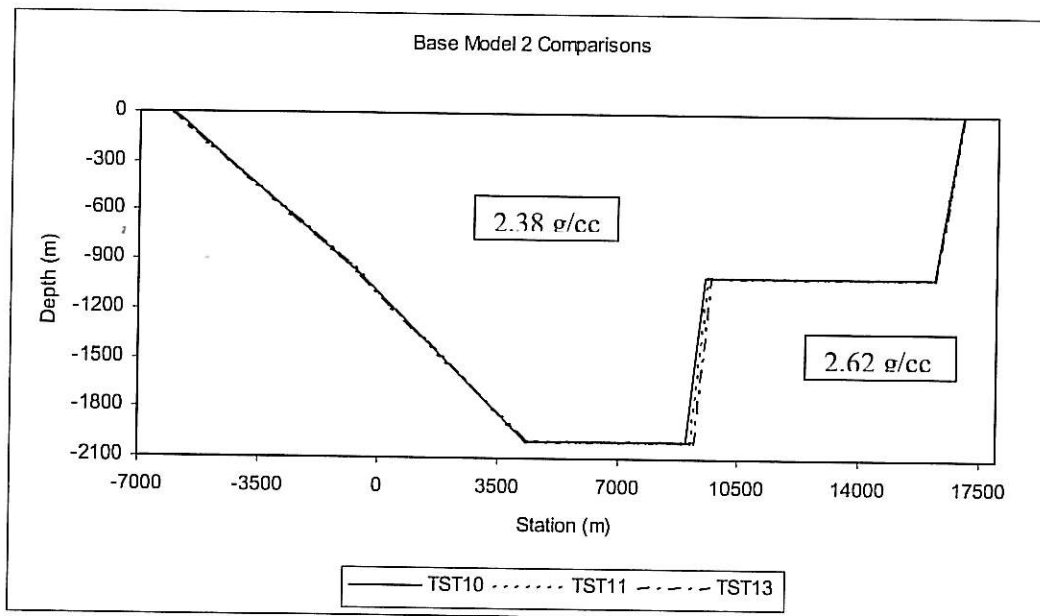


Figure C8

END TST13



**Figure C9** Base model 2 comparisons

**GHP3949**

**APPENDIX D**

**Additional photographs: Structures**

Photographs of interesting features and structures that were inaccessible for or unsuited to measurements were taken during the field investigations. The coordinates of the vantage points are given, as well as bearing towards the feature of interest, where available. A Brunton compass was used to estimate apparent dip and strike where possible. These data are not absolute due to the inability to align the observer exactly with the feature strike, but care has been taken to obtain accurate dips and strikes.



**Figure D1** Dip of Cretaceous sediments as seen from the De Rust – Uniondale road, 3 km west of Meiringspoort. View is looking south, dip approximately  $20^{\circ}$  east.



**Figure D2** Photograph of the TMG/Buffelskloof contact at the northern edge of the basin, at the end of the gravity Profile 1. View is from the Kruisrivier dirt road, looking east.

The gravity Profile 1 ended on the TMS outcrops north of the Cango fault line, near Kruisrivier. The field relationship of the Uitenhage rocks against the TMG at the northern edge of the basin at this location is shown in Fig. D2. It is clear from the photograph that the contact dips at  $\approx 30^\circ$ , and not at  $70^\circ$  as would be expected in the case of a normal fault as northern boundary for the Cretaceous sediments (Cango/Swartberg Fault).

This could suggest that the deposition in this region was not controlled or bounded by the Cango Fault alone, and that post-depositional tectonics tilted the layers to their present position. This would indicate a tilt of up to  $40^\circ$ . Drilling work over the TMS – Uitenhage contact zone at Schoemanshoek to the east of the area in Figure D2 indicated the dip of a fracture zone in the TMS to be in the order of  $75^\circ$  south (Whittingham, GH1501). The intersections of the TMS/Uitenhage contact seen in the Schoemanshoek boreholes indicate that the Uitenhage material is underlain by shallow TMS south of the inferred fault, as is also indicated by the gravity data. Presence of a major fault in this area was not confirmed by the drilling work, suggesting that the basin might not be solely fault bounded at the northern edge.



**Figure D3** A view of Cretaceous material outcrops from slightly south of the Figure D2 vantage point above, showing Buffelskloof Formation dipping at  $\approx 35^\circ$  N. The outcrop in the middle background is the same as in Figure D2 above, with TMS outcrops to the left. View is from the Kruisrivier road (at  $33^\circ 30' 45.8''$  S;  $021^\circ 52' 16.7''$  E) looking  $103^\circ$

The view in Figure D3 from the same area shows Buffelskloof Formation dipping at  $\approx 35^\circ$  N, while in Figure D2 the bedding dip seems to be  $\approx 15^\circ$ . This indicates possible tilting of around  $20^\circ$  between the blocks of Cretaceous material in the two figures. If the Buffelskloof was deposited from the north (with bedding planes dipping south), a total tilt of at least  $35^\circ$  for the block shown in Figure D3 is plausible. Figure D2 however indicates that the amount of tilting is not fixed. The lineations visible in the Buffelskloof in the figures above is assumed to be related to primary bedding. Close visual inspection of outcrops show unsorted conglomerate in a muddy matrix, with almost no small-scale indication of bedding. If the lineations indeed represent bedding, then differential movement between blocks of Buffelskloof Formation after deposition is certain. Uitenhage material close to Dysselsdorp also shows similar dip variations over short distances (Figure D4). These variations could indicate north-south striking faults, resulting in differential movement between blocks of Cretaceous material during the continued post-Cretaceous North-South extension postulated by Kleywegt.



**Figure D4** View of Uitenhage material showing horizontal strata in the foreground with  $\approx 12^\circ$  dip in background. (Vergelegen road,  $33^\circ 30' 16.2''$  E;  $022^\circ 20' 45.4''$  S, looking  $48^\circ$ )

Evidence of post-Cretaceous faulting is also present to the east of Dysselsdorp near the southern edge of the Cretaceous basin. Triangular-shaped planar faces on Enon material are visible along the southern side of a drainage feature, south of the De Rust – Oudtshoorn road (Figure D5). The geomorphology of this area resembles textbook examples of normal fault planes, and the planar surfaces are inconsistent with erosion landforms. (Similar features are present in the TMG outcrops along the Swartberg Fault, east of Toorwaterpoort, near Uniondale.) The geomorphology is not linked to the canal along the foot of the faces, as becomes evident on site.

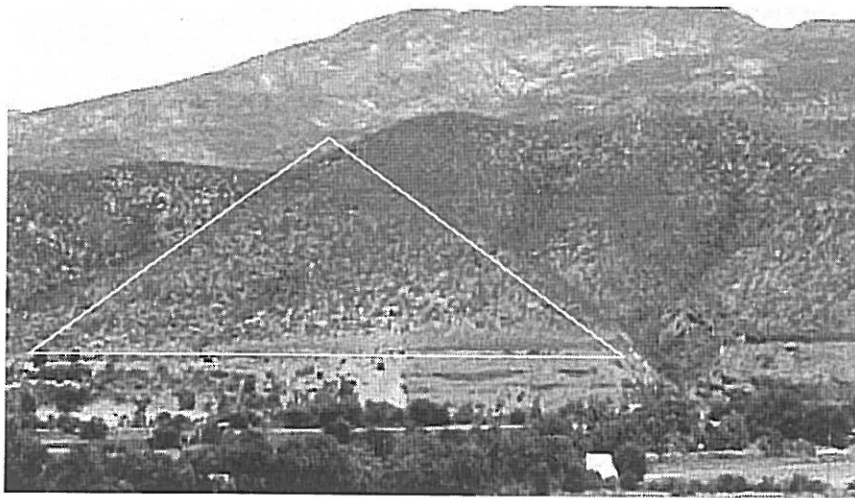


**Figure D5** Fault faces on Enon conglomerate to the east of Dysseldsdorp (View from De Rust – Oudtshoorn tar road, looking south. Mountain in background is TMG)

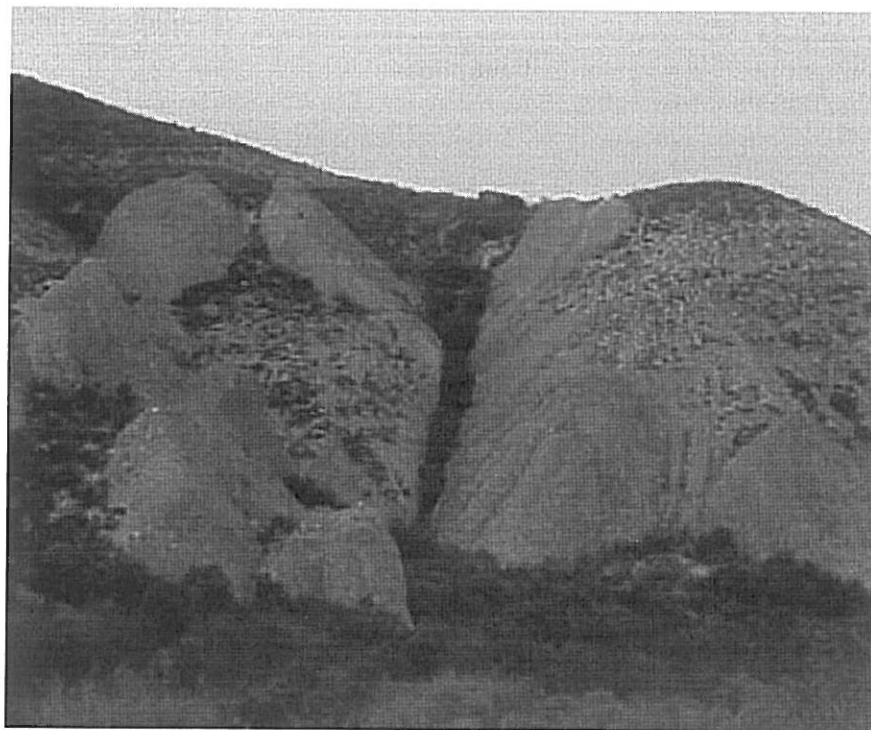


**Figure D6** Joint in Buffelskloof Formation, Vergelegen road. (  $022^{\circ} 22' 30.9''$  E,  $33^{\circ} 31' 3.2''$  S, looking  $99^{\circ}$ ) Apparent dip is  $80^{\circ}$  N, strike direction  $\approx 279^{\circ}$ . (Brunton Readings)



**Figure D7** Joint in Buffelskloof formation. (Vergelegen road,  $022^{\circ}19'9.2''$  E,  $33^{\circ}31'14.8''$  S) Apparent dip:  $82^{\circ}$ , Strike:  $249^{\circ}$  (Brunton readings)



**Figure D8** Open joint in Enon, southern edge of basin (Kamanassie Dam – Oudtshoorn road). Apparent dip:  $76^\circ$ , Strike  $276^\circ$  (Brunton readings)

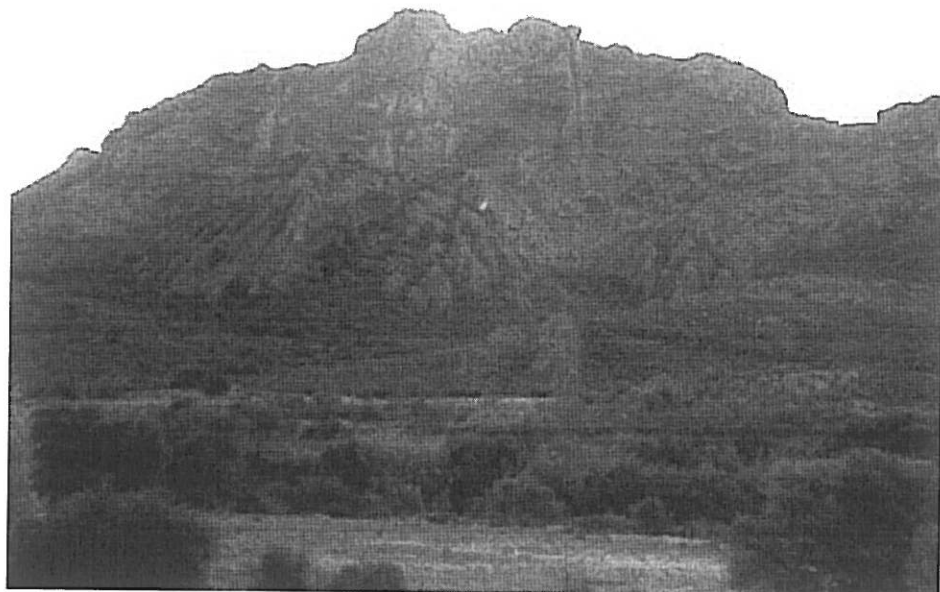


**Figure D9** Large joints in massive Buffelskloof formation, near Buffelskloof on Kruisrivier road, near northern edge of basin. (021° 52' 16.7" E, 33° 30' 45.8" S, looking 257°) The erosion pattern in the foreground follows the same strike.

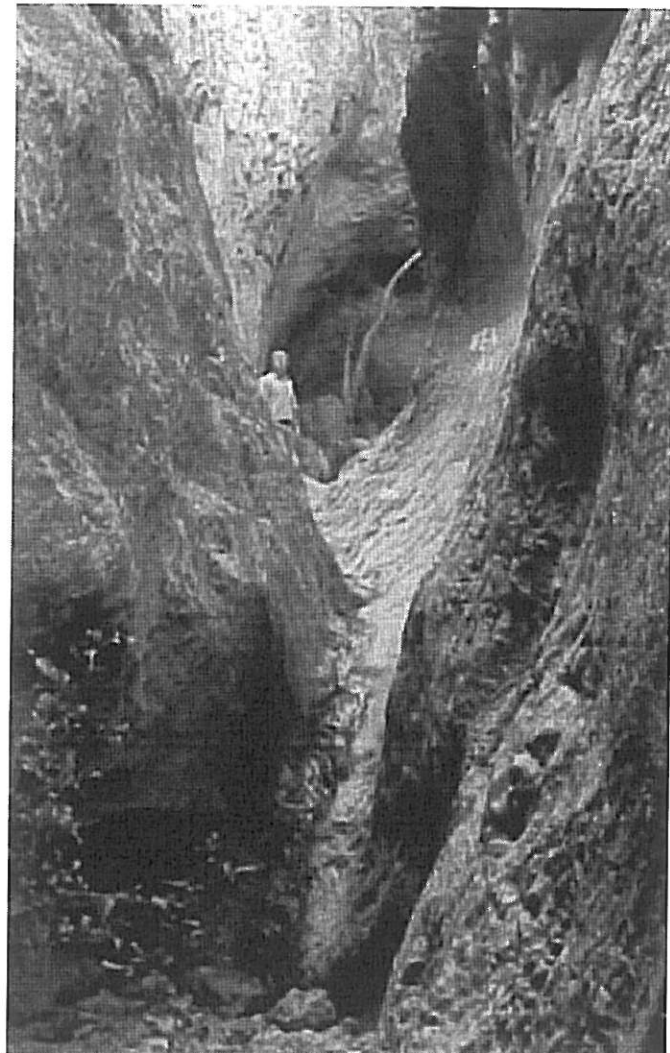


**Figure D10** Eroded joint in TMS near borehole KG1, south of Calitzdorp. Dip is  $83^\circ$  towards  $281^\circ$  (strike  $191^\circ$ : almost north - south). The joint shown forms a cliff face at the end of the kloof where KG 1 is situated. This prominent cliff face, at the western edge of the basin, is related to a postulated north – south fault system at the western edge of the basin.

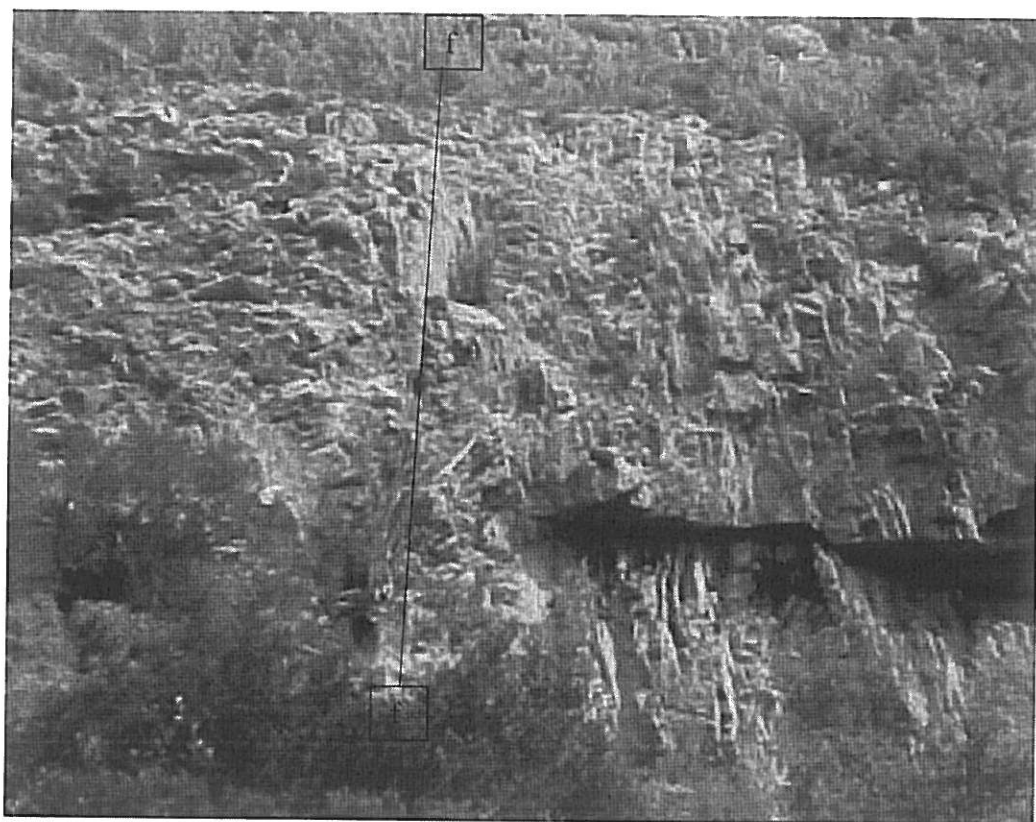


**Figure D11** Horizontal joint butting against fault, borehole KG 1, Calitzdorp. The joint patterns in the TMS on either side of the fault plane are different. Fault strikes  $51^\circ$ , dip is  $\approx 80^\circ$ .



**Figure D12** View of fault plane in TMS near borehole KG 1, Calitzdorp. Fault strikes  $51^\circ$ , dip  $\approx 80^\circ$ . Borehole KG1 is situated to the right of this fault plane.

GHP3949

APPENDIX E



**Hermanus Magnetic Observatory**

Magnetic Observatory, P.O. Box 32, Hermanus, 7200  
Telephone: +27 (28) 3121196 Telefax: +27 (28) 3122039

Date: 08 June 2003  
To: Paul Smith  
Company: Department of Water Affairs & Forestry  
Tel: 058 821 0384  
From: Michelle Van Der Ventel  
Subject: Magnetic Declination

**Message**

**MAGNETIC DECLINATION (D)**

MEAN ANNUAL CHANGE	LATITUDE	LONGITUDE	MAGNETIC DECLINATION
(2003/07/01)	(2000-2002)		
	33° 30' 00" S	21° 40' 00" E	24° 12' WEST
	8.1' P.A.	WESTWARDS	

**Data listing: Structural measurements**

Measurements were taken with a Kassel Coclac structural measurement compass (measured dip, dip azimuth) and a Brunton-type compass (eye-sighted dip, strike) with magnetic declination set to zero. Measurements were corrected for magnetic declination of 24 degrees West before plotting. The data listing include date of measurement, site number, site description where applicable, Latitude and Longitude (DD.MM.SS) taken with a hand held GPS, elevation where acquired, formation type, structure type, structure type, relevant dip, magnetic azimuth and corrected azimuth (true azimuth).

Measurements were mostly restricted to sites next to existing roads, for ease of access. Remote structures estimated with the Brunton compass are shown in Appendix D.

<u>Date</u>	<u>Site</u>	<u>X</u>	<u>Y</u>	<u>Elevation</u> (m)	<u>Formation</u>	<u>Structure</u>	<u>Dip</u>	<u>Azimuth</u> (Magnetic)	<u>Azimuth</u> (True)
9/03/2002	<b>Site 1</b> (West of Calitzdorp)	021/40/28.9E	033/31/37.9S		Kirkwood	Bedding	25	97	73
							21	89	65
		021/40/32.6E	33/31/39.4S				18	78	54
							23	88	64
		021/40/42.4E	33/31/42.3S				29	89	65
							28	89	65
9/03/2002	<b>Site 2</b> (Profile 1)	021/40/44.9E	33/31/43.0S				38	120	96
							32	99	75
		021/40/50.7E	33/31/44.5S				33	95	71
							35	87	63
							36	88	64
							31	92	68
9/03/2002	<b>Site 3</b>	021/53/58.8E	33/36/45.9S		Kirkwood	Bedding	8	24	0
							5	103	79
		021/54/04.8E	33/36/18.9S		Kirkwood (Mudstone in conglomerate)	Bedding	5	84	60
9/03/2002	<b>Site 4</b>	021/53/47.2E	33/35/40.2S		Kirkwood	Bedding	5	282	258
							9	30	6
							10	265	241
							10	308	284
							7	2	338

<u>Date</u>	<u>Site</u>	<u>X</u>	<u>Y</u>	<u>Elevation</u> (m)	<u>Formation</u>	<u>Structure</u>	<u>Dip</u>	<u>Azimuth</u> (Magnetic)	<u>Azimuth</u> (True)
10/3/2002	Site 5	021/51/16.1E	33/31/12.3S		Buffelskloof	Bedding	6 10	166 188	142 164
10/3/2002	Site 6	021/51/57.5E	33/30/54.4S		Buffelskloof	Joint with vertical striaitions	61 62	195 201	171 181
					Buffelskloof	Joint with vertical striaitions	82 82 83	13 17 17	349 353 353
10/03/2002	Site 7 (Oudishoorn - Calitzdorp tar road)	022/02/19.1E	33/35/52.3S		Kirkwood	Bedding	15 6	214 264	190 240
10/3/2002	Site 8	022/01/51.9E	33/35/46.4S		Kirkwood	Bedding	5 5 5	188 234 211	164 210 187
10/3/2002	Site 9	022/01/24.3E	33/35/41.0S		Kirkwood	Bedding	2	3	339
					Vertical joint in sandstone		84 78	196 176	172 152

<u>Date</u>	<u>Site</u>	<u>X</u>	<u>Y</u>	<u>Elevation</u> (m)	<u>Formation</u>	<u>Structure</u>	<u>Dip</u>	<u>Azimuth</u> (Magnetic)	<u>Azimuth</u> (True)
10/03/2002	Site 10	022/27/27.4E	33/34/11.4S		TMS, Enon	Fault plane, TMS/Enon contact	60 90 71	227 230 214	203 206 190

(Dysselsdorp.  
Varkieskloof.  
Enon against TMS)

<u>Date</u>	<u>Site</u>	<u>X</u>	<u>Y</u>	<u>Elevation</u> (m)	<u>Formation</u>	<u>Structure</u>	<u>Dip</u>	<u>Azimuth</u> (Magnetic)	<u>Azimuth</u> (True)
1/10/2003	Site 11 (Vergelegen road)	022/20/11.7E	33/30/51.7S		Buffelskloof	Joint	70	219	195
2/10/2003	Site 12	022/22/16.4E	33/30/51.7S	450	Buffelskloof (Eroded)	Joints	85 75	22 28	358 4
				274					
2/10/2003	Site 13	022/19/2.9E	33/31/18.4S	545	Buffelskloof (Mudstone)	Joints	80 88 79 77	232 232 238 223	208 208 214 199
2/10/2003	Site 11	022/20/11.7E	33/30/51.7S		Buffelskloof	Joint lineation on Surface	40	282	258
						Surface	46 43	279 280	255 256
2/10/2003	Site 14	022/24/21.5E	33/36/50.8S	414	Kirkwood (Mudstone)	Bedding	5 11	282 265	258 241
						Brunton Apparent dip (NW)	1 5		(NW) (NW)



<u>Date</u>	<u>Site</u>	<u>X</u>	<u>Y</u>	<u>Elevation</u> (m)	<u>Formation</u>	<u>Structure</u>	<u>Dip</u>	<u>Azimuth</u> (Magnetic)	<u>Azimuth</u> (True)
3/10/2003	<b>Site 17</b> (Southern edge of Basin)	022/23/28.9E	33/39/10S	400	Bokkeveld shale	Joint 1	74 82	287 278	263 254
3/10/2003	<b>Site 18</b> (Kamanassie - Oudtshoorn road)	022/18/41.3E	33/37/20.4S	323	Kirkwood (Mudstone)	Bedding	5 2 4	355 34 52	331 10 28
3/10/2003						Joint 1	88 90 74 81	8 179 184 190	344 155 160 166
4/10/2003	<b>Site 19</b>	021/56/40.E	33/36/43.1S	244	Kirkwood (Mudstone)	Bedding	84 88 67	254 268 272	230 244 248
							6 20	287 358	263 334



<u>Date</u>	<u>Site</u>	<u>X</u>	<u>Y</u>	<u>Elevation</u> (m)	<u>Formation</u>	<u>Structure</u>	<u>Dip</u>	<u>Azimuth</u> (Magnetic)	<u>Azimuth</u> (True)
4/10/2003	<b>Site 21</b>	021/49/6.5E	33/37/24.3S	219	Kirkwood	Bedding	20	141	117
4/10/2003	<b>Site 1</b>  (Caltzendorf Township)			235	TMS	Joint	82	131	107
4/10/2003	<b>Site 22</b>  (Borehole KG 1, Caltzendorf)	021/39/26.7E	33/32/56.3S	235	TMS	Joint	79	252	228
				72	Fault (E-W)	78	351	327	351
				85		81	342	318	342
				72	356	72	333	309	333

## **GH3949**

### **APPENDIX G**

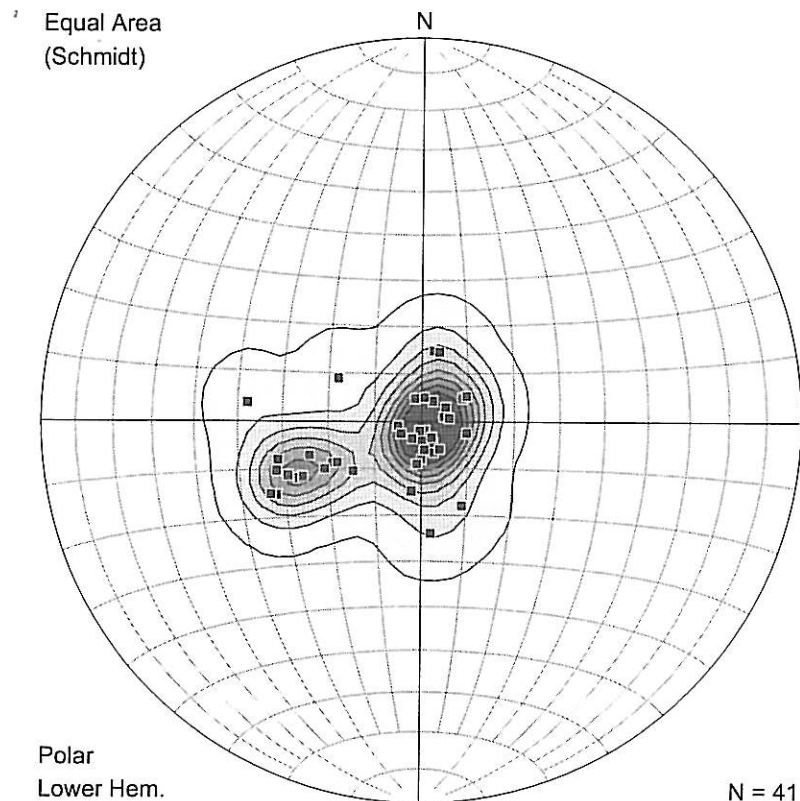
#### **Structural Data Plots**

The following plots of the structural measurements were produced with the *Spheristat* software package. Data are presented as lower hemisphere Schmidt net polar projections of poles to planes, as well as rose diagrams showing dominant directions.

## Data plots: Uitenhage Group Bedding

Plot 1

Kirkwood Formation

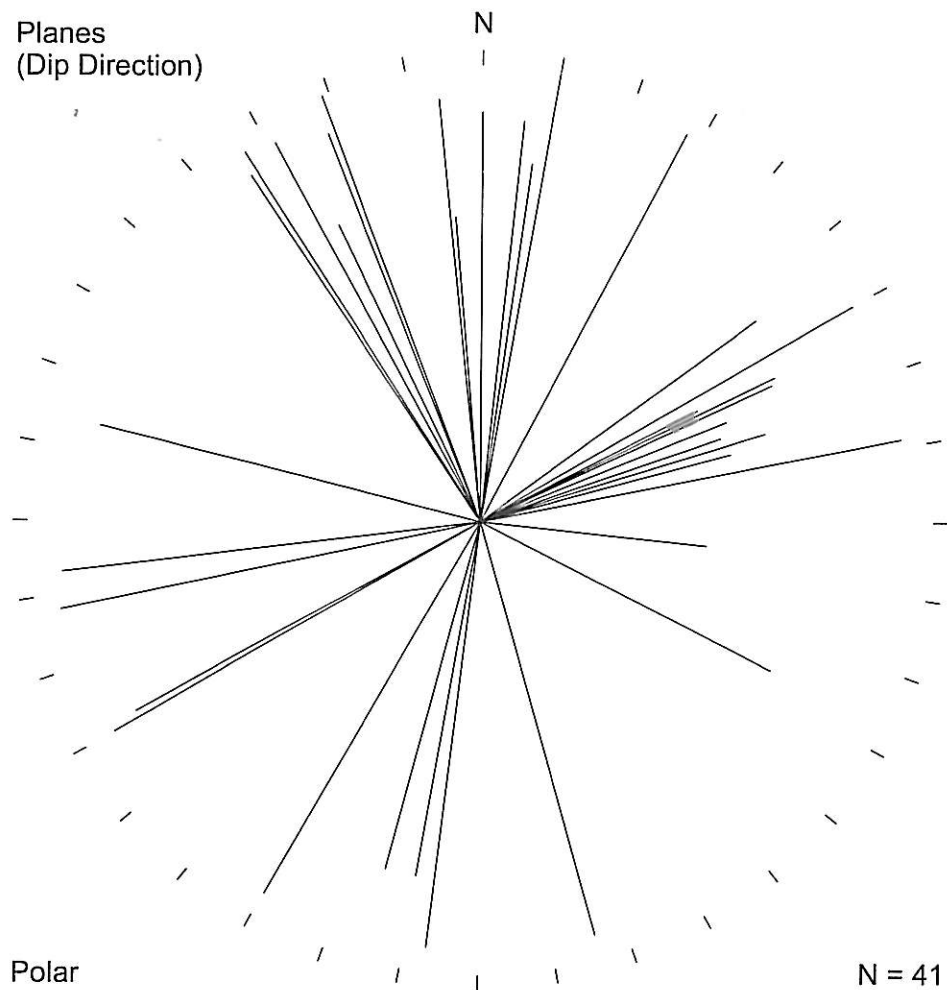


Schmidt net lower hemisphere plot for poles to bedding planes for all measured Kirkwood Formation data.

Number of readings: 41

**Plot 2**

**Kirkwood Formation**

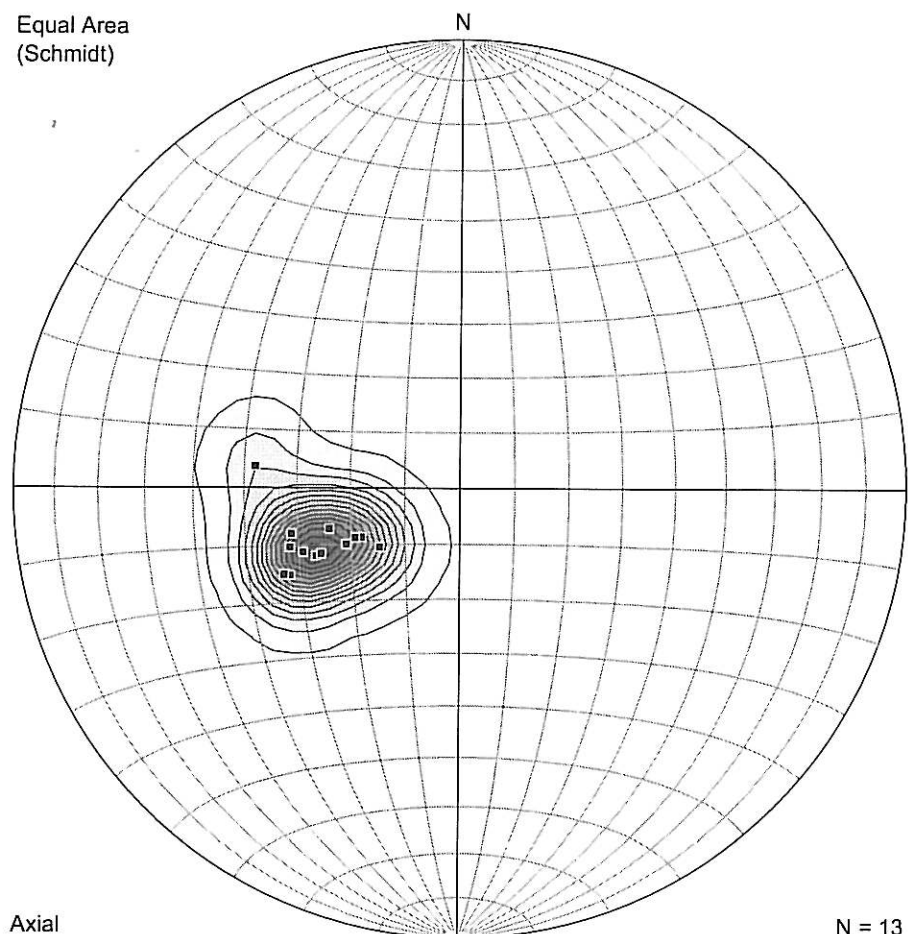


Rose diagram of dip direction distribution for all measured Kirkwood Formation bedding planes. Bar lengths indicate separate measurements, not dip angles.

Number of data points: 41

Plot 3

Site 1

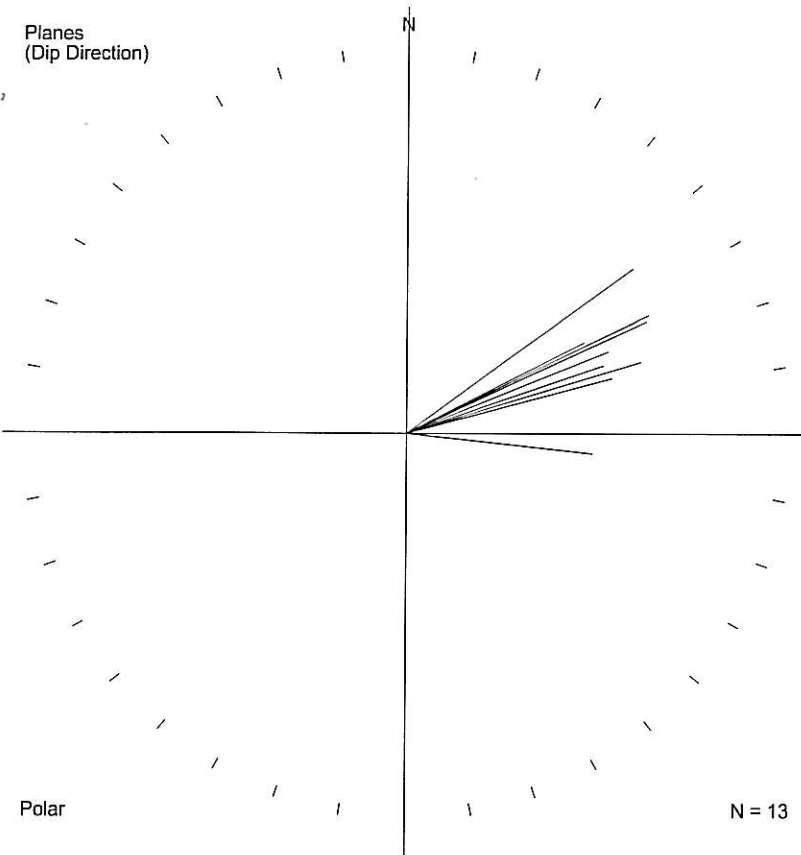


Schmidt net lower hemisphere plot of poles to bedding planes for Kirkwood Formation at Site 1 (Calitzdorp, western edge of basin).

Number of readings: 13  
Mean dip:  $28^\circ$   
Mean dip direction:  $69.3^\circ$

**Plot 4**

**Site 1**

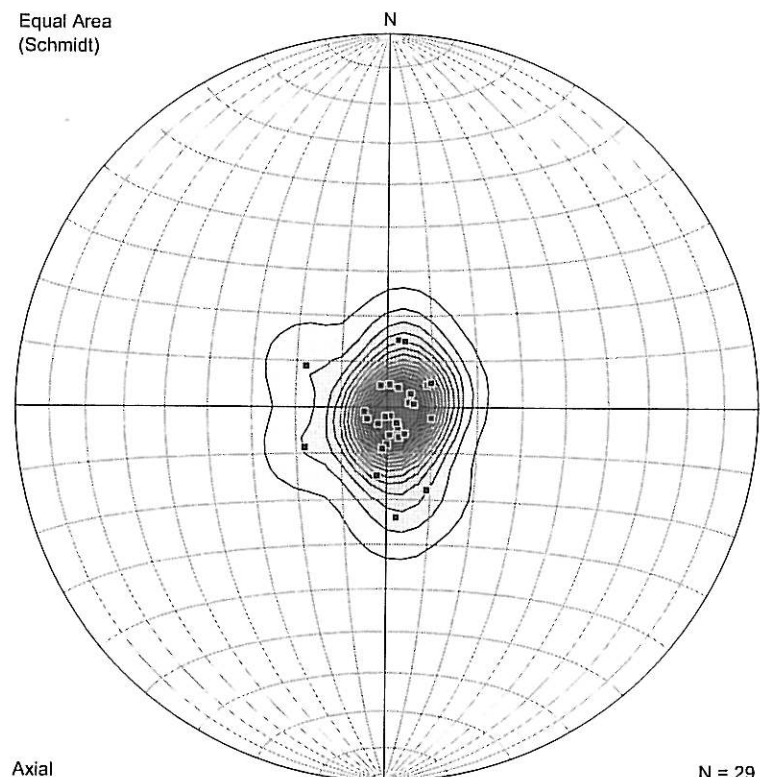


Rose diagram of dip direction distribution for Kirkwood Formation bedding planes measured at Site 1.

Number of data points: 13

**Plot 5**

**Kirkwood Formation Site 2 – Site 21**

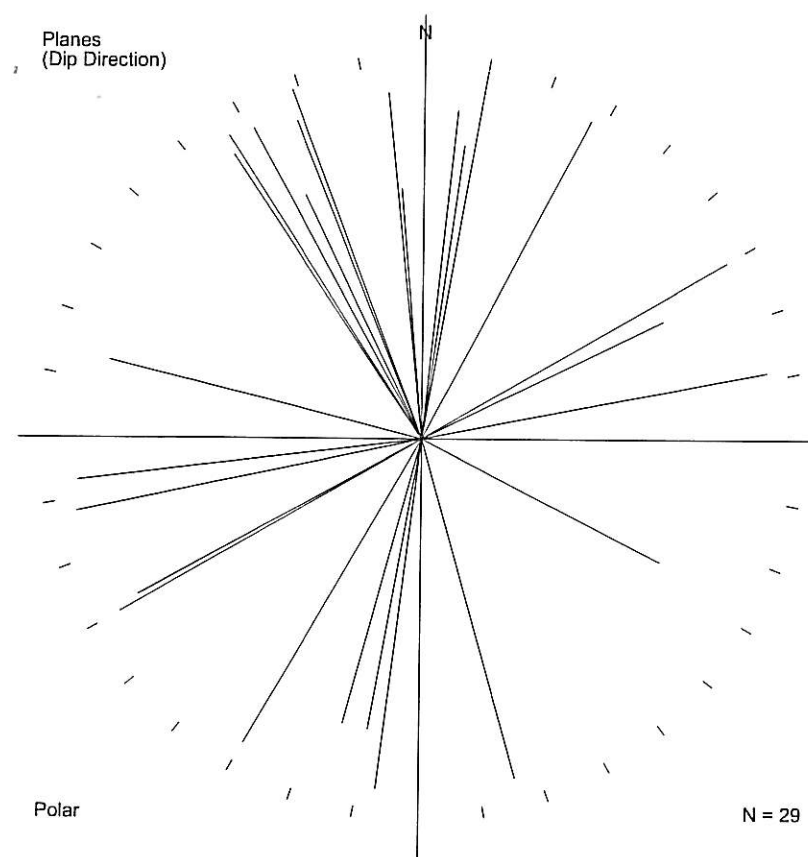


Schmidt net lower hemisphere plot of poles to bedding planes for Kirkwood Formation at Sites 2 - 21 (Sandstones and mudstones, Mid-basin)

Number of readings:	29
Mean bedding dip:	2.4°
Mean dip direction:	312.3°

**Plot 6**

**Kirkwood Formation Site 2 – Site 21**



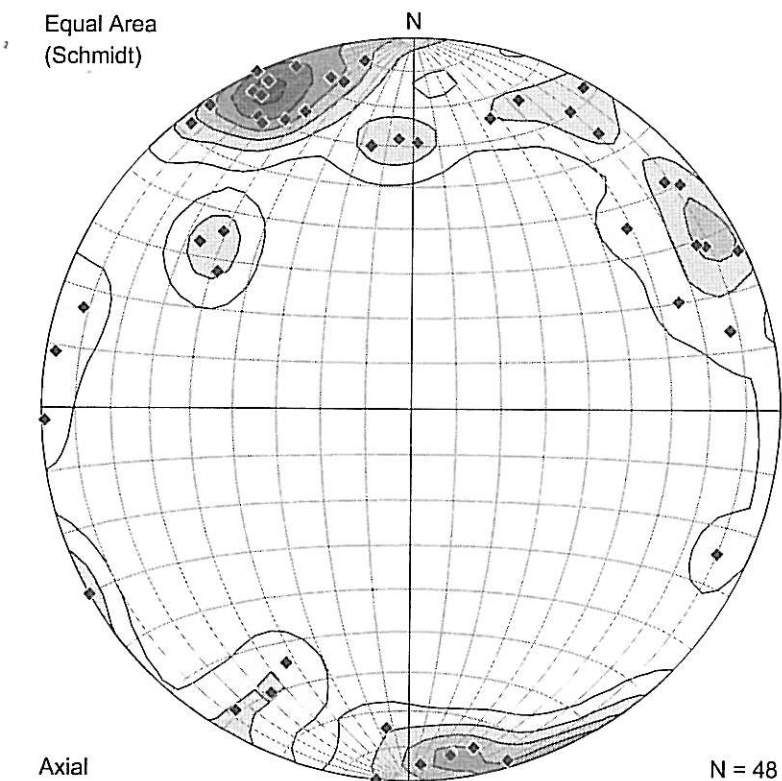
Rose diagram of dip direction distribution for Kirkwood Formation bedding planes measured at Sites 2 - 21 (Sandstones and mudstones, Mid-basin).

Number of data points: 29

Data plots: Uitenhage Group joints

Plot 7

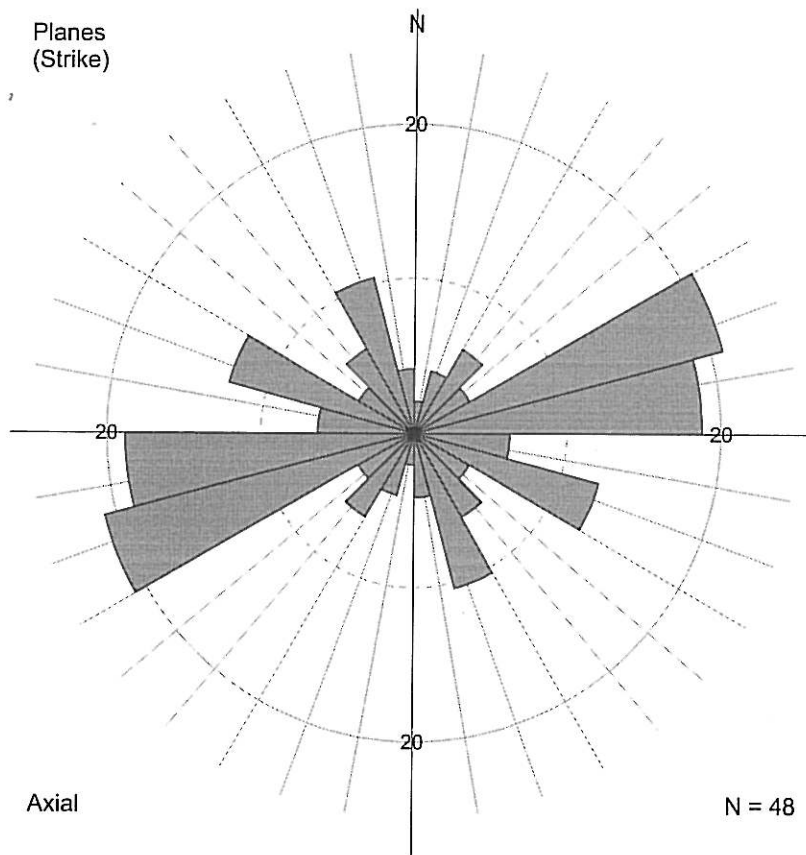
Combined plot of all sites



Schmidt net lower hemisphere plot of poles to joint planes for all joints measured in the Cretaceous sediments (Kirkwood, Enon and Buffelskloof Formations).

Number of readings: 48

**Plot 8**  
**All Cretaceous sediment joints**



Rose diagram showing the strike directions of all joints in the Cretaceous beds.

Number of data points: 48

Class interval:  $15^\circ$

Frequency distribution:  $0 - 15: 2.1\%$ ;  $15 - 30: 4.1\%$ ;  $30 - 45: 6.3\%$

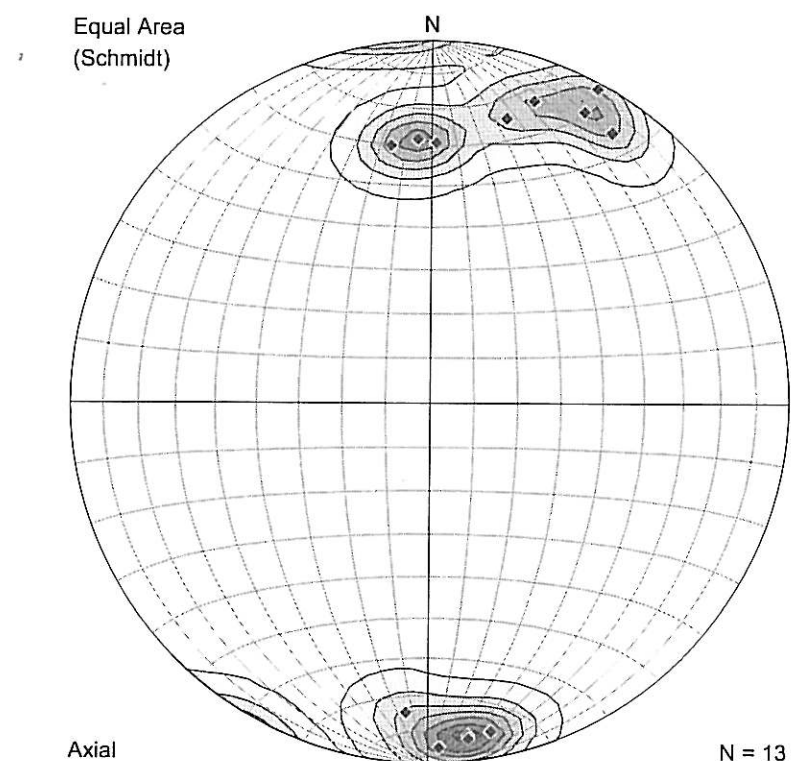
$45 - 60: 4.1\%$ ;  $60 - 75: 20.8\%$ ;  $75 - 90: 18.8\%$

$90 - 105: 6.3\%$ ;  $105 - 120: 12.5\%$ ;  $120 - 135: 4.2\%$

$135 - 150: 6.3\%$ ;  $150 - 165: 10.4\%$ ;  $165 - 180: 4.1\%$

**Plot 9**

**Buffelskloof Formation**

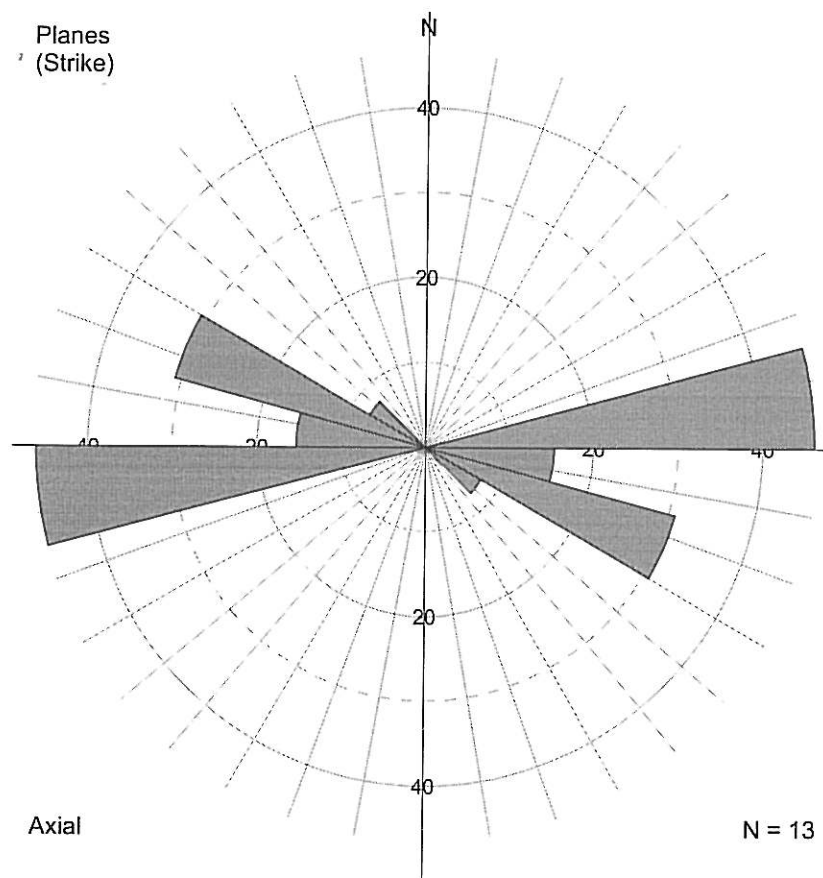


Schmidt net lower hemisphere plot of poles to joint planes in Buffelskloof Formation.

Number of points: 13

**Plot 10**

**Buffelskloof Formation**



Rose diagram of strike direction frequency distribution of joints in Buffelskloof Formation.

Number of points:

13

Class interval:

15°

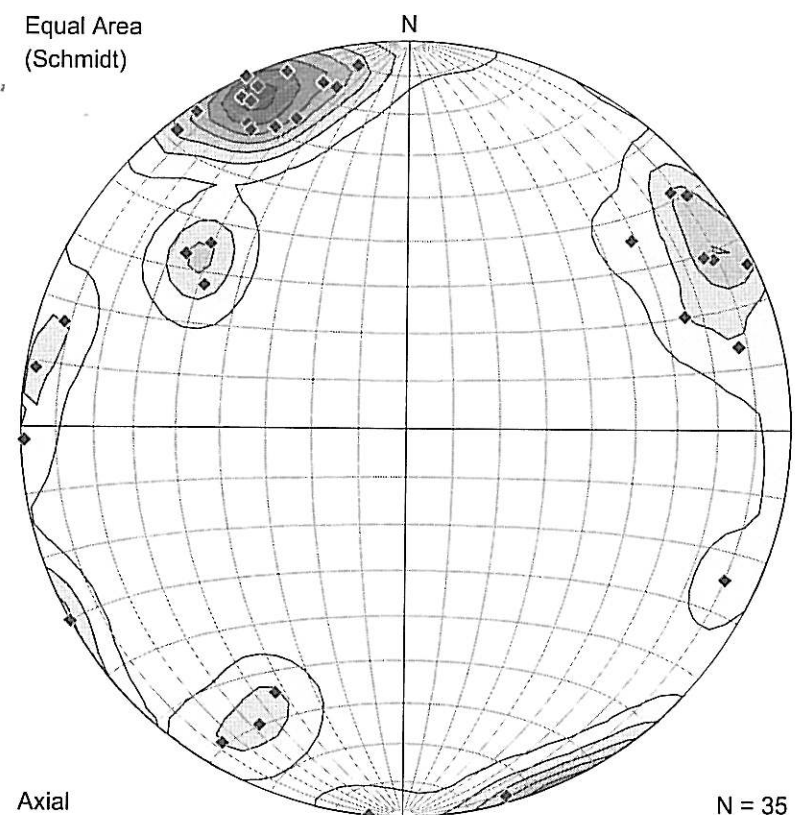
Frequency distribution:

0 – 75: 0%; 75 – 90: 46.2%; 90 – 105: 15.4%;

105 – 120: 30.8%; 120 – 135: 7.7%; 135 – 180: 0%

**Plot 11**

**Kirkwood Formation**

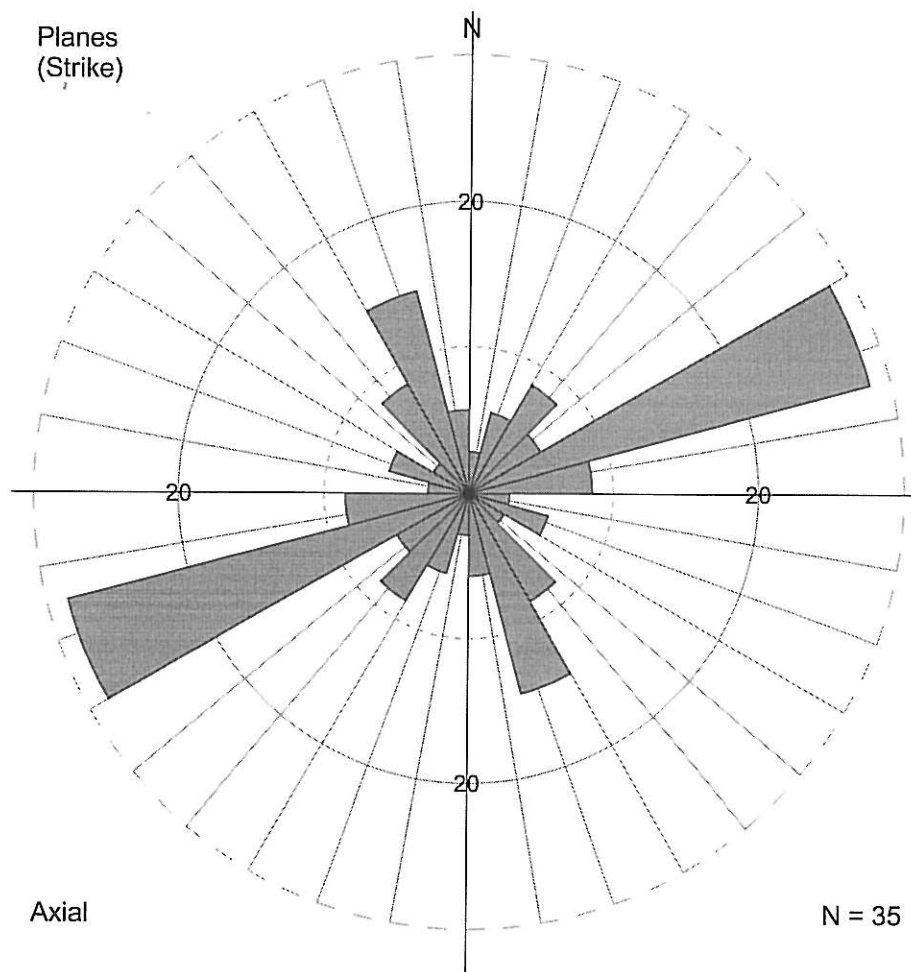


Schmidt net lower hemisphere plot of poles to joint planes in Kirkwood Formation.

Number of points: 35

**Plot 12**

**Kirkwood Formation**



Rose diagram of strike direction frequency distribution of joints in Kirkwood Formation

Number of points: 35

Class interval:  $15^\circ$

Frequency distribution: 0 – 15: 2.9%; 15 – 30: 5.7%; 30 – 45: 8.6%

45 – 60: 5.7%; 60 – 75: 28.6%; 75 – 90: 8.6%

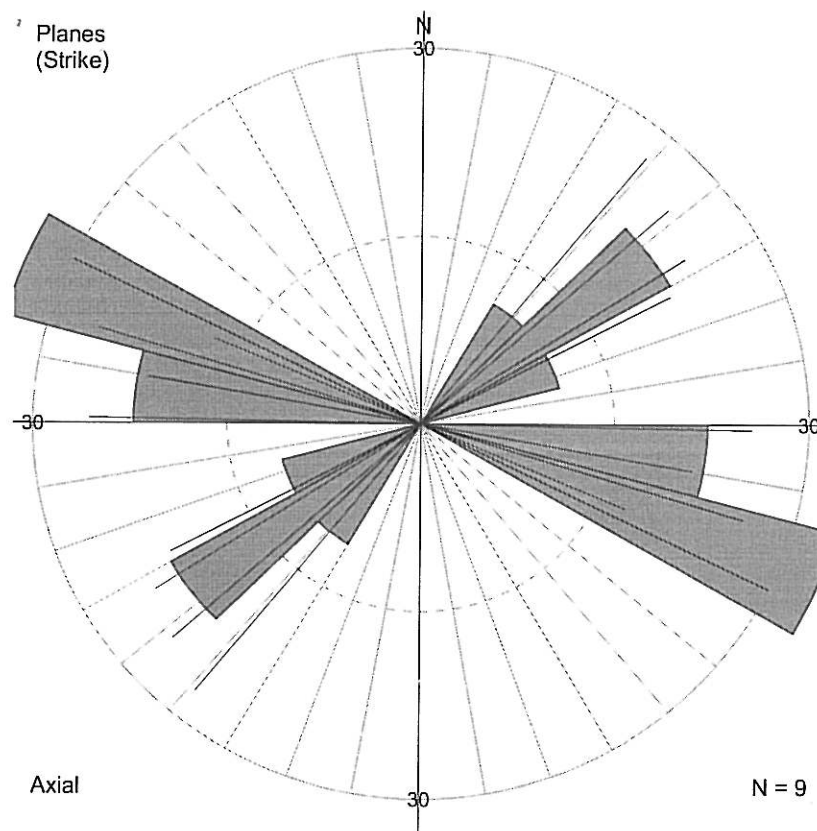
90 – 105: 2.9%; 105 – 120: 5.7%; 120 – 135: 2.9%;

135 – 150: 8.6%; 150 – 165: 14.3%; 165 – 180: 5.7%

## Data Plots: Table Mountain Group

### Plot 13

### Faults in TMS.



Rose diagram and frequency distribution of strike directions of faults measured in TMS. Principal stress direction appears to have been around 81 degrees. A single normal fault measured in Kirkwood Formation strikes 69 degrees.

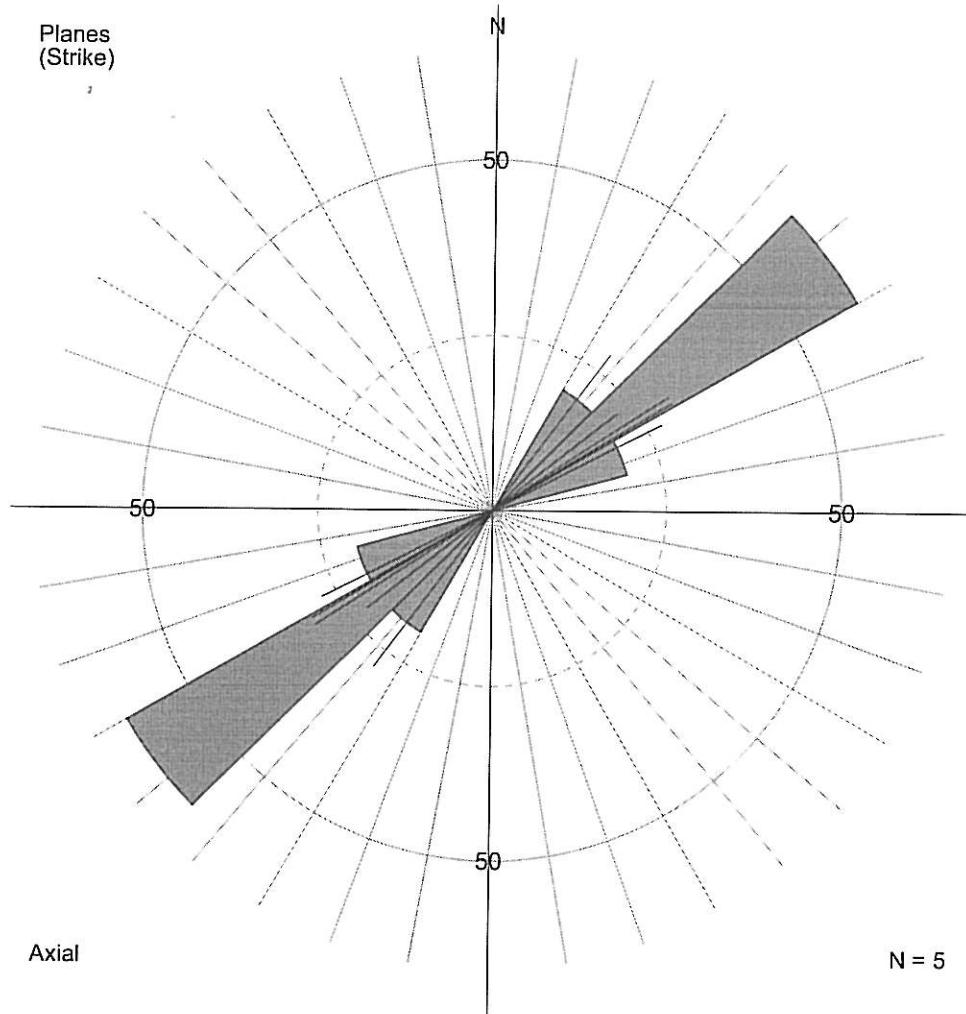
Number of sites: 2 (Site 10, Site 22)

Number of readings: 9

Class interval:  $15^{\circ}$

Plot 14

Joints in TMS

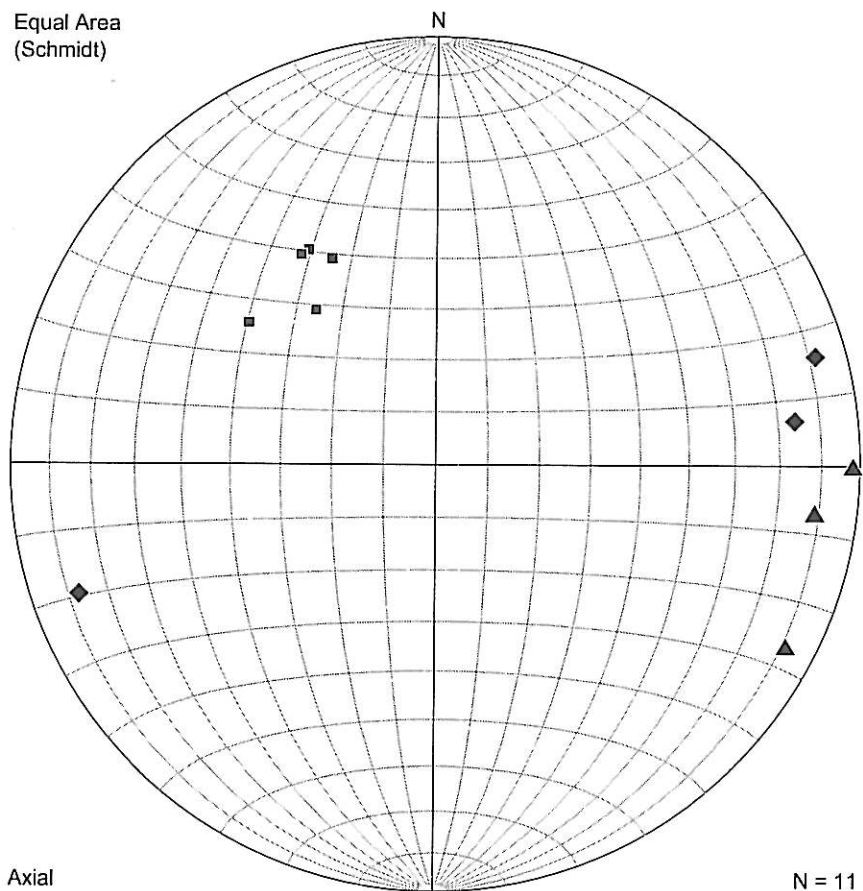


Rose diagram and frequency distribution of strike directions of joints measured in TMS.

Number of sites: 1 (Site 10)  
Number of readings: 5  
Class interval:  $15^{\circ}$

### Plot 15

#### Joints in TMS and Bokkeveld Shale



Schmidt net lower hemisphere plot of poles to joint planes in TMS and Bokkeveld shale (Sites 10, 17, 22). (All measured data.)

Number of readings: 11

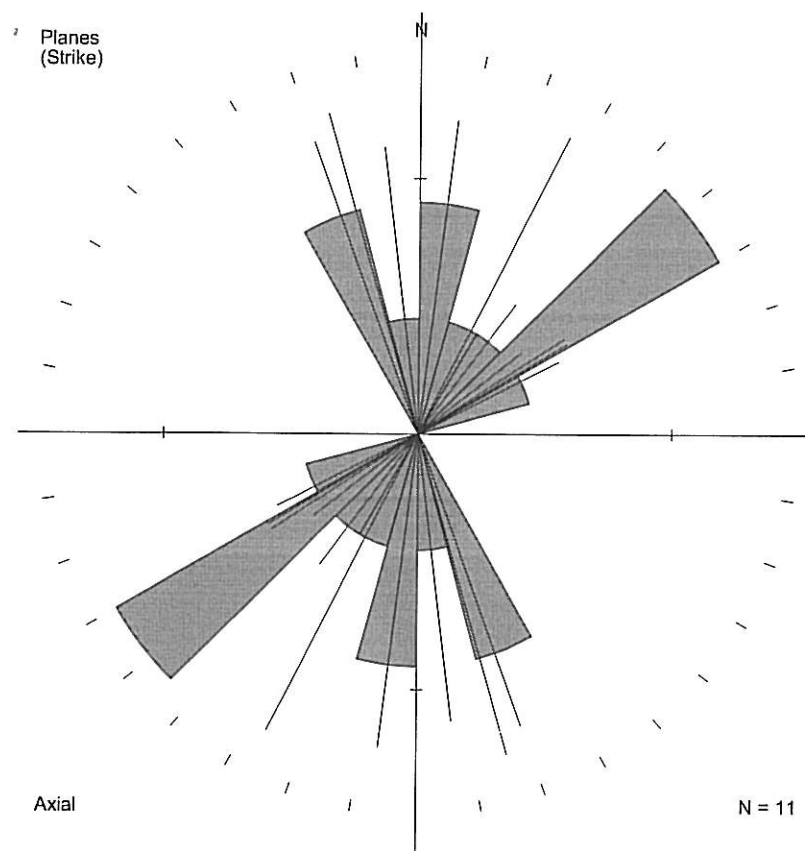
Site 10, TMS (Dysselsdorp) - squares

Site 22 TMS (Calitzdorp) - diamonds

Site 17 Bokkeveld Shale Southern edge of basin - triangles

**Plot 16**

**Joints in TMS and Bokkeveld Shale**



Rose diagram and frequency distribution of strike directions of joints measured in TMS and Bokkeveld Shale (Sites 10, 17, 22). (All measured data)

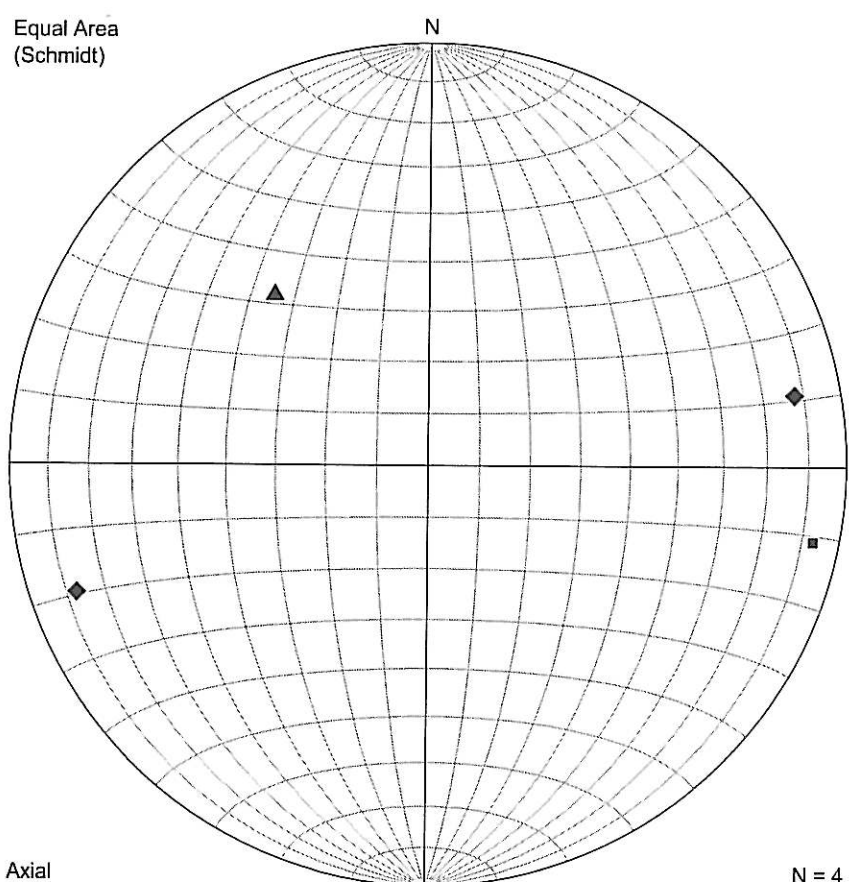
Number of sites: 3 (Site 10, 17, 22)

Number of readings: 11

Class interval:  $15^{\circ}$

**Plot 17**

**TMS and Bokkeveld shale**



Schmidt net lower hemisphere plot of averaged poles to joint planes in TMS and Bokkeveld shale (Sites 10, 17, 22).

Number of sites: 3

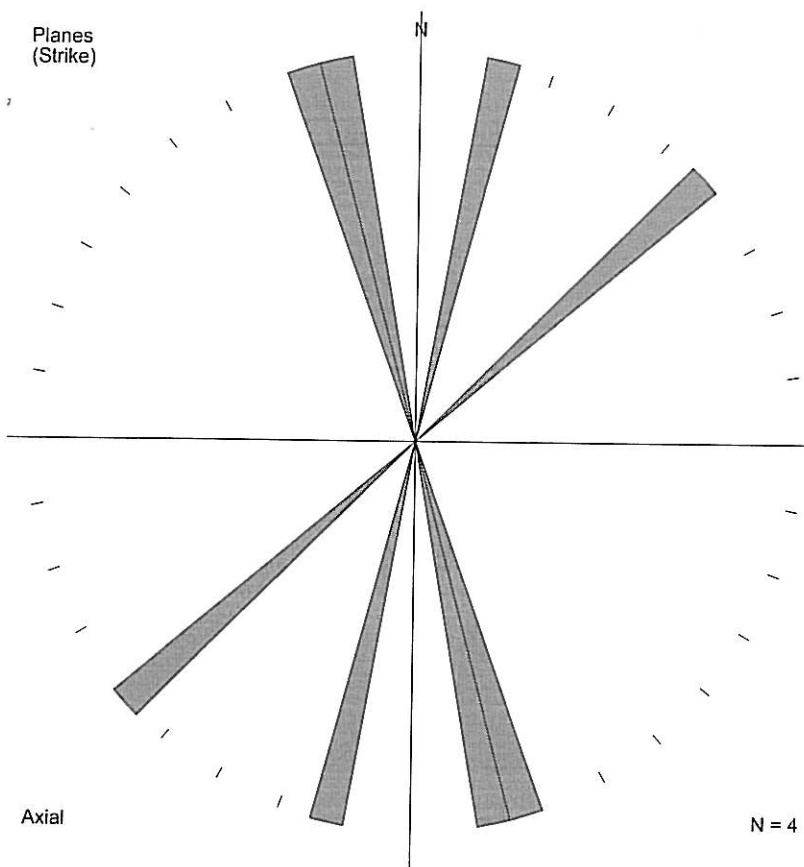
Site 10, TMS (Dysselsdorp) - triangles

Site 22 TMS (Calitzdorp) - squares

Site 17 Bokkeveld Shale Southern edge of basin - diamonds

**Plot 18**

**TMS and Bokkeveld shale**



Rose diagram of averaged strike directions of joints measured in TMS and Bokkeveld Shale (Sites 10, 17, 22).

Number of sites:	3 (Site 10, 17, 22)
Number of readings:	11
Class interval:	10°
Strike directions:	
	TMS Site 10: 53°
	TMS Site 22: 11°
	Bokkeveld Shale Site 17: 164°